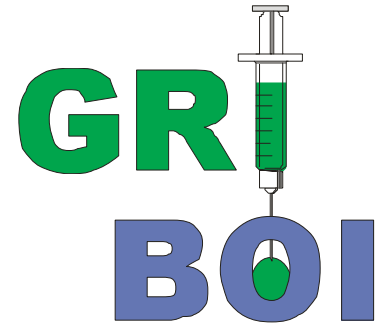
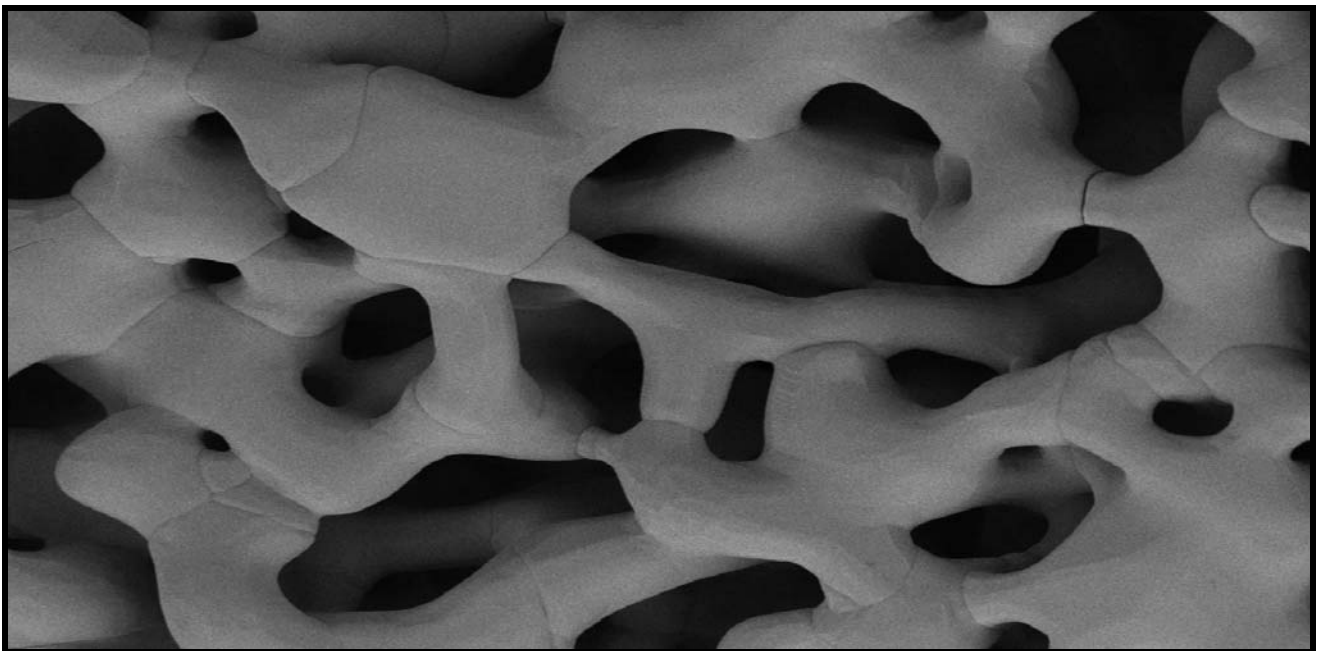


# Proceedings of the 16<sup>th</sup> Interdisciplinary Research Conference on Biomaterials



*Groupe de Recherche Interdisciplinaire  
sur les Biomatériaux Ostéo-articulaires  
Injectables*



**March 16<sup>th</sup> – 18<sup>th</sup>, 2006**  
**Bern, Switzerland**

# Table of Contents

<b>Introduction</b> .....	<b>1</b>
<b>Scientific Program</b> .....	<b>2</b>
<b>Podium Presentations</b> .....	<b>10</b>
<i>Session A: Clinical Applications and Experiences</i> .....	<b>10</b>
<i>Session B: Material Synthesis and Characterization</i> .....	<b>16</b>
<i>Session C: Drug Delivery Applications</i> .....	<b>25</b>
<i>Session D: Live Surgery &amp; Clinical Experiences</i> .....	<b>30</b>
<i>Session E: In Vivo Studies</i> .....	<b>33</b>
<i>Session F: Biomechanics</i> .....	<b>41</b>
<b>Posters</b> .....	<b>48</b>
<b>Sponsors</b> .....	<b>92</b>
<b>European Cells &amp; Materials Journal</b> .....	<b>93</b>

Cover Illustration: *b*-Tricalcium phosphate blocks, M. Bohner and R.G. Richards

# Introduction

## Dear Colleagues

It is our pleasure to welcome you to Bern for the 16th Interdisciplinary Research Conference on Biomaterials (Groupe de Recherche Interdisciplinaire sur les Biomatériaux Ostéo-articulaires Injectables). Our goal for this meeting was to build on the success of previous GRIBOI meetings and to offer a stimulating and multidisciplinary examination of current and future bone substitutes and injectable biomaterials. It was our desire to attract a larger number of clinicians to the meeting to provide the clinical context for the advances which are being made in the development of novel biomaterials. With the current scientific program, we feel that we are offering not only a detailed look into the technical aspects of biomaterials, but also a broad and insightful overview of the application of these materials and the clinical experiences which are beginning to be collected. We can now draw on the results of multi-year follow-up studies to objectively characterize the performance and potential of the technical developments which we are making. It is our desire that, by limiting the meeting to a modest size without parallel sessions, we will stimulate enthusiastic and productive discussions during the oral and poster sessions, exchanging opinions and insights between scientists and clinicians.

We would like especially to acknowledge the contribution of the scientific committee. Without the careful and timely review of the submitted abstracts it would not have been possible to assemble such a high quality program.

We wish you a productive meeting.

Yours Sincerely,

Marc Bohner, Stephen Ferguson, Paul Heini

Co-Chairmen, GRIBOI 2006

## Program Committee

G. Baroud, Ph.D.  
University of Sherbrooke

Marc Bohner, Ph.D.  
Robert Mathys Foundation

Stephen Ferguson, Ph.D.  
University of Bern

Paul Heini, M.D.  
University of Bern

J. Lemaître, Ph.D.  
Swiss Federal Institute of  
Technology Lausanne

T. Steffen, M.D., Ph.D.  
McGill University

S. Belkoff, Ph.D.  
Johns Hopkins University and  
Bayview Medical Center

K. Dai, M.D.  
Shanghai 2nd Medical University

P. Hardouin, M.D., Ph.D.  
Université du Littoral

S. J. Kalita, Ph.D.  
University of Central Florida

D. Rüfenacht, M.D.  
University of Geneva

# Scientific Program

**Thursday, March 16<sup>th</sup>**

**8:00 – 9:00      Registration**

**9:00 – 10:30    Keynote Lectures: Clinical Applications and Experiences**

9:00 – 9:45      Jorrit-Jan Verlaan, MD, PhD: Utrecht University

9:45 – 10:30    Paul Heini, PhD: University of Bern

**10:30 – 11:00    Coffee Break**

**11:00 – 12:15    Podium Presentations: Clinical Applications and Experiences**

11:00 – 11:15    Injectable bone cements in the treatment of spinal fractures, osteopromotive capacity and surgical considerations  
S. Becker, K. Franz, I. Wilke, M. Ogon

11:15 – 11:30    The use of a nanoparticles hydroxylapatite gel as a bone substitute  
C. Schwartz, S. Malincenco, R. Bordei

11:30 – 11:45    ChronOS™ Inject in children with bone cysts resistant to conventional treatment  
T. Slongo, A. Joeris

11:45 – 12:00    Three years of use of a tri-calcium phosphate ( $\beta$ ) substitute in bone and joint surgery  
P. Chelius

12:00 – 12:15    Clinical applications of bioactive glasses in dental, cranial and load bearing bones  
A. Yli-Urpo

**12:15 – 14:00    Lunch and Poster Session**

**14:00 – 15:30    Keynote Lectures: Material Synthesis and Characterization**

14:00 – 14:45    Marc Bohner, PhD: Robert Mathys Foundation

14:45 – 15:30    Stephen Belkoff, PhD: Johns Hopkins University, Bayview Medical Center

**15:30 – 16:00    Coffee Break**

**16:00 – 18:00    Podium Presentations: Material Synthesis and Characterization**

16:00 – 16:15    Evaluation of the cohesiveness of injectable Ca-aluminate based materials in water and simulated body fluid during curing  
H. Spengler, L. Hermansson, H. Engqvist

16:15 – 16:30    Fluoro-apatite and calcium phosphate nanoparticles by flame synthesis  
T. Brunner, S. Loher, W.J. Stark

- 16:30 – 16:45     Injectable PLGA microsphere / calcium phosphate cements: Physical properties and degradation characteristics  
W.J.E.M. Habraken, J.G.C. Wolke, A.G. Mikos, J.A. Jansen
- 16:45 – 17:00     Calcium carbonate biphasic cement concept to control cement resorption  
C. Combes, C. Rey
- 17:00 – 17:15     A new injectable calcium-strontium phosphate bone cement and PLAGA composite  
G. Romieu, S. Munier, H. Garreau, M. Vert, P. Boudeville
- 17:15 – 17:30     Anisotropic bone scaffolds  
O. Zamoum, O. Mecherri , M. Fiallo , P. Sharrock
- 17:30 – 17:45     Influence of platelet-rich plasma on osteogenic differentiation of mesenchymal stem cells and ectopic bone formation in calcium phosphate ceramics  
P. Kasten, J. Vogel, R. Luginbühl, I. Beyen, M. Bohner, B. Gasser, W. Richter
- 17:45 – 18:00     Disperse cement filling in vertebroplasty may reduce risk of secondary tissue damage  
K. Sun, E. Mendel, L. Rhines, A. Burton, M. Liebschner
- 18:00 – 19:30     Posters and Aperos**

**Friday, March 17<sup>th</sup>**

**8:00 – 9:30        Keynote Lectures: Drug Delivery Applications**

8:00 – 8:45        Jeff Hollinger, DDS, PhD: University of Maryland

8:45 – 9:30        Thierry Stoll, MSc: Synthes

**9:30 – 10:00     Coffee Break**

**10:00 – 11:00    Podium Presentations: Drug Delivery Applications**

10:00 – 10:15     In vitro study Of BMP-2 gene transfected bone marrow derived mesenchymal stem cells in APA microcapsules  
T.T. Tang, H.F. Ding, R. Liu, B.G. Li, C.F. Yu, J.R. Lou, K.R. Dai

10:15 – 10:30     Fibrin-fibronectin sealing system in combination with beta-tricalcium phosphate as a carrier for recombinant human bone morphogenetic protein-2: Effects on bone formation in rat calvarial defects  
J.-Y. Hong, S.-J. Hong, S.-W. Jung, Y.-J. Um, S.-B. Lee, K.-S. Cho, C.-S. Kim

10:30 – 10:45     An injectable composite of osteogenic protein-1 (OP-1, rhBMP-7) and hydroxyapatite enables early in vivo cement stabilization and biointegration. A controlled, randomized study in the sheep spine.  
T.R. Blatter, W. Schmölz, A. Weckbach, C. Toth, L. Claes, H.-J. Wilke

10:45 – 11:00     Mineral / organic composite bone grafts: Characterization and evaluation as drug delivery systems  
S. Girod, H. Ternet, M. Frèche, J.L. Lacout, F. Rodriguez

- 11:00 – 12:00**     **Live Surgery Broadcast: Paul Heini**  
**Concurrent Podium Presentations: Clinical Experiences**
- 11:00 – 11:15     Three years experience with standalone kyphoplasty and calcium phosphate cement in traumatic fractures.  
G. Maestretti, C. Cremer, Ph. Otten
- 11:30 – 11:45     Limited suitability of calcium phosphate in the treatment of osteoporotic vertebral body fractures  
T.R. Blattert
- 12:00 – 14:00**     **Lunch and Poster Session**
- 14:00 – 15:30**     **Keynote Lectures: In Vivo Studies**
- 14:00 – 14:45     Jörg Krebs, DVM: University of Bern
- 14:45 – 15:30     Georg Watzek, MD, PhD: Medical University of Vienna
- 15:30 – 16:00**     **Coffee Break**
- 16:00 – 17:45**     **Podium Presentations: In Vivo Studies**
- 16:00 – 16:15     A new concept of antibiotic loaded HAP/TCP bone substitute for prophylactic action: ATANTIK Genta - In vivo study  
A. Bignon, E. Viguier, F. Laurent, D. Goehrig, G. Boivin, J. Chevalier
- 16:15 – 16:30     A poly (D, L-Lactide) / allogenic bone composite for bone tissue engineering  
Q. Li, C. Zhou
- 16:30 – 16:45     Enhanced osseointegration of bone-implant interface by BMP-2 gene medication  
K.R. Dai, M. Yan, T.T. Tang
- 16:45 – 17:00     Effects of recombinant human bone morphogenetic protein-2 and acellular dermal matrix on bone formation in rat calvarial defects  
Y.-J. Um, D.-S. Song, J.-Y. Hong, S.-W. Jung, S.-B. Lee, K.-S. Cho, C.-S. Kim
- 17:00 – 17:15     Chitosan containing calcium phosphate cement: preparation and clinical study  
K. Poret, M. Frèche, S. Goncalvez, J.L.Lacout, F. Rodriguez
- 17:15 – 17:30     Clinical evaluation of an injectable, in-situ curing nucleus replacement  
U. Berlemann, O. Schwarzenbach, C. Etter, S. Kitchell
- 17:30 – 17:45     Quantitative kinetic analysis of gene expression during human osteoblastic adhesion on orthopaedic materials  
M. Rouahi, E. Champion, P. Hardouin, K. Anselme
- 17 :45 – 18 :15**     **GRIBOI General Assembly**
- 20 :00 -**             **Social Event and Dinner**

## Saturday, March 18th

### 8 :00 – 9:30      **Keynote Lectures : Biomechanics**

8:00 – 8:45      Gamal Baroud, PhD: University of Sherbrooke

8:45 – 9:30      Thomas Steffen, MD, PhD: McGill University

### 9:30 – 10:00      **Coffee Break**

### 10:00 – 11:30      **Podium Presentations: Biomechanics**

10:00 – 10:15      The effect of strontium on the rheology and mechanical properties of zinc based glass polyalkenoate cements  
D. Boyd, M.R. Towler

10:15 – 10:30      Local compressive and tensile stiffness measured in tissues with regular patterns of hyaline-fibrocartilage regions  
A. Marsano, D. Wendt, R. Raiteri, R. Gottardi, S. Dickinson, A.P. Hollander, D. Wirz, A.U. Daniels, T.M. Quinn, M. Stolz, I. Martin

10:30 – 10:45      KyphOs FS™ calcium phosphate for balloon kyphoplasty: Verification of Compressive Strength and Instructions for Use  
J. Schwardt, T. Slater, S. Lee, J. Meyer, R. Wenz

10:45 – 11:00      Vertebral cancellous bone augmented with stiffness-adapted PMMA cement does not show acute failure under dynamic loading  
A. Boger, P. Heini, M. Bohner, E. Schneider

11:00 – 11:15      Effect of solution viscosity on cement injectability  
P.J. Leamy, M. Lehmicke, M.T. Fulmer

11:15 – 11:30      Injectable calcium phosphate cement with water washout resistance  
Y. Wang, J. Wei, H. Hong, H. Guo, C. Liu

### 11:30 – 12:00      **Awards and Concluding Remarks**

## POSTERS

Activation and biomechanical assessment of an injectable hybrid osteoconductive - osteogenic bone substitute  
S. Becker, I. Boecken, M. Bohner, G. Bigolin, M. Alini

The effect of pulsed jet lavage in vertebroplasty on injection forces of PMMA bone cement, material distribution and potential fat embolism: A cadaver study  
L. M. Benneker, A. Gisepp

Biodegradable polymers in spinal surgery - posterior lumbar interbody fusion with resorbable polymer interbody cage. Case report  
D. Bludovsky, M. Choc

Fluorcanasite / frankamenite based glass-ceramics for bone tissue repair  
S. Bandyopadhyay-Ghosh, A. Johnson, I. M. Reaney, K. Hurrell-Gillingham, I. M. Brook, P. V. Hatton

- Synthesis and in vitro cell culture of Zn-doped calcium phosphates  
C. L. Burchfield, A. E. Tate, S. Jalota, S. B. Bhaduri, A. C. Tas
- Laser preconditioning on irradiated bone: A preliminary intravital study  
S. Desmons, C. Delfosse, P. Rochon, G. Leroy, S. Mordon, G. Penel
- Pure and doped bioactive glasses synthesised by melt derived and sol-gel methods  
E. Dietrich, H. Oudadesse, A. Lucas-Girot, Y. Legal, M. Mami, R. Sridi-Dorbez
- Injectable bone substitutes of silica-contained calcium phosphates and a hydrophilic polymer  
S.V. Dorozhkin
- Using XRD, FTIR and TG analysis to monitor conversion of a novel, injectable calcium phosphate cement  
M. Geiger, A. Hina, S. Sofia, N. Warne
- Effect of Mg<sup>2+</sup> content on lattice parameter and phase transformation temperature of  $\beta$ -a TCP  
F. Goetz-Neunhoeffler, J. Neubauer, M. Göbbels, R. Enderle
- A novel experimental approach to imaging and quantifying newly bone formation around bone substitutes  
A. Gorustovich, M. Sivak, M.B. Guglielmotti
- Evaluation of in vitro bioactivity of different types of biomaterials  
L. Hermansson, A. Faris, H. Engqvist
- Vertebroplasty and kyphoplasty: A systematic review of 69 clinical studies  
P.A. Hulme, J. Krebs, S.J. Ferguson, U. Berlemann
- Mechanical evaluation of a bioactive calcium aluminate cement for vertebral body augmentation  
P.A. Hulme, P.F. Heini, T. Persson, H. Spengler, K. Björklund, L. Hermansson, S.J. Ferguson
- Comparison of milling techniques in the production of  $\beta$ -TCP  
V. Jack, F. Buchanan, N. Dunne, M. Bohner
- Powder metallurgy (PM) processed titanium based biocomposite for bone substitute material  
M. Karanjai, R. Sundaresan, T.R. Ramamohan, B.P. Kashyap
- Preparation of hydroxyapatite-gelatin composite scaffold for bone tissue engineering  
M. Kazemzadeh Narbat, M. Solati, M. Pazouki
- Poly(lactide-co-glycolide)/nano-hydroxyapatite composite for bone regeneration  
S.-S. Kim, M.S. Park, O. Jeon, C.Y. Choi, B.-S. Kim
- Effects of vertebral bone augmentation on intervertebral discs  
J. Krebs, S.J. Ferguson, B.G. Goss, N. Aebli
- Cardiovascular consequences of pulmonary cement embolism  
J. Krebs, N. Aebli, B.G. Goss, S. Sugiyama, S.J. Ferguson
- Fabrication of porous AL<sub>2</sub>O<sub>3</sub> and T-ZRO<sub>2</sub> ceramics and evaluation of their biocompatibility  
B.T. Lee, A.K. Gain, H.Y. Song
- Phases evolution of bioactive glasses during crystallization for orthopaedic and tissue engineering applications  
L. Lefebvre, J. Chevalier, D. Bernache, L. Gremillard, R. Zenati

The study of PLGA/TCP scaffold with bovine BMP were implanted in bone defects peri-implant  
P. Lei, X.E. Xing

Autologous marrow stromal cells enhance further osseointegration earlier in porous coated-apatite titanium implants in rabbit  
P. Lei, W. Mingxi, X.E. Xing

Study of degradability of the CAO-MgO-B<sub>2</sub>O<sub>3</sub>-P<sub>2</sub>O<sub>5</sub>-SiO<sub>2</sub> glasses  
X. Li, L. Wei, W. Wu, H. Guo, C. Liu

Development of an advanced injection device for highly viscous materials  
M. Loeffel, J. Kowal, P. F. Heini, J. Burger, L.-P. Nolte

Bone substitutes produced by wet shaping techniques  
J. Luyten, S. Mullens, I. Thijs, J. Coymans, S. Impens

Distal radius fracture and injectable cement : useful or not?  
Prospective continue study of 48 cases with minimal follow up of 3 years  
L.Obert, G. Leclerc, D. Lepage, Y. Tropet, P. Garbuio

Post traumatic arthritis secondary to intra articular malunion of distal radius treated by chondro costal graft  
L. Obert, D. Lepage, J. Pauchot, Y. Tropet, P. Garbuio

Extra articular malunion of the distal radius treated by corrective osteotomie and injectable cement  
L. Obert, D. Lepage, S. Rochet, Y. Tropet, P. Garbuio

Impact simulation for cranioplasty using a non-linear finite element model  
H.K. Park, J.H. Park, H.D. Han, J.H. Chung

Preparation and characterization of nanofiber matrices for tissue engineering  
H.H. Park, K.E. Park, K.Y. Lee, W.H. Park

In vitro biocompatibility test of nano alumina and characterization by Rietveld analysis  
D. Saha, S. Dhabal

The effect of sintering temperature on mechanical properties of aluminium-oxide reinforced hydroxyapatite (BHA) composites  
S. Salman, O. Gunduz, F.N. Oktar

Fabrication of silver nanoparticles and their antimicrobial mechanisms  
H.Y. Song, K.K. Ko, I.H. Oh, B.T. Lee

Morphological changes during 42 months of PMMA vertebroplasty: A case study  
C.M.Sprecher, A.Gisep, S.Milz, U.Haupt, K.Yen, P.Heini

Determination of impurities in calcium phosphate ceramics  
E.I. Suvorova, P.A. Buffat

Acrylic vertebroplasty alters vertebral load distribution and causes reduction in strength of adjacent vertebrae  
W. Tawackoli, K. Sun, M. Fukshansky, A. Burton, L. Rhines, E. Mendel, M. Liebschner

Strength restoration by sacroplasty of simulated sacral insufficiency fractures  
M.D. Waites, S.C. Mears, J.M. Mathis, S.M. Belkoff

Injectable bioactive nano biomaterials for bone tissue engineering  
Y. Wang, J. Wei, H. Guo, H. Hong, C. Liu

Research and expressions of the bioglass cement

L. Wei, X. Li, G. Wu

Chemical- physical characterization and histological outcomes after implantation of KyphOs™ and KyphOs R™ in vertebral bodies of sheep

R. Wenz, J.Meyer, M. Sankaran, J. Schwardt

Hydroxyapatite coating for fixation of biomedical implants

K. L. Yadav

## **Session A:**

# **Clinical Applications and Experiences**

### **Keynote Lectures**

Jorrit-Jan Verlaan, MD, PhD  
Utrecht University

Paul Heini, MD  
Inselspital, University of Bern

# **Injectable Bone Cements in the Treatment of Spinal Fractures, Osteopromotive Capacity and Surgical Considerations**

S. Becker<sup>1</sup>, K. Franz<sup>2</sup>, I. Wilke<sup>2</sup>, M. Ogon<sup>1</sup>

<sup>1</sup>*Spine Center Orthopaedic Hospital Speising Vienna AUT, <sup>2</sup>Research Center for medical and biological technologies FZMB, Bad Langensalza D*

**INTRODUCTION:** Recent developments focus on injectable calcium – phosphate – cements for different indications in orthopaedics and traumatology including spinal fractures and osteoporosis. We performed a study and compared 4 different injectable bone cements regarding toxicity, cell growth and cell differentiation. Furthermore we used 2 of them (Calcibon, KyphOs) in the treatment of vertebral fractures on patients and summarize clinical and technical considerations.

**METHODS:** 4 injectable bone cements, three CP cements (ChronOS inject – Synthes, Calcibon - Biomet Merck, KyphOs – Kyphon) and one non resorbable glass – ceramic (Cortoss - Orthovita) were compared. Mesenchymal stem cells from sheep were seeded for the cytotoxic test on 6-well plates (50.000 cells /well). After 3 days of cultivation, a toxicity test (trypanblue), cellproliferationtest (MTT, Absorption 550 nm) and histology was performed. After 16 days of cultivation cell growth/differentiation (2 mio cells seeded onto the sample) was performed by histology, AP synthesis, protein absorption and histology.

Between 2002 and 2005 we performed 315 conventional kyphoplasties on 180 patients. 15 patients were under the age of 40 and showed traumatic fractures and were treated with resorbable bone substances. Maximum follow-up 2.5 years.

**RESULTS:** No significant toxic influences were found in Calcibon and ChronOS inject. KyphOs showed a 16.7% increased toxicity if compared to control. No viable cells were found after seeding on Cortoss. The same results were seen on cell growth, best growth in the Calcibon and ChronOS inject groups followed by 50% less growth in the KyphOs groups and virtually no cell growth in the Cortoss group. After 16 days all surviving cells produced similar AP levels with again the ChronOS group showing the highest levels. No protein absorption was found in the Calcibon and Cortoss groups. Histological studies could only be performed on ChronOS inject, as the other materials were too hard to cut and broke in pieces.

No vertebra treated with resorbable bone substance refractured during the follow-up period. The resorption of the bone substance varied largely and all patients had still visible artificial substance within the bone after 2 years. However, CT and MRI follow-up showed no resorption zone or osteonecrosis around the cements, all were in the state of remodelling.

**DISCUSSION & CONCLUSIONS:** All three CP – cements stimulate mesenchymal stem cell proliferation into osteoblasts and osteoblast growth; however Calcibon and ChronOS inject are superior to KyphOs. Astonishingly Cortoss was toxic for MSC and subsequently no growth occurred. We conclude that under lab conditions it is difficult to simulate the actual ingrowth and remodelling of bone cements. All cements are in clinical use; however we prefer the use of resorbable bone cements in young patients. Technically all used cements need a cavity to be injected in which we realise with a kyphoplasty balloon. The indication of treating traumatic fractures is clinically most important, in our experience within a clinical research group using these cements in different centers, only A1 and A3.1 fractures may yield good results in the future.

## **REFERENCES:**

- Heini PF, Berlemann U. Bone substitutes in vertebroplasty. *Eur Spine J.* 2001 Oct;10 Suppl 2:205-13.
- Hillmeier J et al. Balloon kyphoplasty of vertebral compression fractures with a new calcium phosphate cement. *Orthopäde.* 2004 Jan;33(1):31-9.
- Bohner M et al. Potential use of biodegradable bone cement in bone surgery: holding strength of screws in reinforced osteoporotic bone. *Orthopaedic Trans* 1992;16:401-402.

# The Use of a Nanoparticles Hydroxylapatite Gel as a Bone Substitute.

C.Schwartz, S.Malincenco & R.Bordei

*Service d'Orthopédie et de Traumatologie, Colmar, F*

**INTRODUCTION:** Synthetic bone substitutes are more and more used in orthopaedic and trauma surgery. Biphasic ceramics give good results but are very slowly and incompletely integrated in new-formed bone. Moreover they are not easy to use in certain circumstances because of their rigidity primarily.

**METHODS:** We used from July 2003 to October 2005 a new injectable bone substitute in hundred cases of trauma and orthopaedic surgery.

The substitute is a matrix of synthetic hydroxylapatite nanoparticules in water. It is elaborated by precipitation without sintering. The crystals remain in their initial needles form about 18 nanometres size. They are as agglomerates of approximately 100 x 5 nanometres in the gel. It presents as an odourless white injectable paste, sterilized with gamma rays; its pH is neutral, its solubility about 2.6 mg per 100 g of water; the most important character is its specific surface about 100 square meters pro gram. It is viscous and remains without hardening in situ. Its application by injection brings a close contact between the product and the surrounding osseous layer. It is stable in its volume, without being eliminated by blood, but does not have any mechanical resistance.

We used this substitute for filling 48 tibia open osteotomies stabilised by plates and screws; medium opening angle was 9°. In none case autograft was associated. In 4 cases biopsy was done after 6 to 12 months when plates were withdrawn. Classical histology, TEM and XRD were done.

**RESULTS:** In 4 cases we saw an asymptomatic aseptic flow, which dry itself up in 15 to 20 days without any treatment. Not other complications were seen; consolidation of the osteotomies occurred in 6 weeks, perhaps faster than with biphasic ceramics; it occurred in all cases except one; to early weight bearing delayed the consolidation to 3 months without new operation but only plaster cast and rest.



*Post operative and 6 months X Rays*

Because of its nanocrystalline structure, the substitute is quickly degraded with formation of new bone which stimulates the cure of osseous lesion. Biopsies showed a rapid micro-vascular invasion and fast colonization by pro osteoblasts then differentiation of those with collagen fibre deposition. The resorption is done by macrophages which invade the site with moderated, focal, giant cells reaction in contact with the material.

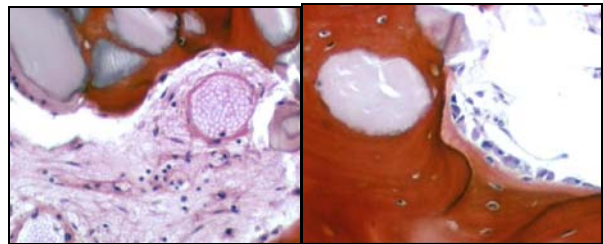


*Fig.1: Biopsy 6 months : angiogenesis,osteoblasts with osteogenesis*

**DISCUSSION & CONCLUSIONS:** The surgeon appreciated the easy way to use this injectable product. He was anxious to see the flow in some cases but reassured when cure without new treatment. Studies are in progress to find the reason of this flow. Bone consolidation was ever fast and good quality; it seems to be a new interesting and practical way for bone substitution in orthopaedic and trauma surgery.

# ChronOS<sup>TM</sup>Inject in Children with Bone Cysts Resistant to Conventional Treatment

T. Slongo<sup>1</sup> & A. Joeris<sup>1</sup>

<sup>1</sup>Dept. Surgical Pediatrics, Children's Hospital, University of Berne, Berne, Switzerland

**INTRODUCTION:** Although a majority of benign bone cysts can be cured by the nowadays established treatments (curettage, corticosteroids, autogenous or allogenic bone grafting, intramedullary nailing) there are a number of cysts, which remain difficult to treat mainly due to the localisation or the patient's age with closed growing plates. Recently a new injectable hydraulic calcium phosphate cement (ChronOS<sup>TM</sup>Inject) was introduced, which shows the induction of bone formation and resorption [1,2]. We therefore hypothesized, that ChronOS<sup>TM</sup>Inject might be a reliable alternative in patients with complicated bone cysts.

**METHODS:** Since 2004 in 7 patients with benign bone cysts, which could not be cured by the established treatments or could not be treated with the established treatments because of the lesion's localisation, the indication for ChronOS<sup>TM</sup>Inject was made. 4 of them were already treated, in 3 the day of surgery is fixed. Follow up was done at our outpatients' clinic. Follow up ranged between 9 and 16 month so far.

**RESULTS:** Among the 4 already treated children the age ranged between 3 and 17 years at the day of treatment. Two times a juvenile bone cyst was diagnosed (tibial head, humeral shaft), once an aneurysmatic bone cyst (proximal humerus) and once a Langerhans-cell-histiozytosis (femoral neck). All 4 children underwent at least one other treatment because of a pathological fracture in prior, either by cast or intramedullary nailing, without healing of the cyst. The indication of ChronOS<sup>TM</sup>Inject was in two cases the cyst's localisation with instability and a high risk of refracture. In two cases a healing of the bone cysts could not be expected anymore due to the patients age. In all cases a stabilisation by intramedullary nailing was done together with the injection of ChronOS<sup>TM</sup>Inject. 15-20 ml of ChronOS<sup>TM</sup>Inject was injected in each bone cyst. The injection together with the intramedullary nailing was done by day surgery, so the children could leave the hospital the same day. A complete healing and consolidation were achieved in all 4 cases. Except of one patient a resorption of ChronOS<sup>TM</sup>Inject

could be observed. Beside a reddish skin and subfebrile temperatures short after operation no adverse effects were seen.

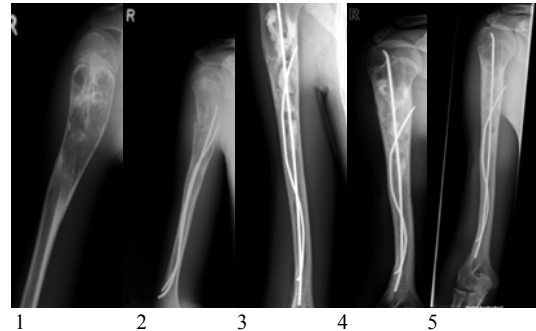


*Fig. 1: 17 year old boy with an aneurysmatic bone cyst. First diagnosis because of a pathological fracture (1), another pathological fracture with TENs in situ (2), 2 month, 5 month and 16 month after injection of ChronOS<sup>TM</sup>Inject (3,4,5). A complete healing with a resorption of ChronOS<sup>TM</sup>Inject, new bone formation and even an unexpected bone remodelling could be observed.*

**DISCUSSION & CONCLUSIONS:** Despite all established treatments large bone cysts in children with closed growing plates or cyst's localisation with a high risk of instability remain an unsolved problem. With the injection of ChronOS<sup>TM</sup>Inject we could achieve a complete healing in 4 patients with complicated bone cysts. No adverse effects were seen. Using ChronOS<sup>TM</sup>Inject a more invasive surgery for autogenous bone grafting and the risk of infection (e.g. hepatitis, HIV) by allogenic bone grafting can be avoided. We believe, that ChronOS<sup>TM</sup>Inject is a promising alternative treatment in children with complicated large long bone cysts, in which the established treatments are unsuccessful. These promising results encourage us for further use of ChronOS<sup>TM</sup>Inject, but larger prospective clinical studies are needed to verify our observations.

**REFERENCES:** <sup>1</sup> D. Apelt, et al (2004) *In vivo behaviour of three different injectable hydraulic calcium phosphate cements*, *Biomater* **25**:1439-51. <sup>2</sup> *Compositional changes of a dicalcium phosphate dehydrate cement after implantation in sheep*, *Biomater* **24**:3463-74

# Three Years of use of a Tri-calcium Phosphate ( $\beta$ ) Substitute in Bone and Joint Surgery

P.Chelius

*General Hospital, 10000 Troyes, France*

**INTRODUCTION:** The bone grafting is a very common procedure in bone surgery and has a great place in the treatment of bone repair. The complication's rate of autologous removal, possible major infectious risk of allograft, directed us towards the use of synthetic substitute and its easier handling.

Three years ago, we made confidence with a tricalcium phosphate substitute; in the same time we started to use locking screw devices for osteosynthesis which allows bridging of the fractured site, and minimal invasive procedure, thus stressing the biological and vascular aspect of the osseous healing.

The purpose of this study is to share our experience using the substitute and, may be, to find, at the moment, what are exactly the indications, the choice of its physical form, the practical use, in preparing the use of the next products or process upstream in the bone formation.

**METHODS:** The field of indication was initially wide, as the same as for autologous graft that we did previously

- acute traumatology to fill the bone loss due to the fracture or after reduction,
- revision surgery in pseudarthrosis or for revision arthroplasty,
- arthrodesis of the spine,
- proximal tibial open osteotomy
- benign bone tumour or bone dystrophy

For most of the cases, we used the substitute alone, and in addition to bone bank, or autologous graft, for few of them, to reduce the cost and the volume of the removal.

We did 184 cases, and we can say that the substitute disappears and it is changed into normal bone; the time to be replaced depends on the site, the volume to fill, the vascular and mechanical conditions.

We always, except for the beginning of our serie, filled the substitute with the blood of the patient under negative pressure in a syringe.

We did not see any adverse effect due to the substitute.

**DISCUSSION & CONCLUSIONS:** If the autologous graft may be considered as the gold standard, the totally resorbable substitute as a tricalcium phosphate ( $\beta$ ) is very useful and its handling is comfortable and safe. With using the locked screw devices the number of indications for grafting will decrease because the gain in stability is so good that the bone can heal by itself in some cases.

The injectible substitute is useful to; it increases the surface of contact between the substitute and the receiving bone so improving the exchanges; its handling has to respond to strong rules; its use for joint's fracture needs a clear intra articular control; we used it in several cases as a temporary spacer to stabilise the bone after reduction and before inserting the final device without any disturbing temporary device, as wires or clamp.

The totally resorbable substitute is specially indicated for benign bone tumour or dystrophy, without any disadvantage for the further X-rays control.

From few "border line" cases, we learned that the most important factors to succeed in these procedures are the characteristics of the receiving site.

We have to answer to some questions:

- What is the location of the defect and the volume to create?
- What is the vascular status?
- What are the mechanical conditions?
- What are the walls of the defect?
- What is the local capacity of bone regeneration?

At the end of these analysis, we think that we can define the need of a substitute and arguments for its choice.

**REFERENCES:** P.Eggli, et.al.*Clinical Orthopaedics*,1988, vol.232

M.Bohner(2001). *Eur. Spine J.* 10 Suppl 2 :114-121

# **Clinical Applications of Bioactive Glasses in Dental, Cranial and Load-Bearing Bones**

A. Yli-Urpo<sup>1</sup>

<sup>1</sup> Institute of Dentistry, University of Turku, Turku, Finland

Tissue reactions on bioactive glass S53P4 have shown bone bonding and good tissue conduction by forming a CaP-layer into a reaction layer on the glass. Immediate reactions in human tissues have shown a good healing and formation of new bone in dental, cranial and orthopaedic applications during follow-up of several years. The results have been promising in tissue repair also under chronic infections and load bearing situations according to follow-up studies. Bioactive glass composite material seems to be promising for different types of large skull defect repair and for guided tissue repair. Reaction and resorption activity of the glass is possible to control by surface area of the glass products. During time, the glass material will gain new bone material and the glass itself will be resorbed in a controlled way and time from the body via urine without harmful reactions.

## **Session B:**

# **Material Synthesis and Characterization**

## **Keynote Lectures**

Marc Boner, PhD  
Robert Mathys Foundation

Stephen Belkoff, PhD  
Johns Hopkins University and Bayview Medical Center

# Evaluation of the Cohesiveness of Injectable Ca-aluminate Based Materials in Water and Simulated Body Fluid During Curing

H. Spengler<sup>1</sup>, L. Hermansson<sup>1,2</sup> and H. Engqvist<sup>1,2</sup>

<sup>1</sup> *Doxa AB, Axel Johanssonsgata 4-6, 754 51 Uppsala, Sweden.* <sup>2</sup> *Materials Science Department, The Angstrom Laboratory, Uppsala University, Box 534, 751 21 Uppsala, Sweden.*

**INTRODUCTION:** Recently much attention has been paid cements for stabilizing osteoporotic vertebral compression fractures. The cements are injected into the compressed vertebrae. Most procedures are performed using PMMA, which however has some negative feature, e.g. high curing temperature and low osseointegration. The drawbacks with PMMA can be overcome by using a non-resorbable bioceramic calcium aluminate based material. The material is delivered as powder and liquid, which are mixed to a paste. The final properties of the hardened material are dependent on the amount of liquid added, the so-called liquid to powder ratio. When injected to the body the paste is also subjected to more liquid in the form of body fluid. Since the material is hydrophilic this can alter the surface composition of the material. There is also a possibility that chemical reactions with the body fluid can occur. This paper compares the surface reactions occurring on the calcium aluminate when injected into water or phosphate buffer solution (PBS).

**METHODS:** The media (i.e. water and PBS) were poured into glass containers and immersed into a 37 °C water bath for tempering. Calcium aluminate paste was prepared by adding liquid to the cement (placed in a capsule). The capsule was thereafter mechanically vibrated for one minute. One ml of cement paste was extruded into the different media at 3 minutes and 6 minutes after mixing.

Images of the extruded material in the media were taken after the material was set, i.e. > 15 minutes, using a digital camera. To analyse the composition of the “cloud” surrounding the material, the “cloud” was collected from the media using a syringe. The samples were evaporated at 110°C in glass beakers. The dried powders were collected on carbon tape and analysed with SEM/EDX.

**RESULTS:** In tap water a cloud is formed around the extruded material (3 minutes after mixing), see Fig. 1a. A smaller cloud forms when the cement is extruded into tap water at 6 minutes after mixing.

In PBS, the cloud seems to consist of agglomerates or flakes, see Fig. 1b.



Fig. 1: Photos of calcium aluminate extruded after 3 minutes into tap water (left) and PBS (right)

Regarding the composition of the cloud, the cloud formed in water showed traces of calcium aluminate constituents, see Fig. 2a. Note especially the presence of Zr (added in the form of ZrO<sub>2</sub> for radio-opacity). ZrO<sub>2</sub> is insoluble in water and thus only appear as grains. For the test in PBS, only ions from the PBS was present in the precipitates, see Fig. 2b. Also, on the surface of the set cement P could be found, indicating apatite formation.

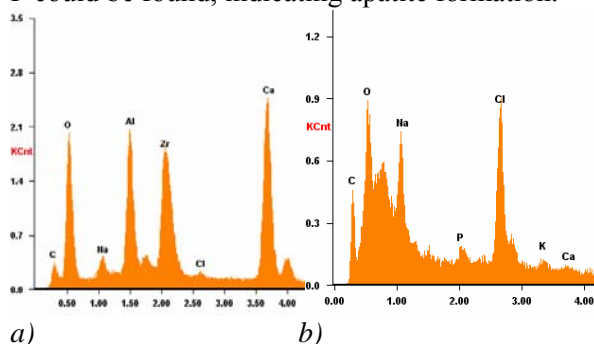


Fig. 2: Elemental composition of the collected powder (SEM/EDS) a) water and b) PBS.

**DISCUSSION & CONCLUSIONS:** A too high liquid to powder ratio leads to dissolution of the outer layer. In water with no flow, this results in precipitation of hydrates outside the surface. During setting the pH is increased, in the PBS this cause precipitation of salts. The salt ions in PBS form apatite at the cement surface, hindering further dissolution. The precipitations of salts or hydrates are strongly reduced when cement is injected at a later stage in the setting process. For a fully set material no precipitates can be seen.

**ACKNOWLEDGEMENTS:** Part of this work was financed by Göran Gustafsson Foundation for academic research.

# Fluoro-apatite and Calcium Phosphate Nanoparticles by Flame Synthesis

T. Brunner, S. Loher, W. J. Stark

*Institute for Chemical and Bioengineering, Department of Chemistry and Applied Biosciences, ETH Hoenggerberg, CH-8093 Zurich, Switzerland*

**INTRODUCTION:** Calcium phosphate biomaterials have attracted a tremendous interest in clinical medicine. Both hydroxyapatite (HAp,  $\text{Ca}_{10}(\text{PO}_4)_6(\text{OH})_2$ ) and tricalcium phosphate (TCP,  $\text{Ca}_3(\text{PO}_4)_2$ ) exhibit excellent biocompatibility and osteoconductivity [1, 2]. In the present study, calcium phosphate nanoparticles with a calcium to phosphorous molar ratio ranging from 1.43 to 1.67 have been synthesized by flame spray pyrolysis [3].

**METHODS:** Precursors of all materials have been prepared by correspondingly mixing calcium carboxylate with tributyl phosphate and optionally adding trifluoroacetic acid. The liquid mixtures were fed through a capillary into a methane/oxygen flame. Oxygen was used to disperse the liquid leaving the capillary (Fig. 1).

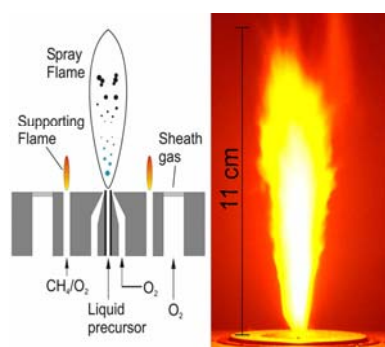


Fig. 1: (a) Sketch of the experimental set-up. (b) The burning spray of a calcium phosphate producing flame synthesis unit.

**RESULTS:** As-prepared calcium phosphate consists of amorphous nanoparticles with a primary particle size of 10-30 nm ( $\text{SSA}_{\text{BET}} \approx 90 \text{ m}^2/\text{g}$ ). Fourier transform infrared (FTIR) spectroscopy reveals the purity of the different calcium phosphates (Fig. 2). Phase pure  $\beta$ -tricalcium phosphate results from the sample with a slight excess of calcium ( $\text{Ca}/\text{P}=1.52$ ) after sintering at  $900^\circ\text{C}$ . Decreasing the  $\text{Ca}/\text{P}$  ratio provokes the formation of  $\beta$ -dicalcium pyrophosphate ( $\beta\text{-Ca}_2\text{P}_2\text{O}_7$ ). Sample  $\text{Ca}/\text{P}=1.67$  (HAp stoichiometry) shows the typical absorption spectra of HAp with the characteristic OH-stretching band at  $3572 \text{ cm}^{-1}$ . Substitution of hydroxyl entails a clear reduction in absorption

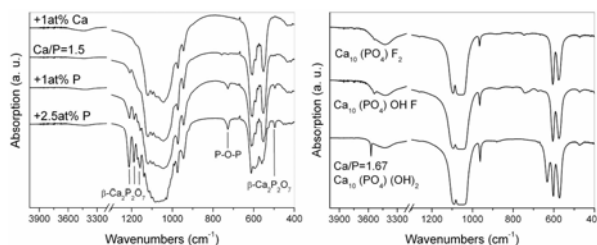


Fig. 2: FTIR spectra of calcium phosphates with increasing  $\text{Ca}/\text{P}$  ratio (left) and spectra of HAp and fluoro-apatite (right).

for said band indicating the ongoing replacement of OH-groups by fluoride.

Electron microscopy images of  $\text{Ca}/\text{P}=1.5$  nanoparticles after calcination at  $700^\circ\text{C}$  (Fig. 3a, b) and  $900^\circ\text{C}$  (Fig. 3c, d), respectively, display highly regular structure with interconnecting micropores suggesting good resorption properties.

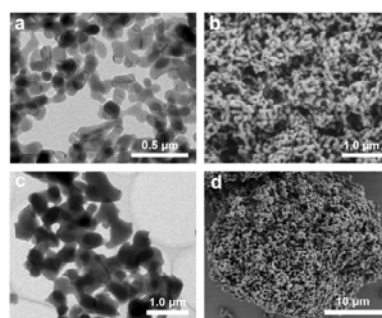


Fig. 3: TEM (left) and SEM (right) images of calcium phosphate.

**DISCUSSION & CONCLUSIONS:** Phase pure  $\beta$ -tricalcium phosphate, HAp, and fluoro-apatite can be easily accessed by flame spray pyrolysis. A high degree of flexibility in morphology, crystallinity and phase composition offer a versatile production tool to biomaterials engineering.

**REFERENCES:** <sup>1</sup> M. Jarcho (1981) *Clin. Orthop. Rel. Res.*:259-278. <sup>2</sup> K. de Groot (1983) in *Bioceramics of Calcium Phosphate* CRC Press. <sup>3</sup> S. Loher, W. J. Stark, M. Maciejewski, et al. (2005) *Chem Mater* 17:36-42.

**ACKNOWLEDGEMENTS:** This research was financially supported by the Swiss Commission for Technology and Innovation, Top Nano 21, 5978.2 and CTI 7021.2.

# Injectable PLGA Microsphere / Calcium Phosphate Cements: Physical properties and degradation characteristics

W.J.E.M.Habraken<sup>1</sup>, J.G.C.Wolke<sup>1</sup>, A.G.Mikos<sup>2</sup>, J.A.Jansen<sup>1</sup>

<sup>1</sup> Department of Periodontology and Biomaterials, Radboud University Nijmegen Medical Centre, The Netherlands <sup>2</sup> Department of Bioengineering, Rice University, Houston, USA

**INTRODUCTION:** Calcium Phosphate (CaP) cements show an excellent biocompatibility and often have a high mechanical strength, but in general degrade relatively slow. To increase degradation rates, macropores can be introduced into the cement, e.g. by the inclusion of biodegradable microspheres into the cement. The aim of this research is to develop an injectable PLGA microsphere/CaP cement with sufficient setting/cohesive properties and good mechanical/physical properties.

**METHODS:** PLGA microspheres were prepared using a w/o/w-double emulsion technique. The CaP-cement used was Calcibon<sup>®</sup>, a commercial apatite cement. 10/90 and 20/80 dry wt% PLGA microsphere/CaP cylindrical scaffolds were prepared as well as microporous cement (reference material). Injectability, setting time, cohesive properties and porosity were determined. Also, a 12-weeks degradation study in PBS (37°C) was performed.

**RESULTS:** Injectability of the cement decreased with an increase in PLGA microsphere content (Fig.1). Initial and final setting time of the PLGA/CaP samples was higher than the microporous sample. Porosity of the different formulations was 40.8% (microporous), 60.2% (10/90) and 69.3% (20/80). The degradation study showed distinct mass loss and a pH decrease of the surrounding medium starting from week 6 with the 10/90 and 20/80 formulations, indicating PLGA erosion. Compression strength of the PLGA microsphere/CaP samples decreased significantly in time, the microporous sample remained constant. After 12 weeks both PLGA/CaP samples showed a structure of spherical micropores (Fig. 2) and a compressive strength of 12.2MPa (10/90) and 4.3 MPa (20/80) was obtained. Signs of cement degradation were also found with the 20/80 formulation.

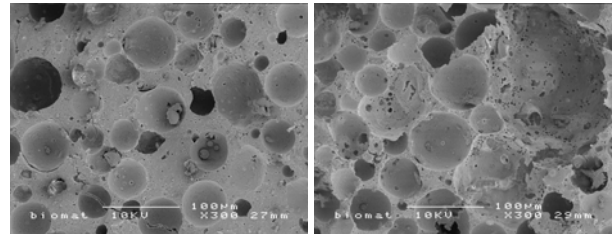


Fig. 1: Injectability graph of microporous CaP(◇), 10/90 PLGA/CaP(□) and 20/80 PLGA/CaP(Δ)

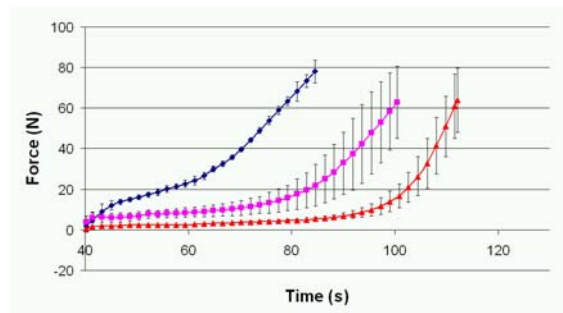


Fig. 2: SEM-micrographs of 10/90 (left) and 20/80 (right) sample at t= 12 weeks(orig. magn. 300x)

**DISCUSSION & CONCLUSIONS:** The addition of PLGA microspheres reduces injectability and increases setting time due to an extra absorption of water. Adding more liquid phase will improve injection properties, but also increases setting time and therefore an optimum must be found. After cement setting the PLGA/CaP structure often shows thin shells between two neighbouring spheres. Though these shells could form a barrier for bone ingrowth, they are very susceptible for degradation. This is due to a local high acid concentration caused by PLGA hydrolysis and increased porosity after the PLGA has disappeared.

**In conclusion:** all physical parameters are well within workable ranges with both 10/90 and 20/80 PLGA microsphere/CaP cements. After 12 weeks the PLGA is totally degraded and a highly porous, but strong scaffold remains.

# Calcium Carbonate Biphasic Cement Concept to Control Cement Resorption

C. Combes & C. Rey

*CIRIMAT UMR CNRS 5085, INPT-ENSIACET, Toulouse, France*

**INTRODUCTION:** Biodegradation and bioactivity properties of ceramics and cements have often been related to the solubility of their constitutive phases. The concept of biphasic calcium phosphate (BCP) ceramics based on an optimum balance between a sparingly soluble phase (hydroxyapatite) and more soluble phase (tricalcium phosphate) to control material resorption has however rarely been applied to control the resorption of ionic cements. Calcium carbonate and biomimetic apatites appear to be one of the most promising associations for bone filling and repair as biodegradation could be controlled by the proportion of the more soluble  $\text{CaCO}_3$  in the cement final composition. We present here a  $\text{CaCO}_3$ -CaP mixed cement concept based on the reactivity of bi- or tri-phasic mixtures of highly reactive calcium carbonate and calcium phosphate (CaP) leading to biphasic cements.

**METHODS:** When mixed with the appropriate amount of aqueous medium, mixtures of metastable crystalline  $\text{CaCO}_3$  (aragonite (Ar) and/or vaterite (V)), representing at least 40 % w/w of the solid phase, and amorphous or crystalline calcium phosphate (dicalcium phosphate dihydrate (DCPD) or amorphous tricalcium phosphate (TCPam)) powders can lead to cements with biphasic final compositions (Table 1). The setting and hardening occurred within 2 h at 37 °C in an atmosphere saturated with  $\text{H}_2\text{O}$ .

The samples were characterised by FTIR spectroscopy and X-ray diffraction analyses. The  $\text{CO}_3^{2-}$  content was determined by coulometry.

**RESULTS:** Depending on the initial carbonate/phosphate ratio, the final composition of cements can vary: mixing either DCPD or TCPam and vaterite mainly led to a mixture of poorly crystalline apatite phase (PCA) analogous to bone mineral and untransformed vaterite whereas only a very few amount of  $\text{CaCO}_3$  remained after the setting of (Ar+V+DCPD) mixtures (table 1 and fig. 1). The setting reaction appeared essentially related to the formation of a highly carbonated PCA phase ( $\cong 10$  %  $\text{CO}_3^{2-}$  for (Ar+V+DCPD) cement). The decrease of the total carbonate content after setting is related to the reaction of  $\text{HPO}_4^{2-}$  ions from DCPD or formed during the fast hydrolysis of

TCPam into a PCA phase on carbonate ions of vaterite and/or aragonite:

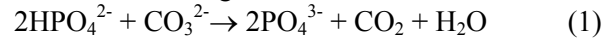


Table 1. Initial and final compositions of examples of  $\text{CaCO}_3$ -CaP mixed cements.

Initial powder mixture		Cement final composition	
Phases (w:w)	% $\text{CO}_3^{2-}$ (w/w)	Phase(s)	% $\text{CO}_3^{2-}$ (w/w)
V+DCPD (1:1)	30.0	PCA+V	17.5
V+TCPam (1:1)	30.0	PCA+V	21.2
Ar+V+DCPD (1:2:4)	26.7	PCA	10.0

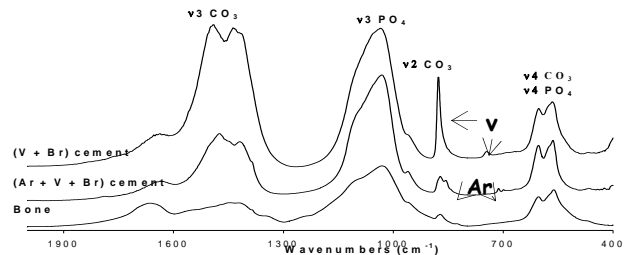


Fig. 1: FTIR spectra of examples of  $\text{CaCO}_3$ -CaP mixed cements after setting and hardening compared to bone FTIR spectrum.

**DISCUSSION & CONCLUSIONS:** The metastable  $\text{CaCO}_3$  (vaterite) in hardened cements is supposed to dissolve or transform into PCA rather rapidly after implantation and could thus determine the bioresorption of the cement. In addition, due to the presence of large amounts of  $\text{CaCO}_3$  which moderates the pH drop generated by PCA formation (stability of pH during cement formation), the cement paste could be associated with ions or biologically active molecules, able to promote tissue repair, and which could be progressively released. As biomimetic cements, *in vivo* biodegradation of such cement compositions releases non-cytotoxic metabolites that are under the control of the organism ( $\text{Ca}^{2+}$ ,  $\text{CO}_3^{2-}$  and  $\text{PO}_4^{3-}$  ions and/or  $\text{CO}_2$ ). Taking advantage of all these interesting features of biphasic  $\text{CaCO}_3$ -CaP mixed cements, we can control and adapt the final composition and consequently the cement biodegradation along with bioactivity properties.

# A New Injectable Calcium-strontium Phosphate Bone Cement and PLAGA Composite

G. Romieu, S. Munier, H. Garreau, M. Vert & P. Boudeville

Centre de Recherche sur les Biopolymères Artificiels *CRBA*, UMR-CNRS 547, Faculté de Pharmacie, 15 Avenue Charles Flahault, BP14491, 34093 Montpellier cedex 5, France

**INTRODUCTION:** Today, injectability, or cement ability to be injected with a syringe, is considered as an essential parameter together with mechanical strength or setting time, because it allows lower invasive surgery and an easier setting up. A new calcium phosphate bone cement containing strontium was developed, based on the partial replacement of calcium by strontium in a DCPD-CaO based-cement [1]. Strontium was incorporated because it plays an important role in osseous mineralization. It occurs naturally in bone mineral where it replaces easily calcium, stimulates osteoblast activity, inhibits partially osteoclast activity, enhances bone strength, increases hydroxyapatite solubility, is more radio-opaque than calcium and has a radio-active isotope. For these reasons, it is involved in osteoporosis treatment and radioactive  $^{89}\text{Sr}$  is used for treating osseous cancer. In this contribution, we wish to report on the properties of a novel organo-mineral composite that combines the injectable strontium-based cement and bioresorbable microspheres of the PLAGA type in order to produce potential macroporosities and allow drug loading.

**METHODS:** The cement paste was prepared by mixing DCPD + CaO + SrCO<sub>3</sub> in powder and a liquid phase with a pestle in a mortar for 30 s or by the push-pull technique between two syringes. The liquid phase was a  $\text{MH}_2\text{PO}_4 + \text{M}_2\text{HPO}_4$  buffer with  $\text{M} = \text{Na}^+$  (NaP) or  $\text{NH}_4^+$  (NH<sub>4</sub>P) pH 7, 0.75 M and the liquid-to-powder ratio (L/P) of 0.5 or 0.6 ml g<sup>-1</sup>. The injectability of the cement was quantified either by  $t_{100\%}$ , *i.e.* the time during which the cement is totally injectable at 22°C, using a variant of the technique proposed by Khairoun *et al.* [3] under the following conditions: paste 2 g, syringe 2.5 ml, opening 2 mm in diameter and 1 cm in length, constant strength 4 kg or by recording the injection strength during the injection at a constant rate [4], 1.5 ml during 15 s each 3 min, Instron 4444 machine, syringe 5 ml and needle 15 cm long and 2.3 mm in diameter.

**RESULTS:** The characteristics of the cement were: compressive strength CS = 20 ± 2 MPa, diametral tensile strength DTS ≈ 2 MPa, initial (I) and final (F) setting times I = 10-16 min and F = 14-19 min, volume expansion = 0.5 % and maximum temperature reached during setting ≤ 41.5°C in an adiabatic environment maintained at

37°C. The replacement of the NaP buffer by a  $\text{NaH}_2\text{PO}_4 + \text{Na}_2$  glycerophosphate buffer (NaGP) pH 6.7, 0.75 M or the inclusion of polymer microspheres (40%w/w) at the same L/P ratios did not influence the mechanical strength. Immersed in water or a 0.05 M, pH 7 NaP buffer 1 h after their preparation, cement samples (with or without polymer) did not disintegrate later on and released slowly but continuously strontium ions over 1 month (solution changed daily). The pH of the solution (unchanged over 1 month) did not exceed 8.6 (water) or 7.4 (NaP buffer).  $t_{100\%}$  was 9 ± 1 min. The injection strength was 22 N, at 25°C, 15 min after the cement preparation and 50 N at 37°C, 8 min after the cement preparation (Fig. 1).

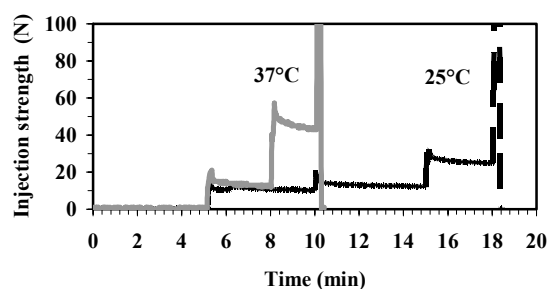


Fig. 1: Variations in injection strength over time during injection of the cement at 25 and 37°C in the same conditions as during vertebroplasty.

**DISCUSSION & CONCLUSIONS:** Considering both mechanical and rheological properties, without polymer microspheres this cement is fluid enough for vertebroplasty. With polymer microspheres, injectability is much lower but this composite is suitable for bone defect filling.

**REFERENCES:** : <sup>1</sup>H. El Briak, D. Durand, J. Nurit, S. Munier, B. Pauvert, P. Boudeville. (2002) *J Biomed Mater Res (Appl Biomater)*, **63**:447-453. <sup>2</sup>P. Boudeville, S. Munier, M. Vert. French patent (2004) Fr 0404714. <sup>3</sup>I. Khairoun, M.G. Boltong *et al.* (1998) *J Mater Sci Mater Med*, **9**:425-428. <sup>4</sup>M. Bohner, B. Gasser, G. Baroud, P. Heini. (2003) *Biomaterials* **24**:2721-2730.

## Anisotropic Bone Scaffolds

O. Zamoum<sup>1</sup>, O. Mecherri<sup>1</sup>, M. Fiallo<sup>2</sup>, P. Sharrock<sup>2</sup>

<sup>1</sup> *Laboratoire de Chimie Analytique, Université Mouloud Mammeri, Tizi Ouzou, Algérie.*

<sup>2</sup> *Laboratoire de Chimie Bioinorganique Médicale, Université Paul Sabatier, Castres, France.*

**INTRODUCTION:** Synthetic anisotropic tissue matrices are desirable for a wide variety of cases. Most non natural biomaterials are homogeneous in composition and structure while natural bone for example has cancellous and cortical parts which play different roles but are closely juxtaposed in the body. We report on the elaboration of a composite material based on hydroxylapatite and polylactic acid for the production of new materials with engineered properties.

**METHODS:** The polylactic acid (PLA) used was Galastic PABR-L-68 from Galactic (Brussels Biotech) which consists of 88% *l* lactic acid residues polymerized by a ring opening reaction of *l*-lactide. The hydroxylapatite (HA) was a fine powder form of less than 10  $\mu\text{m}$  size provided by MediCal calcium phosphates (Toulouse) which contained HA and 30% tricalcium phosphate. The solvent used was industrial grade chloroform stabilized with methanol. The porogen used was natural sea salt of fine and coarse particle sizes.

The samples were made by dissolving the desired amount of polymer in solvent overnight and thereafter introducing the required amount of minerals and mixing until a homogeneous paste was obtained. The desired amount of porogen was incorporated then the paste was placed in a mould with one open face and air dried at room temperature until solid. The extracted sample was further oven dried at 40°C before immersion in distilled water. Following salt dissolution the samples were again oven dried and rectified with sand paper.

**RESULTS:** Despite much effort we could not make a composite containing 75% HA. Samples were made containing 0%, 30%, 50% and 66% HA by weight. The composites containing more minerals were harder and dried more quickly than those containing more polymer. Collapse of the porous structures was observed when the composites were immersed in water before complete removal of solvent. The anisotropic samples were made by superimposing different layers in the mould before drying.

**DISCUSSION & CONCLUSIONS:** Functional coatings such as HA on Titanium promote surface bioactivity by modifying an inert substrate.

Similarly, organic molecules have been grafted on mineral surfaces<sup>1</sup> and organic structures have been mineralized in a biomimetic way<sup>2</sup>. Using HA and PLA as basic ingredients, we elaborated a series of composite and anisotropic materials based on these arranged as functional gradients. The objective was to ascertain the extent to which the gradients could be feasible. The 50% HA 50% PLA composite was made with intended porosities of 0% to 50%. Composites with lower porosities took longer to leach out the porogen but had better mechanical strength. An anisotropic sample was made by moulding three simultaneous layers of 0%, 35% and 50% porogen contents. Transverse observation of the material confirmed the presence of a strong base material intimately bound to a porous material of increasing porosity. Conversely, a cylindrical specimen was made with high interior porosity and high external strength. Such materials are intended to offer choices for resorption rates, for the inclusion of pharmaceutical principles, or the recolonisation or differentiation of cells<sup>3</sup>. We also realized a biomaterial with anisotropic composition. This specimen had a 50% HA porous composition on one side, and a porous 100% PLA composition on the other. Such a material could be advantageous for simultaneous osteoblast binding on one side together with chondrocyte development on the other. We believe solvent casting is unique in providing a means for polymer diffusion leading to strong binding between layers of different composition or structure. This allows the modulation of biomaterial strength. Contrary to sintered ceramics, metal screws can be fixed into the composites without fractures.

**REFERENCES:** <sup>1</sup> C. Zahraoui (1999) *Greffage de biomolécules sur un nouveau biomatériau à base d'hydroxylapatite-application aux implants osseux*, Thèse Université Paul Sabatier, Toulouse. <sup>2</sup> Y.F. Chouet al. (2004) *Biomaterials* **25**:5323-31. <sup>3</sup> D.Tadic et al. (2004) *Biomaterials* **25**:3335-40.

# Influence of Platelet-rich Plasma on Osteogenic Differentiation of Mesenchymal Stem Cells and Ectopic Bone Formation in Calcium Phosphate Ceramics

P.Kasten<sup>1</sup>, J.Vogel<sup>1</sup>, R.Luginbühl<sup>2</sup>, I.Beyen<sup>1</sup>, M.Bohner<sup>2</sup>, B.Gasser<sup>2</sup>, Richter,W<sup>1</sup>

<sup>1</sup>*Department of Orthopaedic Surgery, University of Heidelberg, Germany*

<sup>2</sup>*Robert Mathys Foundation, Bettlach, CH*

**INTRODUCTION:** Ceramics such as  $\beta$ -tricalcium phosphates ( $\beta$ -TCP, specific surface area  $< 0.5 \text{ m}^2/\text{g}$ ) or Calcium-deficient hydroxyapatite (CDHA, specific surface area  $48 \text{ m}^2/\text{g}$ ) can be combined with expanded mesenchymal stem cells (MSC) and growth factors to accelerate bone healing. In 1998, Marx and coworkers reported that adding platelet-rich plasma (PRP) to an autogenous cancellous bone graft resulted in a faster maturation rate and higher bone formation rate in alveolar defects. The aim of this study was to evaluate whether a combination of expanded MSC with PRP in resorbable calcium phosphate ceramics can promote osteogenesis and enhance ectopic bone formation in a SCID mouse model. We evaluated whether the effects of PRP depend on the type of carrier and the stage of osteogenic differentiation of the applied MSC.

**METHODS:** CDHA and  $\beta$ -TCP ceramic blocks were loaded with human MSC. Half of the specimens were treated with five-fold concentrated PRP. Furthermore, we compared undifferentiated MSC with MSC that were cultured under osteogenic conditions for 2 weeks *in vitro* on the scaffolds. Bone formation and osteogenic differentiation were evaluated by histology, alkaline phosphatase (ALP) enzyme activity, and osteocalcin (OC) content 4 and 8 weeks after ectopic implantation in SCID mice.

**RESULTS:** Ectopic bone formation was enhanced in MSC/CDHA (7/32) compared to MSC/ $\beta$ -TCP (2/30) composites; however, there was only a trend to more bone formation on CDHA after addition of PRP.

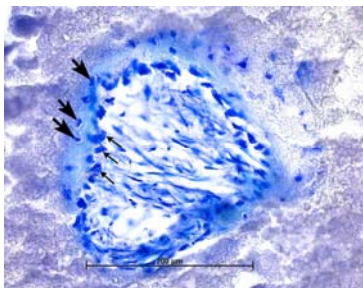


Fig. 1. Toluidine blue staining of a CDHA sample with PRP and undifferentiated MSC after 8 weeks shows bone formation in the outer parts of a peripheral

ceramic pore with osteoblasts (small arrows) and osteocytes (large arrows) (200 x magnification).

The addition of PRP to the composites increased the specific ALP activity significantly ( $P=0.006$ ) on CDHA, but on  $\beta$ -TCP a similar trend did not reach significance.

The specific ALP activity was significantly higher in MSC-loaded samples compared to empty scaffolds ( $p<0.001$ ) in CDHA and  $\beta$ -TCP ceramics. Mean ALP activity values were significantly higher in the undifferentiated MSC/ $\beta$ -TCP group compared with biocomposites subjected to osteogenic induction.

Although higher mean values of OC were obtained in cell-loaded CDHA with PRP versus without PRP, this difference did not reach significance. In contrast to  $\beta$ -TCP biocomposites, MSC/CDHA samples revealed a significantly higher OC content than the empty ceramic ( $P=0.031$ ) but no significant difference was seen between the undifferentiated and induced MSC/CDHA samples.

**DISCUSSION & CONCLUSIONS:** PRP in combination with MSC loaded on CDHA had a positive effect on osteogenic differentiation regarding ALP activity, but due to a large donor-dependent MSC variability a trend towards better ectopic bone formation did not reach significance. MSC/ $\beta$ -TCP groups failed to profit from the addition of PRP. In conclusion, the effect of PRP depended on the ceramic and the differentiation status of the MSC, however it did not clearly promote osteogenesis of human bone-marrow-derived MSC.

**ACKNOWLEDGEMENTS:** The study was supported by a grant of the Dr. h.c. Robert Mathys Foundation and an AO research grant.

# Disperse Cement Filling in Vertebroplasty May Reduce Risk of Secondary Tissue Damage

K. Sun<sup>1</sup>; E. Mendel<sup>2</sup>; L. Rhines<sup>2</sup>; A. Burton<sup>2</sup>; M. Liebschner<sup>1</sup>

<sup>1</sup> *Rice University, Houston, TX*, <sup>2</sup> *MD Anderson Cancer Center, Houston, TX*

**INTRODUCTION:** There is an increased risk of fracture in untreated adjacent vertebrae after PMMA vertebroplasty (abstract by Tawackoli et al). The compact distribution of PMMA within the vertebrae caused stress concentrations in the bone tissue directly above and below the PMMA, which altered the load transfer to the adjacent vertebrae [1-3]. We hypothesized that a more dispersed fill of the vertebrae with an alternative cement (CORTOSS, Orthovita, Inc.) will provide a more uniform structural reinforcement, alleviating the high stresses and minimizing stress-riser effects. The objective of this study was to determine the effects of cement distribution patterns and material properties on vertebral mechanics.

**METHODS:** An untreated, PMMA and CORTOSS treated specimen specific finite element models of the same fractured vertebral body (L4, female, 90 years old) were generated from postoperative quantitative computed tomography (QCT) scans (Fig 1). The three-dimensional compact fill pattern of PMMA from another vertebra was extracted through multiple X-ray projections. Uniaxial compression was simulated with intervertebral discs and alternatively potting cement to replicate an *in-vitro* experimental setup as boundary conditions. Cement material properties were also varied.

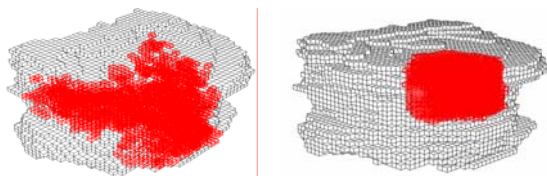


Fig 1: The dispersed fill pattern of CORTOSS (left) and compact fill pattern of PMMA (right) within the same vertebral body model.

**RESULTS:** The potting cement applied a uniform loading condition on the vertebral body, which resulted in the generation of stress-risers in the bone elements directly above and below the PMMA cement. Stress concentrations were absent in the CORTOSS treated model with either potting cement or intervertebral discs (Fig 2).

Vertebral stiffness augmentation under disc boundary conditions was higher with the dispersed

cement fill pattern with CORTOSS than with a compact cement fill pattern with PMMA for the same volume of cement (Fig 3).

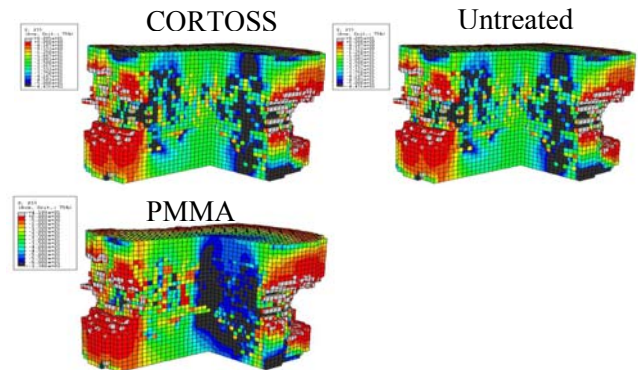


Fig 2: Stress distribution in the untreated, CORTOSS and PMMA treated models potted with PMMA. Higher stresses in blue.

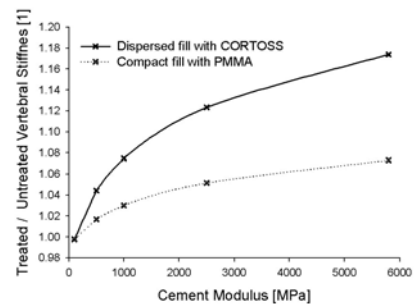


Fig 3: The effect of cement distribution patterns under different cement moduli.

**DISCUSSION & CONCLUSION:** The minimal intravertebral stress-risers with a dispersed cement fill may indicate a lowered risk of subsequent damage in the adjacent untreated vertebrae. The higher stiffness augmentation with a dispersed cement distribution pattern implies that a smaller cement volume fill would achieve the same level of augmentation than a compact fill, possibly reducing the risk of complications from cement leakages.

**ACKNOWLEDGMENTS:** Thanks to Orthovita, Inc. and Alistair Templeton.

**REFERENCES:** <sup>1</sup> Baroud, G., et al. (2003) *Eur Spine J*, **12**:421-6. <sup>2</sup> Polikeit, A., et al. (2003) *Spine*, **28**:991-6. <sup>3</sup> Sun, K. and Liebschner, M. (2004) *Ann Biomed Engin*, **32**:77-91.

**Session C:**  
**Drug Delivery**  
**Applications**

**Keynote Lectures**

Jeff Hollinger, DDS, PhD  
University of Maryland

Thierry Stoll, MSc  
Synthes

# In Vitro Study Of BMP-2 Gene Transfected Bone Marrow Derived Mesenchymal Stem Cells In APA microcapsules

T.T.Tang<sup>1</sup>, H.F.Ding<sup>1</sup>, R.Liu<sup>2</sup>, B.G.Li<sup>2</sup>, C.F.Yu<sup>1</sup>, J.R.Lou<sup>3</sup>, K.R.Dai<sup>1</sup>.

<sup>1</sup>Department of Orthopedic Surgery, Shanghai Ninth People's Hospital, Shanghai Jiaotong University School of Medicine, Shanghai, China. <sup>2</sup>Cryogenics and Foodstuff Refrigeration Research Centre, Shanghai University of Science and Technology, Shanghai, China. <sup>3</sup>Shanghai Institute of Biological Products, Shanghai, China.

**INTRODUCTION** An alternative approach to somatic gene therapy is to deliver a therapeutic protein by implanting non-autologous recombinant cells that are immunologically protected from graft rejection with alginate microcapsules. This study is to investigate the in vitro characterization of BMP-2 gene modified bone marrow derived mesenchymal stem cells(MSCs) encapsulation in alginate.

**METHODS:** An electrostatic droplet generator was employed to produce BMP-2 or  $\beta$ -gal (control gene) gene modified MSCs encapsulated in alginate-poly-L-lysine alginate (APA) microcapsules. The viability of the encapsulated cells was demonstrated by the X-gal staining. The BMP-2 proteins secreted from the encapsulated gene modified stem cells were determined by the ELISA methods. An co-culture system (fig.1) was used to evaluate the effects of gene products from the microcapsules on the non-gene modified MSCs.

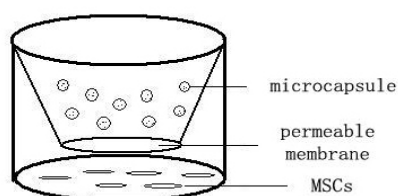


Fig.1: Co-culture system: permeable membrane (pore size:7 $\mu$ m) permits diffusion of media components

**RESULTS:** The X-gal staining of the encapsulated cells were still positive 28 days after encapsulation(fig.2). The secreted BMP-2 proteins could be detected 30 days after encapsulation(fig.3). The ALP activity in co-cultured MSCs was higher than it was in control group with statistical significant difference( $P < 0.05$ ) which indicated that the gene products could induced the MSCs differentiated into the osteoblast.

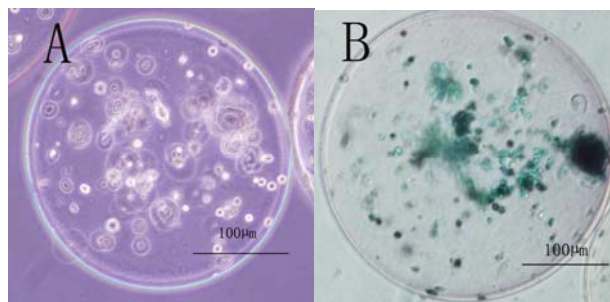


Fig.2: A:microcapsule with good shape.B:X-gal staining at the 28th day after microencapsulation

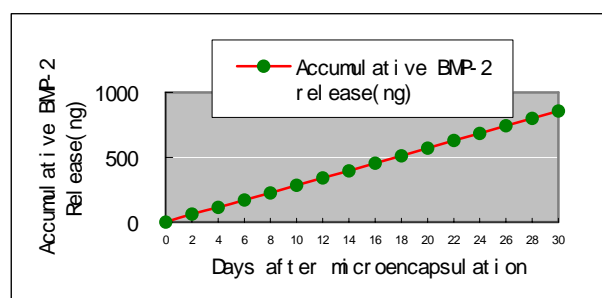


Fig.3: Accumulative BMP-2 release from the encapsulated cells

**DISCUSSION & CONCLUSIONS:** The results demonstrated that the gene modified cells could survive in the APA microcapsules and were capable of a constitutive synthesis and delivery of biologically active BMP-2 proteins for at least 28 days and thus are of potential utility for enhancement of bone repair and bone regeneration. Both in vitro and in vivo study is needed to evaluate the immuno-isolation effect of the microcapsules in the future.

**ACKNOWLEDGEMENTS:** This research was supported by grants from Shanghai Science and Technology Development Fund (No. 05JC14034)

# Fibrin-Fibronectin Sealing System in Combination with Beta-Tricalcium Phosphate as a Carrier for Recombinant Human Bone Morphogenetic Protein-2: Effects on Bone Formation in Rat Calvarial Defects

J.-Y. Hong<sup>1</sup>, S.-J. Hong<sup>1</sup>, S.-W. Jung<sup>1</sup>, Y.-J. Um<sup>1</sup>, S.-B. Lee<sup>1</sup>, K.-S. Cho<sup>1,2</sup>, C.-S. Kim<sup>1,2</sup>

<sup>1</sup>*Department of Periodontology, Research institute for periodontal regeneration, College of dentistry, Yonsei University, Seoul, Korea* <sup>2</sup>*Department of Periodontology, Research institute for periodontal regeneration, College of dentistry, Brain Korea 21 project for Medical Science, Yonsei University, Seoul, Korea*

**INTRODUCTION:** Bone morphogenetic proteins (BMPs) are being evaluated as potential candidates for periodontal and bone regenerative therapy. In spite of good prospects for BMP applications, an ideal carrier system for BMPs has not yet been identified. The purpose of this study was to evaluate the osteogenic effect of a fibrin-fibronectin sealing system (FFSS) combined with Beta-tricalcium phosphate (Beta-TCP) as a carrier system for rhBMP-2 in the rat calvarial defect model.

**METHODS:** Eight-mm critical-size calvarial defects were created in 100 male Sprague-Dawley rats. The animals were divided into 5 groups of 20 animals each. The defects were treated with rhBMP-2/FFSS, rhBMP-2/FFSS/ Beta -TCP, FFSS and Beta-TCP carrier control or were left untreated as a sham-surgery control. Defects were evaluated by histologic and histometric parameters following a 2- and 8-week healing interval (10 animals/group/healing intervals).

**RESULTS:** The FFSS/ Beta-TCP carrier group was significantly greater in new bone area (Table 1) at 2 weeks ( $p < 0.05$ ) and augmented area at 2 and 8 weeks ( $p < 0.01$ ) relative to the FFSS carrier group. New bone area (Table 1) and augmented area in the rhBMP-2/FFSS/ Beta -TCP group were significantly greater than in the rhBMP-2/FFSS group at 8 weeks ( $p < 0.01$ ). On histologic observation, FFSS remnants were observed at 2 weeks, but by 8 weeks, the FFSS appeared to be completely resorbed. rhBMP-2 combined with FFSS/ Beta-TCP produced significantly more new bone formation and augmentation in this calvarial defect model.

Table 1. New bone area (group means  $\pm$  SD; n=9, mm<sup>2</sup>)

	2 weeks	8 weeks
Sham-surgery control	0.2 $\pm$ 0.1	0.4 $\pm$ 0.1 <sup>□</sup>
FFSS	0.4 $\pm$ 0.2	2.3 $\pm$ 0.7 <sup>*□</sup>
FFSS/ $\beta$ -TCP	1.4 $\pm$ 1.2 <sup>*¶</sup>	2.1 $\pm$ 0.3 <sup>*□</sup>
rhBMP-2/FFSS	2.6 $\pm$ 0.6 <sup>*¶†</sup>	3.4 $\pm$ 0.5 <sup>*¶†□</sup>
rhBMP-2/FFSS/ $\beta$ -TCP	2.8 $\pm$ 1.4 <sup>*¶†</sup>	5.3 $\pm$ 2.1 <sup>*¶†‡□</sup>

\*: Statistically significant difference compared to surgical control group ( $P < 0.05$ )

¶: Statistically significant difference compared to FFSS group ( $P < 0.05$ )

†: Statistically significant difference compared to FFSS/ $\beta$ -TCP group ( $P < 0.05$ )

‡: Statistically significant difference compared to rhBMP-2/FFSS ( $P < 0.01$ )

§: Statistically significant difference compared to 2 weeks ( $P < 0.05$ )

**DISCUSSION & CONCLUSIONS:** FFSS/ Beta -TCP may be considered as an available carrier for rhBMP-2.

**REFERENCES:** <sup>1</sup>Chang-Sung Kim, Joon-Il Kim, Jin Kim, Seong-Ho Choi, Jung-Kiu Chai, Chong-Kwan Kim, Kyoo-Sung Cho(2005) Ectopic Bone Formation of Recombinant Human Bone Morphogenetic Proteins -2 using Absorbable Collagen Sponge and beta Tricalcium Phosphate as Carriers; *Histological and Immunohistochemical evaluation. Biomaterials* 26(15):2501-2507. <sup>2</sup>Suk-Ju Hyun, Dong-Kwan Han, Seong-Ho Choi, Jung-Kiu Chai, DDS, Kyoo-Sung Cho, Chong-Kwan Kim, Chang-Sung Kim (2005) The Effect of Recombinant Human Bone Morphogenetic Protein-2, 4 and 7 on Bone Formation in Rat Calvarial Defect. *Journal of Periodontology* ;76:1667-1674.

# An Injectable Composite of Osteogenic Protein-1 (OP-1, rhBMP-7) and Hydroxyapatite Enables Early *In Vivo* Cement Stabilization and Biointegration. A Controlled, Randomized Study in the Sheep Spine.

T.R.Blatter<sup>1</sup>, W.Schmölz<sup>2</sup>, A.Weckbach<sup>3</sup>, C.Toth<sup>4</sup>, L.Claes<sup>2</sup> & H.-J.Wilke<sup>2</sup>

<sup>1</sup> Clinic for Trauma, Reconstructive, and Plastic Surgery, Leipzig University, Leipzig, D. <sup>2</sup> Institute of Orthopaedic Research and Biomechanics, Ulm University, Ulm, D. <sup>3</sup> Clinic for Trauma and Reconstructive Surgery, Würzburg University, Würzburg, D. <sup>4</sup> Stryker Biotech, Hopkinton, Massachusetts, USA

**INTRODUCTION:** Lumbar interbody fusion by means of hydroxyapatite- or calcium phosphate-cements proved to be unsuccessful in clinical and experimental settings. Since these biomaterials cannot withstand shear and bending forces, fracture and subsequent fragmentation of the biomaterials will result along with final resorption of the debris [1].

Objective of this *in vivo* study was to investigate the ability of OP-1 to induce osseous stabilization of a hydroxyapatite-cement early enough to prevent it from fragmentation and resorption thus enabling integration of the biomaterial and spinal fusion. For this reason, an injectable composite of di-/tetra-hydroxyapatite and microencapsulated OP-1 (2.2 mg) was developed.

**METHODS:** Endpoints of this controlled, randomized, prospective study were total cement leftover, radiographic interbody fusion rates, and biomechanical properties at 8 weeks post op. In 14 sheep, L4/L6 were instrumented posteriorly with an internal fixator, intervertebral disc L4/L5 was removed under transpedicular endoscopic control, and end plates L4/L5 were decorticated. In 7 randomly assigned sheep, the created defect in L4/L5 was then augmented transpedicularly with the composite (HA-OP-1). The remaining 7 animals were treated with the hydroxyapatite cement without OP-1 (HA).

Following euthanasia, the ratio between total volume of cement leftover ( $V_{8weeks}$ ) and total volume of cement initially applied ( $V_{0weeks}$ ) was measured by means of CT-assisted volumetry. Fusion rates were evaluated radiologically (plain X-ray and CT). Range of motion and neutral zone were determined by biomechanical testing applying pure moments of  $\pm 3.75$  and  $\pm 7.5$  Nm in each principle motion plane.

**RESULTS:**  $V_{8weeks}/V_{0weeks}$  was significantly higher in the HA-OP-1 group ( $p=0.007$ ):  $79.9\% \pm 13.8\%$  (HA-OP-1) versus  $54.0\% \pm 6.8\%$  (HA).

Radiomorphologic evaluation of the HA group revealed gross fragmentation of the formerly solid cement mass, especially within the interbody space along with loss of contact at the bone-cement interface. In contrast, cement masses in the HA-OP-1 group remained solid. Radiographic fusion rate was 5/7 in the HA-OP-1 group versus 0/7 in the HA group ( $p=0.002$ , Wilcoxon-test).

Biomechanical testing, however, could not show an improvement of the stability in the segments treated with OP-1:

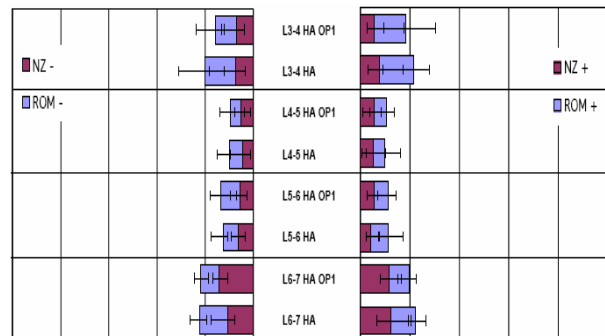


Fig. 1: Median values for range of motion (ROM) and neutral zone (NZ) during lateral bending upon  $\pm 3.75$  Nm (posterior instrumentation dismantled).

## DISCUSSION & CONCLUSIONS:

Biointegration of the osteoconductive carrier without OP-1 does not occur, since shear and bending forces cause early cement fracture with subsequent fragmentation and gross resorption. In contrast, the osteoinductive effect of OP-1 enables early callus sheathing and *in vivo* stabilization of the composite resulting in biointegration and radiographic spinal fusion in 5/7 cases. The initial layers of bridging bone, however, proved to be still fragile at 8 weeks post op. to withstand biomechanical forces.

**REFERENCES:** <sup>1</sup> T.R. Blatter, G. Delling, A. Weckbach (2003) *Eur Spine J* 12:216-23.

**ACKNOWLEDGEMENTS:** This research was supported by Deutsche Forschungsgemeinschaft

# Mineral/Organic Composite Bone Grafts: Characterization and Evaluation as Drug Delivery Systems

S. Girod<sup>1</sup>, H. Ternet<sup>1</sup>, M. Frèche<sup>2</sup>, J.L. Lacout<sup>2</sup>, F. Rodriguez<sup>1</sup>.

<sup>1</sup>Université Paul Sabatier, GEFSOD E.A. 2631, Faculté Sciences Pharmaceutiques, Toulouse, FR. <sup>2</sup> CIRIMAT, C.N.R.S. U.M.R. 5085, ENSIACET-INP, Toulouse, FR

**INTRODUCTION:** Calcium phosphate cements are widely used in hard tissue repair because of their moldability and in-situ self-hardening ability to form hydroxyapatite [1]. The aim of our study was to test the ability of pectin microspheres to be incorporated into a calcium phosphate cement, to characterize the resulting composites and evaluate their potentiality as drug delivery systems.

**METHODS:** Pectins presenting various esterification (DE) and amidation (DA) degrees (CP Kelco), were used to prepare microspheres by ionotropic gelation with calcium ions. The resulting microspheres were characterized in terms of morphology, size distribution and pH sensitivity (seen by swelling in pH conditions mimicking those occurring in the cement while setting and hardening). Their efficiency of encapsulation of an anti-inflammatory drug, ibuprofen, was also tested. Then pectin microspheres were incorporated into extemporaneous calcium phosphate cement (Cementek, Teknimed) [2]. The influence of the pectin/cement (P/C) weight ratio on the setting, mechanical properties and chemical evolution of the cement were studied. Then, the composite ability to release ibuprofen was evaluated by comparing microspheres alone and included into the cement.

**RESULTS:** All the pectin samples tested allowed to obtain microspheres with a spherical shape and a smooth surface (Figure 1).

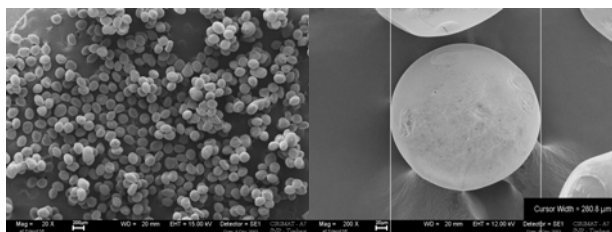


Fig. 1: Morphology of microspheres obtained from a pectin with a DE30% and a DA of 19%.

Their size distributions were monomodal, centered on 250 µm. According to pectins DE and DA, various pH sensitivities were observed. A pectin with medium swelling properties, a DE of 30% and a DA of 19%, was chosen to be incorporated into

the cement. According to formulation tests, an incorporation ratio of pectin microspheres ranging from 0 to 6% w/w allowed to obtain composites with maintained malleability and cohesion. The setting times of the resulting composites diminished according to pectin ratio but remained compatible with a surgical implantation. The crystalline evolution of the mineral part of the composites was slowed but not prevented. In terms of release properties, the composites allowed a controlled liberation of ibuprofen, due to pH variation and consecutive pectin microspheres degradation. After one month, microspheres were completely degraded: macropores appeared into the cement structure (Figure 2).

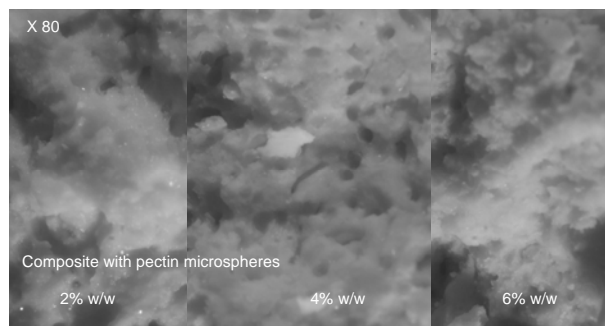


Fig. 2: Optical microscopy on composites after 1 month in water (original magnification: x80).

**DISCUSSION & CONCLUSIONS:** Pectin microspheres inclusion into calcium phosphate cement seems promising. P/C ratio and pectin type (in terms of DE and DA) appear to be key parameters which can modulate the resulting composite properties in terms of release properties and final macroporosity. In vivo tests on rabbits are under investigation to verify the potential of these composites.

**REFERENCES:** <sup>1</sup>M. Bohner et al (2005) *Biomaterials* 26:6423-29. <sup>2</sup>J.L. Lacout et al (1998) patent n° 98.03459

**ACKNOWLEDGEMENTS:** The authors wish to thank TEKNIMED Society for its participation

## **Session D:**

# **Live Surgery Clinical Experiences**

## **Surgeon**

Paul Heini, MD  
Inselspital, University of Bern

# Three Years Experience with Standalone Kyphoplasty and Calcium Phosphate Cement in Traumatic Fractures

G.Maestretti, C.Cremer, P. Otten

*Department of Orthopaedic Surgery, Kantonspital Fribourg, Fribourg, Switzerland*

**STUDY DESIGN:** Prospective study to investigate the clinical and radiological results of balloon kyphoplasty and cement augmentation with Calcium Phosphate in traumatic fractures.

**OBJECTIVES:** Evaluation of radiological and computer tomography results, VAS, Roland Morris score and complications in 28 patients with acute traumatic compression fractures type A, treated with a standalone balloon kyphoplasty and cement augmentation with calcium phosphate (Calcibon™). Follow-up time at a mean of 30 month (24-37 months).

**METHODS:** From August 2002 to August 2003, 28 patients with traumatic compression fracture (Magerl type A) without neurological deficit consecutively underwent 33 balloon kyphoplasties with Calcibon™. We report here the pre, postoperative and the follow-up results (12, 24 months), applying the visual analogue scale VAS (0-10) for pain rating, the Roland Morris (0-24) disability score, CT-scan examination, detailed radiographic evaluation of vertebral body deformity and segmental kyphosis measurement. The preoperative X-ray measurements, VAS and the 7 days Roland Morris scores are compared with the 1 and minimum 2 years follow-up findings.

**RESULTS:** The mean initial vertebral deformity (VB kyphosis) was 17°, corrected to a postoperative of 6°. We noted a loss of correction at (the minimum) two years follow-up in comparison to the postoperative standing X-ray at 24 h of 3° vertebral deformity and 3° segmental kyphosis. The VAS score demonstrates a decrease over time from a mean of 8,7 to 3,1 at seven days and to 0,8 at the last follow-up. The Roland Morris disability score demonstrates a similar improvement. We noticed no major complications related to the procedure. All patients with vertebral fractures as sole medical problem were discharged within 48 hours. All active patients returned to work within 3 months.

**CONCLUSIONS:** Balloon kyphoplasty is an alternative mini-invasive technique to reduce the height of vertebral body in acute fractures. The utilisation of Calcium Phosphat Cement (Calcibon™) is recommended only in fractures type A1 and A3.1 due to the intrinsic characteristic of this biological cement. With this indication, our preliminary results demonstrate a new feasible, seemingly safe treatment of this kind of fracture, allowing a rapid treatment of pain, early discharge and return to normal activities.

# Limited Suitability of Calcium Phosphate in the Treatment of Osteoporotic Vertebral Body Fractures – A Prospective, Randomized, Clinical Trial of Percutaneous Balloon Kyphoplasty Comparing Calcium Phosphate Versus Polymethylmethacrylate

T.R.Blatter<sup>1</sup>

<sup>1</sup> *Clinic for Trauma, Reconstructive, and Plastic Surgery, Leipzig University, Leipzig, D.*

**INTRODUCTION:** In kyphoplasty and vertebroplasty, polymethylmethacrylate (PMMA) currently represents the standard augmentation material. It is characterized, however, by a lack of osteointegration and its limited biocompatibility.

**METHODS:** This prospective, randomized trial investigated the feasibility of calcium phosphate (CaP) for augmentation of osteoporotic vertebral body fractures by means of percutaneous balloon kyphoplasty in comparison to PMMA. Inclusion criteria were osteoporotic fractures of vertebral bodies in the thorocolumbar spine, patient age  $\geq 65$  years, and fracture age  $\leq 4$  months. Exclusion criteria were tumor lesions and additional posterior instrumentation.

**RESULTS:** A total of 60 osteoporotic vertebral body fractures in 56 patients were included. CaP and PMMA were randomly applied in 30 cases each. All 60 fractures were classified type A (acc. to Magerl et al.). Of these, 19 were classified type A3.

52/56 patients experienced p.op. pain relief ( $2.1 \pm 1.9$  to  $8.2 \pm 1.5$  on a Visual Analogue Scale from 0

“worst” to 10 “best”). Endplate angles were restored by  $6.2^\circ \pm 2.9$  on average. For both parameters (pain relief and restoration of endplate angle), no statistically significant difference was found between the groups.

Cement-specific complications were vascular embolism using PMMA (n=2); subtotal “cement-washout” using CaP (n=1); and substantial loss of correction on radiographs 6 weeks p.op. due to cement failure in all fractures type A3, if CaP had been applied (n=9). There was no case of cement failure, when PMMA had been used.

**DISCUSSION & CONCLUSIONS:** Currently in kyphoplasty, a routine use of CaP cannot be recommended. Due to its minor resistance to bending, extension, and shear forces compared to PMMA, there is a high risk for cement failure and subsequent loss of correction in the well defined

clinical setting of osteoporotic vertebral body fractures type A3.

## **Session E:**

### **In Vivo Studies**

#### **Keynote Lectures**

Jörg Krebs, DVM  
University of Bern

Georg Watzek, MD, PhD  
Medical University of Vienna

# A New Concept of Antibiotic Loaded HAP/TCP Bone Substitute for Prophylactic Action: ATLANTIK Genta – In Vivo Study

A.Bignon<sup>1</sup>, E.Viguiier<sup>2</sup>, F.Laurent<sup>3</sup>, D.Goehrig<sup>4</sup>, G.Boivin<sup>4</sup>, J.Chevalier<sup>5</sup>

<sup>1</sup> *MEDICAL BIOMAT, Vaulx-en-Velin, FR.* <sup>2</sup> *EA3090, ENVL, Marcy l'étoile, FR.* <sup>3</sup> *UMR CNRS 5557 – Ecologie Microbienne, Lyon, FR.* <sup>4</sup> *INSERM U403, Université Claude Bernard Lyon I, Lyon, FR.* <sup>5</sup> *UMR CNRS 5510, GEMPPM, Villeurbanne, FR.*

**INTRODUCTION:** Infections and their consequences are a considerable problem in orthopedic surgery. Despite systemic prophylaxis, infection rates after orthopedic surgery are above 1%. Antibiotic loaded PMMA bone cements have been shown to enhance the efficiency of intravenous prophylactic treatments for total hip replacement<sup>1</sup>. However, less than 10% of the load is released during the first 5-10 days of implantation<sup>2</sup>: the remaining antibiotic is released at low levels over many months<sup>3</sup> and could select antibiotic-resistant strains<sup>2</sup>. The recommendations for the use of antibiotic in prophylactic applications are to obtain high levels, with treatment duration inferior to 48 hours. A new HAP/TCP bone substitute loaded with 125 mg of Gentamicin was designed for prophylactic use in bone filling applications. Its aim was to enhance the efficacy of systemic prophylactic treatments by increasing the local antibiotic concentration without selecting resistant strains.

**METHODS:** A commercial bone substitute composed of 70% Hydroxyapatite and 30%  $\beta$ -Tricalcium Phosphate<sup>4</sup> containing 125 mg of Gentamicin (ATLANTIK Genta, Medical Biomat, France) was used in this study. The release rate of Gentamicin from the bone substitute was investigated after implantation in the femoral condyle of 5 sheep. In order to investigate the local and systemic Gentamicin concentrations, synovial fluids and blood samples were assessed by immunoassay over a 5 day period.

**RESULTS:** The mean Gentamicin concentration peak obtained in blood was 4.2  $\mu\text{g/ml}$  and the mean local Gentamicin concentration obtained in synovial fluids during the first 8 hours was 305  $\mu\text{g/ml}$ . There were differences in local Gentamicin concentrations between individuals but for all animals, the local Gentamicin concentrations measured during the first 8 hours were higher than the minimal bactericidal concentration of the majority of the germs responsible for infections in orthopedic surgery, *i.e.* 6-12  $\mu\text{g/ml}$ . After 48 hours, the concentration in blood and synovial fluids was less than

0.5  $\mu\text{g/ml}$ . The Gentamicin amount remaining in the implant explanted at day 8 was less than 0.003% of the initial amount.

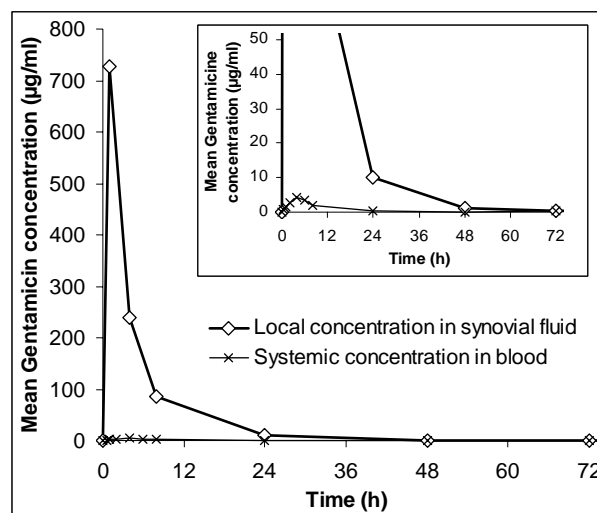


Fig. 1: Mean Gentamicin concentrations in synovial fluid and blood measured after implantation of ATLANTIK Genta bone substitute in the condyle of femur of 5 sheep.

**DISCUSSION & CONCLUSIONS:** Local delivery of antibiotics has the advantage of achieving high local levels of the drug with little risk of systemic toxicity, whereas systemic antibiotics have a low penetration in bone tissues. In this study, the gentamicin release rate from the HAP/TCP bone substitute fits the recommendations for prophylaxis: high levels of antibiotic for a maximum duration of 48 hours. Gentamicin loaded HAP/TCP bone substitutes should be an effective prophylactic tool in orthopedic surgery if combined with systemic prophylaxis.

**REFERENCES:** <sup>1</sup> L.B. Engesaeter, et al (2003) *Acta Orthop Scand* **74**(6):644-51. <sup>2</sup> H. van de Belt, D. Neut, W. Schenk, et al (2001) *Acta Orthop Scand* **72**(6):557-71. <sup>3</sup> F. Langlais, L. Bunetel, A. Segui, et al (1988) *Rev Chir Orthop Reparatrice Appar Mot* **74**(6):493-503. <sup>4</sup> A. Bignon, J. Chouteau, J. Chevalier, et al (2003) *J Mater Sci Mater Med* **14**(12):1089-97.

# A Poly (D, L-lactide) /Allogenic Bone Composite for Bone Tissue Engineering

Q.Li, C.Zhou

*Biomaterials Research Lab, Material Science and Engineering Department, Jinan University  
Guangzhou, 510632, PR China*

**INTRODUCTION:** Porous polymer composites are one of the most heated research topics for bone tissue engineering. In vitro and vivo tests demonstrated that porous composites can be used as the matrices for bone cell growth and differentiation, and showed that composites had better osteoconductivity compared with the porous polymers alone<sup>1</sup>. Allogenic bone has been used very widely for the bone defect treatments. In this study, a novel PLA (poly D, L-lactide) /allogenic bone composite was prepared by a novel method—supercritical carbon dioxide fluid technology ((SC-CO<sub>2</sub>-FT).

**METHODS:** The PLA (poly D, L-lactide) /allogenic bone composite was prepared with PLA (Mn=1 ×10<sup>4</sup>, diameter=150μm-200μm) and allogenic bone (diameter=80μm-100μm) mixed with NaCl(diameter=100μm -200μm ).After PLA, allogenic bone and NaCl were homogeneously mixed ,the mixture was placed in a disk mold and then put into supercritical carbon dioxide equipment at 20mpa,35° for 30 minutes, with the exposure time of less than 15 minutes. The NaCl was subsequently removed from the composites by leaching the composite in the distilled water with shaking for 48 hours, with the water changed every 8 hours, and then the composites were dried under the vacuum.

**RESULTS:** The composites were determined by scanning electron microscopy, porosity analysis and vivo implantation studies. The results showed that the pore formed by SC-CO<sub>2</sub> technique was appropriate to be used as materials, the materials had a interconnected porous structure, the porosity was over 80%, furthermore, the most outstanding virtues of these composites were that a large number of micropores (diameter=10-20μm) were generated on the tri-dimensional pores surface while avoiding the use of organic solvent. The vivo tests results also showed that the well-formed tissue grown homogeneously in the composite, in addition the allogenic bone of the composite had been absorbed slowly along with the PLA degrading.

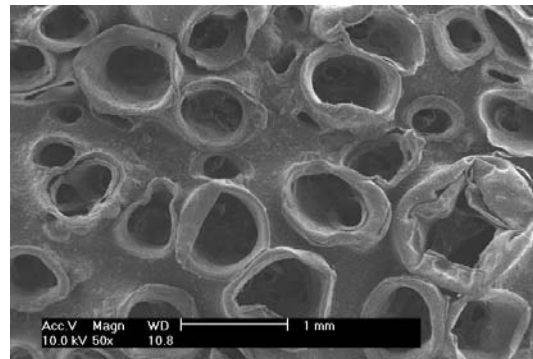


*Fig. 1: SEM of the PLA/allogenic bone composites*

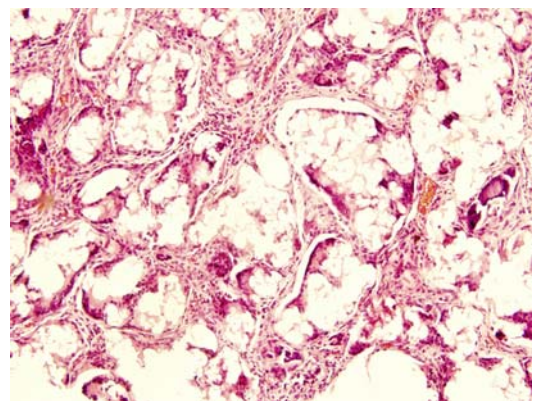


*Fig. 2: Histological studies of PLA /allogenic bone composite explanted from the mice at 4 weeks.*

**DISCUSSION & CONCLUSIONS:** The results indicated that the processes and the novel composites were both feasible, and the results also demonstrated that the composites had the potential for integration with bone. The clinic use of the novel PLA/allogenic bone composites biomaterial prepared by SC-CO<sub>2</sub>-FT will be awaited for the further research.

**REFERENCES:** <sup>1</sup> Kai Zhang, Yunbing Wang, Marc A. Hill Myer, Lorraine F. Francis. Processing and properties of porous poly (D, L-lactide)/ bioactive glass composites. *Biomaterials* 2004; 25: 2489-250

**ACKNOWLEDGEMENTS:** National Natural Science Foundation supported this work, we thank for Nanfang Medical University for donating the allogenic bone

# Enhanced Osseointegration of Bone-implant Interface by BMP-2 Gene Medication

K.R.Dai, M.Yan, T.T.Tang

*Department of Orthopaedics, Ninth People's Hospital, Shanghai Jiaotong University School of Medicine, Shanghai, P.R. China*

**INTRODUCTION:** The purpose of the study is to investigate the effects of BMP-2 gene therapy for the reconstruction of peri-implant bone defect and peri-implant osteolysis on the bone-implant interface.

**METHODS:** A 3mm bone defect around Ti alloy implant was created in bilateral lateral femur condyle of 18 adult Beagle dogs. (1) In the 28 defects of 14 dogs, two defects were left empty as blank group. By means of impaction grafting technique, the other 26 defects were filled with freeze-dried allograft, freeze-dried allograft loading autogenous bone marrow stromal cells (BMSCs) or freeze-dried allograft loading autogenous BMSCs transfected by Adv-BMP2 gene. (2) TiAIV particles were injected into bone-implant interface of 8 defects of the other 4 dogs for inducing peri-implant osteolysis. Eight weeks after injection, revision surgeries were performed and the osteolysis area were filled with freeze-dried allograft or freeze-dried allograft loading autogenous BMSCs transfected by Adv-BMP2 gene.

The healing and osseointegration of bone-implant interface were evaluated by histological, histomorphometric and biomechanical investigations at 6th weeks and 12th weeks after implantation.

**RESULTS:** The results were summarized as follows. (1) Histologically, at 6th weeks, new bone formation was found on the implant surface in

gene group, and point contact between bone and implant was observed, the bone-implant contact (BIC) ratio was around 10%. And only soft tissue was found at bone-implant interface in all other groups. At 12th weeks, there was thick soft tissue membrane between new bone and implant in the blank group. In non-cell group and cell group, most of the interface was filled by connective fibrous tissue with point contact between bone and implant and BIC ratio was lower than 10%. In gene group, the interface was mainly filled by bone tissue and area contact between bone and implant was found, the BIC ratio was significantly higher than all the other groups ( $P < 0.001$ ). The

mechanical strength of interface increased by time in all groups, with the gene group far higher than others at all the post-op. times ( $P < 0.001$ ).

(2) Eight weeks after the TiAIV particles injection, typical osteolytic changes were found around the implant. At 12th weeks after revision, the BIC ratio and strength of interface in gene therapy group were higher than those of freeze-dried bone group.

**CONCLUSIONS:** As a conclusion, BMP-2 gene therapy can enhance the osseointegration of bone-implant interface. The results of management of peri-implant osteolysis could be improved by using IBG technique combined BMP-2 gene medication.

# Effects of Recombinant Human Bone Morphogenetic Protein-2 and Acellular Dermal Matrix on Bone Formation in Rat Calvarial Defects

Y.-J.Um<sup>1</sup>, D.-S.Song<sup>1</sup>, J.-Y.Hong<sup>1</sup>, S.-W.Jung<sup>1</sup>, S.-B.Lee<sup>1</sup>, K.-S.Cho<sup>1,2</sup>, C.-S.Kim<sup>1,2</sup>

<sup>1</sup>Department of Periodontology, Research institute for periodontal regeneration, College of dentistry, Yonsei University, Seoul, Korea <sup>2</sup>Department of Periodontology, Research institute for periodontal regeneration, College of dentistry, Brain Korea 21 project for Medical Science, Yonsei University, Seoul, Korea

**INTRODUCTION:** To achieve the osteoinductive effect of BMPs, carrier systems are essential. Carrier systems for delivering BMPs should be biocompatible and biodegradable to minimize local tissue response and to allow replacement by newly formed bone. And it has to be easy to apply and be easy to manufacture. The purpose of this study was to evaluate the possibility of the acellular dermal matrix (ADM) as a barrier membrane for bone regeneration, and to evaluate the osteogenic effect of ADM as a carrier system for rhBMP-2 in the rat calvarial defect model.

**METHODS:** An 8-mm, calvarial, critical-size osteotomy defect was created in each of 60 male Sprague-Dawley rats (weight 250~300g). Three groups of 20 animals, each received either rhBMP-2 (0.025mg/ml) in an ADM carrier, ADM only, or negative surgical control. And each group was divided into 2- and 8- week healing intervals.

The groups were evaluated by histologic and histomorphometric parameters (10 animals/groups/healing intervals). Data were expressed as means±standard deviations (m±SD). Comparisons between experimental and control groups were made using two-way ANOVA and post hoc t-test. Comparisons between 2 weeks and 8 weeks were made using paired t-test. The level of statistical difference was defined as P< 0.05.

**RESULTS:** The ADM group and rhBMP-2/ADM group results in enhanced local bone formation in the rat calvarial defect at both 2 and 8 weeks. The amount of defect closure, new bone formation (Table 1) were significantly greater in the rhBMP-2/ADM group relative to ADM group (P<0.05). At 8 weeks, the majority of ADM in the defect was contracted, and integrated with surrounding host tissues. In addition, host cell infiltration and neovascularization of the ADM in the absence of an inflammatory response were observed, and the newly formed bone around ADM showed a continuous remodeling and consolidation.

Table 1. New bone formation (group means ± SD; n=10, %)

	2 weeks	8 weeks
control	4.8 [±] 0.7	8.2 [±] 1.4*
ADM	10.5 [±] 4.5	29.1 [±] 11.4 <sup>††</sup>
rhBMP-2/ADM	16.6 [±] 7.7 <sup>†††</sup>	42.5 [±] 14.6 <sup>†††</sup>

\*: Statistically significant difference compared to 2 weeks (P<0.05)

††: Statistically significant difference compared to the control group (P<0.05)

†††: Statistically significant difference compared to the ADM group (P<0.05)

**DISCUSSION & CONCLUSIONS:** The results of the present study indicated that ADM may be used as a barrier membrane for bone regeneration and that may be employed as a delivery system for BMPs.

**REFERENCES:** <sup>1</sup>Chang-Sung Kim, Joon-Il Kim, Jin Kim, Seong-Ho Choi, Jung-Kiu Chai, Chong-Kwan Kim, Kyoo-Sung Cho (2005) Ectopic Bone Formation of Recombinant Human Bone Morphogenetic Proteins -2 using Absorbable Collagen Sponge and beta Tricalcium Phosphate as Carriers, Histological and Immunohistochemical evaluation. *Biomaterials* 26(15):2501-2507. <sup>2</sup>Suk-Ju Hyun, Dong-Kwan Han, Seong-Ho Choi, Jung-Kiu Chai, DDS, Kyoo-Sung Cho, Chong-Kwan Kim, Chang-Sung Kim (2005) The Effect of Recombinant Human Bone Morphogenetic Protein-2, 4 and 7 on Bone Formation in Rat Calvarial Defect. *Journal of Periodontology* 76:1667-1674.

**ACKNOWLEDGEMENTS:** This work was supported by the Korea Research Foundation Grant funded by the Korean Government (MOEHRD) (KRF-2005-041-E00390).

# Chitosan Containing Calcium Phosphate Cement: Preparation and Clinical Study

K. Poret<sup>2</sup>, M. Frèche<sup>1</sup>, S. Goncalvez<sup>3</sup>, J.L. Lacout<sup>1</sup>, F. Rodriguez<sup>2</sup>

<sup>1</sup>*CIRIMAT UMR 5085, ENSIACET INPT, Toulouse, FR.* <sup>2</sup>*Laboratoire de Pharmacie Galénique GEFSOD EA 2631, Toulouse, FR.* <sup>3</sup>*TEKNIMED S.A. - Biomatériaux et Implants Orthopédiques, L'Union, FR.*

**INTRODUCTION:** Phosphocalcium cements have been the focus of many recent works intended to improve their properties and to extend their applications. Two points have to be addressed : their injectability and their biological degradation rate. Improvements can be made by the inclusion of synthetic or natural polymers. The healing properties and the activity on the bone regeneration of the chitosan are previously described [1]. This work relates to the re-formulation of an existing cement, Cementek<sup>R</sup>, by addition of chitosan and presents the first clinical results on animal experiments.

**METHODS:** Cementek<sup>R</sup> cement was prepared by mixing a liquid phase with a solid phase [2]. The chitosan used was provided by Primex; it is in the form of a powder with particle dimensions smaller than 100 microns and its desacetylation degree is 74%. The chitosan was introduced either into the liquid phase, or in the solid phase such that the percentage in the final cement varied from 0 to 10% (w/w). When the chitosan was introduced into the solid phase, it was necessary to increase the liquid/solid ratio (L/S). The chemical maturation of the cement was followed by X ray diffraction. Measurements of the setting time and of the compressive strength were carried out on each sample either in wet or dry medium.

A clinical animal study was carried out, with cements containing 5% of chitosan in solid phase, on bony defects in the femur of rats and on the sternums of sheep.

**RESULTS:** The addition of chitosan, either in the liquid phase or in the solid phase of the cements, did not disturb their chemical and structural maturation. All the prepared formulations evolved towards an hydroxyapatite.

The addition of chitosan in the solid phase modified the consistency of the pasty cement which became more malleable and more homogeneous than pure Cementek. This addition also modified the setting time which decreased from 20 minutes for pure Cementek to about 8 minutes depending on the chitosan amount.

The mechanical properties in compression are preserved, even slightly improved in the presence of chitosan.

The in vivo tests were performed on cements containing 5% of chitosan in the solid phase, after sterilization by gamma irradiation. A first experimentation series, which concerned the implantation of cement in a bony defect in the femur, was carried out on 80 rats. After only 3 weeks, the formation of cartilage indicated that the chitosan made it possible to induce the growing of cartilage starting from cells in the perioste and the medullary tissue.

A second experimentation series, concerning the reconstruction of the sternum, was carried out on sheep. After 6 weeks, the treated bone appeared to be in an osseous rebuilding phase ; new trabecular bone was formed as well as cartilage, which indicates that the formation of new bone follows a process of ossification of the endochondral type. After 12 weeks, microscopic examinations indicated supplements in regeneration of the damaged bone.

**DISCUSSION & CONCLUSIONS:** Various formulations of ionic cements containing chitosan were developed. The presence of chitosan did not interfere with the succession of acidic-basic reactions of dissolution and precipitation which lead to the final phase of hydroxyapatite. The setting time and the mechanical properties remain convenient for practical use. The clinical animal study showed that, due to the activity of the chitosan, the compensation for the osseous damages is complete in a reduced time.

**REFERENCES:** <sup>1</sup>J. Ma, H. Wang, et al (2001) *Biomaterials* **22**:331-336. <sup>2</sup>M. Frèche, J. L. Lacout, Z.Hatim (1999) *Surgical or dental hydroxyapatite-based biomaterial preparation FR2776282*.

**ACKNOWLEDGEMENTS:** The authors gratefully acknowledge Professor Silbermann and his team for the clinical study and PRIMEX Society for providing them with the chitosan.

# Clinical Evaluation of an Injectable, In-Situ Curing Nucleus Replacement

U. Berlemann<sup>1</sup>, O. Schwarzenbach<sup>1</sup>, C. Etter<sup>2</sup>, S. Kitchell<sup>3</sup>

<sup>1</sup> Spine Center, Thun, CH

<sup>2</sup> Swiss Spine Institute, Basel, CH

<sup>3</sup> Health Sciences Center, University of Oregon, Eugene OR, USA

**INTRODUCTION:** Literature indicates that following microdiscectomy significant loss of disc height with corresponding recurrent back and/or leg pain may occur.<sup>1,2</sup> Loss of disc tissue due to herniations and/or surgery can accelerate degeneration of the disc.<sup>3,4</sup> NuCore™ Injectable Nucleus is an in-situ curing silk-elastin protein polymer hydrogel. It mimics the properties of the natural nucleus and is intended as a replacement for natural nucleus lost to herniation and/or discectomy. The hydrogel is injected as a fluid through the annulus, and adheres to the surrounding discal tissue as it cures. The material is designed to immediately fill the nuclear void and seal the annulotomy (or annular defect); and in the long term, preserve natural biomechanics, and prevent recurrent herniation and further degeneration of the disc.

**METHODS:** Pre-clinical studies showed the NuCore™ Injectable Nucleus restores biomechanics; and is biocompatible, resistant to expulsion forces, and highly durable under simulated *in vivo* loading. A multi-center pilot clinical study is underway to evaluate NuCore™ Injectable Nucleus as an adjunct to microdiscectomy. At the time of this writing, the material has been implanted into twelve patients aged between 23 and 48 years (6 females, 6 males) following a standard microdiscectomy procedure for monosegmental radicular pain non-responsive to conservative treatment. L5/S1 was treated in ten cases and L4/5 in two cases.

**RESULTS:** All surgeries were successfully completed using between 0.3 and 2.6cc of hydrogel, with an average injection volume of 1.1cc. Four patients currently are at twelve months follow-up and five have reached six months. In all cases, pain subsided as normally expected following standard microdiscectomy. Neurologic evaluation, Oswestry index, SF36 and VAS scores were taken pre- and post-operatively, and at six, twelve, twenty-six, and fifty-two weeks post-op. All measures showed significant improvement in all patients. Average ODI scores dropped from 47 preoperatively to less than 10 at follow-up. Leg pain dropped from an average

preoperative score of 7.3 to less than 1.0 at follow-up. All categories of the SF36 showed substantial improvement over preoperative scores. All of these improvements were maintained over the course of completed follow-ups. No patient had any device related complication. MRI investigations confirmed stable positioning of the implants at all time-points, and no recurrent herniations. Preliminary analysis of standing plain films indicated improved disc height maintenance relative to published literature, with an average loss of disc height at completed follow-ups of five percent.

**DISCUSSION & CONCLUSIONS:** To our knowledge, this is the first injectable nucleus replacement to have been implanted as an adjunct to microdiscectomy. Early clinical results indicate that NuCore™ Injectable Nucleus can be reliably used as a nuclear defect-filler. All patients are doing well clinically, and disc height and function appear to be maintained over the course of follow-up. Though early results indicate potential benefits, further follow-up will be necessary to fully determine the long-term functional benefits of this treatment. Additional clinical studies have been approved to investigate the use of this hydrogel as an early intervention in degenerative disc disease.

**REFERENCES:** <sup>1</sup> Yorimitsu, et al (2001) *Long-term Outcomes of Standard Discectomy for Lumbar Disc Herniation*, Spine 26:652-657. <sup>2</sup> Vaughan, et al (1988) *Results of L4-L5 Disc Excision Alone Versus Disc Excision and Fusion*, Spine 13:690-695. <sup>3</sup> Mochida, et al (2001) *The Risks and Benefits of Percutaneous Nucleotomy for Lumbar Disc Herniation*, JBJS Br 83:501-505. <sup>4</sup> Kambin, et al (1995) *Development of Degenerative Spondylosis of the Lumbar Spine after Partial Discectomy*, Spine 20:599-607.

**ACKNOWLEDGEMENTS:** Spine Wave, Inc. has provided materials for the pre-clinical and clinical studies presented.

# Quantitative Kinetic Analysis of Gene Expression During Human Osteoblastic Adhesion on Orthopaedic Materials

M.Rouahi<sup>1</sup>, E.Champion<sup>2</sup>, P.Hardouin<sup>1</sup> & K.Anselme<sup>3</sup>

<sup>1</sup> *Laboratoire de Recherche sur les Biomatériaux et Biotechnologie, Boulogne sur mer, France.*

<sup>2</sup> *Sciences des Procédés Céramiques et de Traitements de Surface (SPCTS), Limoges, France.*

<sup>3</sup> *Institut de Chimie des Surfaces et Interfaces, Mulhouse, France.*

**INTRODUCTION:** Little information was found in the literature about the expression on calcium phosphate materials of genes specific of cellular adhesion molecules although more were found on titanium-based substrates. Hence, the goal of this work was to study by a kinetic approach from 30 minutes to 4 days the adhesion of human osteosarcoma Saos2 cells on microporous (mHA) and non microporous hydroxyapatite (pHA) in comparison to polished titanium. Our strategy associated the visualization of adhesion proteins inside the cells by immunohistochemistry and the quantitative expression of genes at mRNA level by real-time PCR. The cell morphology was assessed using scanning electron microscopy and the number of cells thanks to biochemical techniques.

**METHODS:** Microporous hydroxyapatite (mHA) discs were provided by BIOCETIS s.a. (France). They were obtained by a humid method using commercial powders of HA (Transtech, USA). The discs were then sintered at high temperature (1250°C). mHA displayed 12.5% of interconnected microporosity. Non microporous hydroxyapatite discs (pHA) were prepared using a laboratory-prepared HA powder which was pressed by uniaxial pressure of 80 Mpa. Discs were sintered at 1220°C and polished with SiC paper. Mirror-polished pure titanium discs, were obtained from the Laboratoire Matériaux (ENSAM, Lille, France). SaOs2 cells were cultured on samples for 30 min, 1h, 4h, 24h or 4 days. Cells on samples were either treated for immunofluorescence, for adhesion assay or for protein and RNA extraction. For these last measurements, cells on each sample were immersed in 0.25 ml of Extract-All (Eurobio, France) and proceeded for protein and RNA extraction. The expression of genes involved in bone cell adhesion and differentiation was quantified by real-time PCR.

**RESULTS:** The cellular attachment was the highest on mHA from 30 minutes to 24 hours although the cell growth on mHA was the lowest after 4 days. Generally, the SaOs-2 osteoblastic cells morphology on mHA was radically different

than on other surfaces with the particularity of the cytoplasmic edge which appeared undistinguishable from the surface. The revelation by specific antibodies of proteins of the cytoskeleton (actin) and the focal adhesions (FAK, phosphotyrosine) confirmed that adhesion and spreading were different on the 3 materials. The actin stress fibers were less numerous and shorter on mHA ceramics. Cells had more focal contacts after 4 hours on mHA compared to other substrates but less after 24 hours. The highest values of total proteins were extracted from mHA at 0.5 and 24 hours and from pHA at 1, 4, and 96 hours. The  $\alpha$ v and  $\beta$ 1 integrin, actin, FAK, and ERK gene expression were found to be different with adhesion time and with materials. C-jun expression was comparable on mHA, titanium and plastic but was largely higher than on pHA at 0.5 and 1 hour. On the contrary, c-fos expression was the highest on pHA after 0.5 hours and the lowest after 1 hour. This difference between c-fos and c-jun expression on pHA after 0.5h could be related to the fact that these two genes may differ in their signalling pathways. The expression of the alkaline phosphatase gene after 4 days was lower on mHA compared to other materials demonstrating that the microstructure of the mHA ceramic was not favourable to SaOs-2 cells differentiation.

**DISCUSSION & CONCLUSIONS:** Finally, it was demonstrated in this study that HA and titanium surfaces influence as well gene expression at early times of adhesion as the synthesis of adhesion proteins but also proliferation and differentiation phases. Indeed, the signal transduction pathways involved in adhesion of SaOs-2 cells on HA and titanium were confirmed by the sequential expression of  $\alpha$ v and  $\beta$ 1 integrins, FAK, and ERK genes followed by the expression of c-jun and c-fos genes for proliferation and alkaline phosphatase gene for differentiation. These results are a new demonstration that adhesion of cells on materials is linked to their nature, their protein adsorption capacity, their microstructure, and that it influences further cellular proliferation and differentiation phases.

# **Session F:**

## **Biomechanics**

### **Keynote Lectures**

Gamal Baroud, PhD  
University of Sherbrooke

Thomas Steffen, MD, PhD  
McGill University

# The Effect of Strontium on the Rheology and Mechanical Properties of Zinc Based Glass Polyalkenoate Cements.

D. Boyd & M.R. Towler

*Materials and Surface Science Institute (MSSI), University of Limerick, Ireland.*

**INTRODUCTION:** Zinc-based glass polyalkenoate cements (Zn-GPCs) have significant potential as skeletal cements due to their bioactive nature<sup>1</sup> and antibacterial properties<sup>2</sup>. However, their mechanical properties contraindicate their use in load bearing applications<sup>1</sup>. In order to increase both radiopacity and therapeutic action, strontium (Sr) can be substituted for calcium in the glass structure due to their similar ionic radii. However, the influence of such a substitution on the rheology and mechanical properties of resultant cements must be monitored.

**METHODS:** Three glass compositions (Table 1) were synthesized. Appropriate amounts of silica, zinc oxide, strontium carbonate and calcium carbonate were weighed out, ball milled and fired in a mullite crucible (1580°C, 1Hr). The melts were then shock quenched and the resulting frit was dried, ground and sieved (<45µm). Glasses were characterized using differential thermal analysis (DTA) and X-ray diffraction (XRD), to respectively evaluate glass transition temperature ( $T_g$ ) and amorphous nature of each glass. Two polyacrylic acids (PAA), E7 ( $M_w$ , 27700) and E9 ( $M_w$ , 80800) were employed. Cements were prepared by mixing 1.0g of glass powder with a 50wt% of PAA solution, using a powder: liquid (P:L) ratio of 1:0.91. Setting times and compressive strengths were determined in accordance with ISO9917<sup>3</sup>. The biaxial strength of the cements was determined by the method of Williams *et al*<sup>4</sup>.

## RESULTS:

**Table 1:** Glass compositions (mol. fraction) and  $T_g$ s.

Glass	SrO	CaO	ZnO	SiO <sub>2</sub>	$T_g$ (°C)
A	0	0.05	0.53	0.42	690
B	0.025	0.025	0.53	0.42	687
C	0.05	0	0.53	0.42	686

**Table 2:** Setting times (s) of cements.

GPC	Setting times
AE9	155
BE9	255
CE9	360

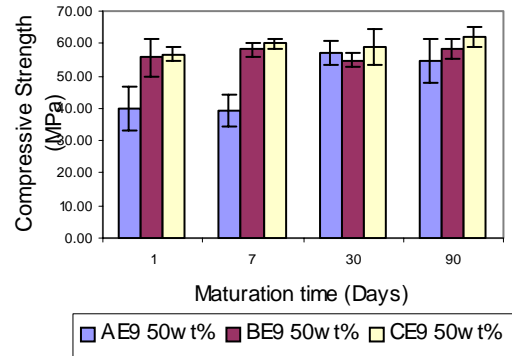


**Figure 1:** Compressive strengths of Zn-GPCs.

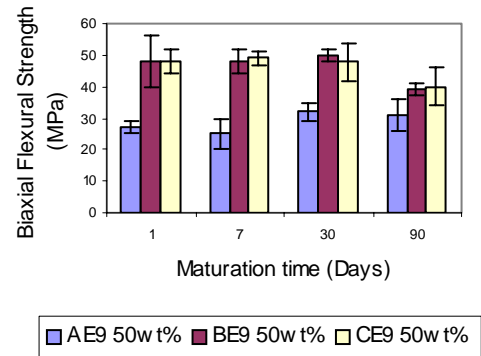


**Figure 2:** Biaxial flexural strengths of Zn-GPCs.

**DISCUSSION & CONCLUSIONS:** The substitution of Ca by Sr in the glass network resulted in no appreciable change in  $T_g$ , indicating that glass structure remains similar irrespective of Sr loading. However, the addition of Sr facilitated increased setting times, compressive strengths and biaxial flexural strengths of resultant cements. This data implies that controlled additions of Sr into such glass networks may provide the appropriate increase in mechanical properties of resultant cements required for load bearing applications.

**REFERENCES:** <sup>1</sup>D. Boyd & M.R. Towler (2005) *J. Mat. Sci. Mat. Med.* **16**:843-850 <sup>2</sup> D. Boyd, H. Li, D.A. Tanner, *et al* (2005) accepted by *J. Mat. Sci. Mat. Med.* <sup>3</sup>International standard ISO9917: 1991 (E). <sup>4</sup>Williams, J. A., Billington, R. W. & Pearson, G. J. (2002) *Dental Materials* **18**:376-379

# Local Compressive and Tensile Stiffness Measured in Tissues with Regular Patterns of Hyaline-Fibrocartilage Regions

A.Marsano<sup>1</sup>, D.Wendt<sup>1</sup>, R.Raiteri<sup>2</sup>, R.Gottardi<sup>2</sup>, S.Dickinson<sup>3</sup>, A.P.Hollander<sup>3</sup>,

D.Wirz<sup>4</sup>, A.U.Daniels<sup>4</sup>, T.M.Quinn<sup>5</sup>, M.Stolz<sup>6</sup>, I.Martin<sup>1</sup>

<sup>1</sup> *Institute for Surgical Research&Hospital Management, University Hospital Basel, Basel, CH*

<sup>2</sup> *University of Bristol, AMBI, Avon Orthopaedic Center, Southmead Hospital, Bristol, UK*

<sup>3</sup> *Department of Biophysical and Electronic Engineering, University of Genoa, I*

<sup>4</sup> *Laboratory for Orthopaedic Biomechanics, Felix Platter Hospital, University of Basel, CH*

<sup>5</sup> *Cartilage Biomechanics Group, Ecole Polytechnique Fédérale de Lausanne (EPFL), CH*

<sup>6</sup> *Maurice E. Mueller Institute for Structural Biology, Biozentrum/University of Basel, CH*

**INTRODUCTION:** With the ultimate goal of engineering a meniscus substitute, we generated bi-zonal hyaline-fibrocartilaginous tissues using articular chondrocytes loaded on hyaluronan-based meshes and cultured in the presence of different hydrodynamic conditions [1, 2]. Specific aim of this study was to demonstrate that the different local biochemical composition of the bi-zonal tissues results in a different local biomechanical function, resembling that of native meniscus.

**METHODS:** Bovine articular chondrocytes were loaded into hyaluronan-based meshes (Hyalograft-C<sup>®</sup>, Fab, Italy) and cultured for 4 weeks in either (i) a static culture system, (ii) a mixed flask (MF), or (iii) a Rotary Cell Culture System (RCCS, Synthecon Inc., USA) [1]. Engineered tissues were assessed histologically, immunohistochemically, biochemically and by scanning electron microscopy. Local compressive stiffness was determined using atomic force microscopy-based,  $\mu\text{m}$ -scale indentation tests [3] at different regions of bisected cartilaginous constructs. Local tensile stiffness was determined by tensile tests performed on concentric rings punched out from the inner and outer regions of engineered tissues.

**RESULTS:** Hyaluronan meshes-based constructs generated in the bioreactor-based systems (MF or RCCS) were characterized by a fibrocartilage-like outer capsule, containing abundant collagen type I (CI), versican and negligible glycosaminoglycans (GAG) or collagen type II (CII), and a hyaline-like inner core, containing abundant CII and GAG, with little CI and versican. In contrast, constructs cultured in the static system did not display any regular pattern in the deposition of CI, CII, GAG or versican. Scattered areas with bundle of parallel collagen fibers were observed only in the outer capsule of MF- or RCCS-grown tissues. Compressive stiffness measured in the inner regions of constructs generated in the MF or the RCCS were significantly higher (respectively 3.8-

and 4.3-fold) than those measured in the corresponding peripheral regions. Conversely, tensile stiffness of the external rings of tissues engineered in the MF or the RCCS were higher than those of the corresponding internal rings (respectively 1.9- and 2.5-fold higher). Control constructs cultured statically had compressive and tensile stiffness that were similar in the inner and outer regions.

**DISCUSSION & CONCLUSIONS:** We found that differences in the local biochemical composition of cartilaginous tissues, introduced by using MF or RCCS, were reflected in different local biomechanical properties. In particular, the inner hyaline-like zones of bioreactor-based constructs had higher strength in compression than in tension, whereas the outer fibro-cartilaginous regions were stronger in tension than compression. Since these structural, biochemical and functional properties resemble the heterogeneous nature of the meniscus, we are currently investigating the use of MF or RCCS for the development of meniscus substitutes.

**REFERENCES:** <sup>1</sup> A. Marsano (In press 2006) Bi-zonal cartilaginous tissues engineered in a rotary cell culture system *Biorheology* <sup>2</sup> Vunjak-Novakovic G, et al (1999) Bioreactor cultivation conditions modulate the composition and mechanical properties of tissue-engineered cartilage, *J Orthop Res*. *J Orthop Res* 17(1):130-8. <sup>3</sup> Stolz M, et al. (2004) Dynamic elastic modulus of porcine articular cartilage determined at two different levels of tissue organization by indentation-type atomic force microscopy *Biophys J*; 86(5):3269-83.

**ACKNOWLEDGEMENTS:** The study was funded by the Swiss Federal Office for Education and Science (B.B.W.), under the Fifth European Framework Growth Program (Meniscus Regeneration, contract G5RD-CT-2002-00703)

# KyphOs FS™ Calcium Phosphate for Balloon Kyphoplasty: Verification of Compressive Strength and Instructions for Use

J. Schwardt<sup>1</sup>, T. Slater<sup>1</sup>, S. Lee<sup>1</sup>, J. Meyer<sup>2</sup> & R. Wenz<sup>2</sup>

<sup>1</sup> Kyphon Inc., Sunnyvale, CA, USA. <sup>2</sup> Sanatis GmbH, Rosbach, Germany

**INTRODUCTION:** KyphOs FS™ Calcium Phosphate Bone Substitute is a biomaterial for use during balloon kyphoplasty (BKP) treatment of type A1.1, A1.2 or A3.1 fractures of the vertebral body (VB). During BKP, a collapsed VB is restored with an inflatable bone tamp, and the resulting void is filled with a biomaterial to support the surrounding bone and prevent further collapse. This report describes results of in vitro compressive strength tests that verify the utility of KyphOs FS for its intended use, and help prescribe intra-operative and post-operative instructions for use. The study aimed to answer the following research questions: (1) Within a reasonable period of time after implantation into a fractured VB, will KyphOs FS attain an appropriate weight-bearing compressive strength, thus allowing safe transfer of the patient from the procedure table? (2) Will KyphOs FS attain its expected final compressive strength after undergoing a significant early load during the initial setting period?

**METHODS:** Cylindrical specimens (6 mm diameter x 12 mm) of KyphOs FS were prepared, immersed in 37°C water for various setting times, and compressed under displacement control at 1 mm/min. In the first protocol, specimens were tested after setting times of 5 minutes to 24 hours. In the second protocol, specimens underwent a single non-destructive load of 1 MPa at early times of 10, 20, and 30 minutes, then returned to the water bath and loaded again to failure after 2 hours. A Tukey-Kramer HSD test was used to detect statistically significant ( $p < 0.05$ ) differences among strength values.

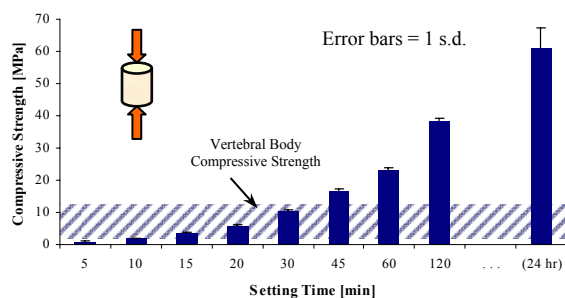


Fig. 1: Mean compressive strength ( $n=6$ ) of specimens at various setting times, compared to the reported 2-12 MPa strength of a VB [1,2].

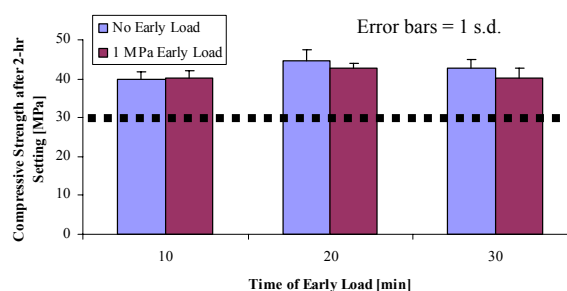


Fig. 2: Mean 2-hour compressive strength ( $n=6$ ), with and without early load. 30 MPa is the minimum expected strength.

**RESULTS:** The compressive strength of KyphOs FS increased over time:  $1.8 \pm 0.2$  MPa after 10 minutes,  $3.4 \pm 0.3$  MPa after 15 minutes,  $5.9 \pm 0.3$  MPa after 20 minutes,  $38.5 \pm 0.8$  MPa after 2 hours, and  $61.2 \pm 6.1$  MPa after 24 hours (Fig. 1). The 2-hour setting strengths in specimens with early loads of 1 MPa are not statistically different than controls with no early loads (Fig. 2).

**DISCUSSION & CONCLUSIONS:** The results suggest that KyphOs FS can attain compressive strength comparable to that of an intact VB within 15-20 minutes after implantation. Thus, the biomaterial is sufficiently strong for safe transfer of the patient within a reasonable setting time. The early load of 1 MPa used in the second protocol is similar to the compressive stress in a lumbar VB of a standing subject [2,3,4]. With or without an early load, the biomaterial attains its expected compressive strength.

Based on these data, KyphOs FS instructions for use have been prescribed as shown in Table 1.

Table 1. Timing Sequence in Instructions for Use

Time Interval	Activity
<b>Period</b>	
<b>4 min : 45 sec</b>	<ul style="list-style-type: none"> <li>▪ Mix Powder &amp; Liquid</li> <li>▪ Transfer to Bone Filler Devices</li> <li>▪ Deliver to VB</li> </ul>
<b>20 min</b>	Waiting period <i>after delivery to VB</i> before moving patient.
<b>24 hr</b>	Bed rest before weight-bearing.

**REFERENCES:** <sup>1</sup>L. Mosekilde (1990) *Bone* 11(2):67-73. <sup>2</sup>K. Singer et al. (1995) *Bone* 17(2):167-174. <sup>3</sup>A. Nachemson (1976) *Spine* 1:59. <sup>4</sup>H.J. Wilke et al. (1999) *Spine* 24(8):755-62

# Vertebral Cancellous Bone Augmented with Stiffness-adapted PMMA Cement does not Show Acute Failure under Dynamic Loading

A. Boger<sup>1</sup>, P. Heini<sup>2</sup>, M. Böhner<sup>3</sup> and E. Schneider<sup>1</sup>

<sup>1</sup> AO Research Institute, Davos, CH. <sup>2</sup> Department of Orthopaedic Surgery, Insel Hospital Bern, CH. <sup>3</sup> Robert Mathys Foundation, Bettlach, CH

**INTRODUCTION:** An increased fracture risk has been reported for the adjacent vertebral bodies after vertebroplasty<sup>1,2</sup>, which may be due to the high stiffness of PMMA. Using stiffness-adapted porous PMMA<sup>3</sup> might reduce this risk. But the reduced failure strength of the porous cement could deteriorate under dynamic loading. The task of this study was to determine stiffness, acute failure, height loss and subsidence of cancellous bone augmented with porous PMMA under dynamic loading.

**MATERIALS & METHODS:** BMD of 12 human lumbar vertebrae (T11 or T12) was measured using pQCT. Two cylindrical biopsies (diameter 10.6 mm) were cored out from the central part of each vertebral body perpendicular to the endplates. The biopsies were randomly assigned to two groups. Each group contained one biopsy of each vertebra to assure identical density distribution in each group. The endplates of the cylinders were removed with a band saw to allow augmentation. Then the biopsies were sawn coplanarly to a length of 20mm. After removing the marrow, one group was augmented with regular PMMA (Vertecem, Synthes Inc.) and the other one with porous PMMA. The porous cement was prepared as described by Boger et. al<sup>3</sup>. For augmentation the biopsy was put into a tube and then cement was infiltrated with a plunger. Young's modulus (YMm) and yield strength (YSm) in compression for the cements<sup>3</sup> are listed in Table 1. After 4h the infiltrated biopsy was rinsed and stored in demin. water at room temperature for 2 days. A dynamic compression test was performed in demin. water (Bionix; MTS Systems). The sinusoidal load controlled cycles had a frequency of 4 Hz and an amplitude from 3.9 N to 390 N corresponding to max. stress of 4.4 MPa (normal disc pressure 1-1.5 MPa). The total test duration was 60min (14.400 cycles). Stress-strain diagrams were analyzed for the initial (YMi) and final stiffness (YMf) of the bone/cement composite as an average of the first and final 10 loading cycles. Height loss was determined from initial and final height. Subsidence was determined as difference in strain at max. load between the average of final and initial 10 cycles. A quasi static

compression test was performed to failure (velocity 5mm/min) (Instron 5866, 10 kN load cell). From the static compression test YMs and YSs were determined according to ISO 5833. Statistical differences between the groups were analyzed using ANOVA, dependent t-test,  $\alpha < 0.05$ .

**RESULTS:** BMD of the vertebrae/biopsies ranged from 0.078 to 0.29 g/cm<sup>3</sup> (mean $\pm$ SD: 0.21 $\pm$ 0.06). No failure occurred during dynamical testing. Stiffness of the composite increased with porous and decreased with regular cement, both around 34% compared to cement alone. All variables were significantly different comparing the two groups. No linear correlation between BMD and height loss, subsidence could be found ( $R^2 < 0.3$ ). A significantly higher height loss and subsidence was found for the biopsy group with porous compare to the ones with regular cement. All constructs showed stiffening due to dynamic loading by 17%. *Table 1. Subsidence, height loss, stiffness and yield strength values (mean  $\pm$  SD)*

PMMA	Porous	regular
YMm / MPa	480 $\pm$ 65	1900 $\pm$ 40
YSm / MPa	11.6 $\pm$ 3.3	100 $\pm$ 5
YMi / MPa	647 $\pm$ 106	1223 $\pm$ 127
YMf / MPa	761 $\pm$ 158	1422 $\pm$ 204
YMs / MPa	642 $\pm$ 131	1262 $\pm$ 183
YSs / MPa	21.1 $\pm$ 4.1	62.5 $\pm$ 10.8
height loss / %	0.53 $\pm$ 0.21	0.16 $\pm$ 0.1
subsidence / %	0.43 $\pm$ 0.23	0.11 $\pm$ 0.05

**DISCUSSION & CONCLUSION:** The bone/cement construct with stiffness adapted cement retains the mechanical properties in failure strength and preserves elasticity similar to trabecular bone alone. Nevertheless, the porous cement will prevent the accumulation of further damage without altering significantly the stress distribution under physiological loading. These data provide baseline data for the human application.

**REFERENCES:** <sup>1</sup> Grados F et. al, (2000), *Rheumatology (Oxford)*, 39:1410-1414. <sup>2</sup> Ferguson SJ et. al, (2002) *J. Bone & Joint Surgery* 84-B: 748-752. <sup>3</sup> Boger et. al, (2005) *Biomedical Material Research Part B*, submitted. The authors thank Synthes Inc. for providing the materials.

# Effect of Solution Viscosity on Cement Injectability

P.J. Leamy, M. Lehmicke and M.T. Fulmer

Synthes Biomaterials Development Center, West Chester, Pennsylvania, USA

**INTRODUCTION:** The addition of viscous water soluble polymers to calcium phosphate cements (CPCs) has been shown to reduce phase separation and increase injectability. It is hypothesized that the increased injectability with polymer addition is attributable to increased solution viscosity which counteracts phase separation. The purpose of this study was to establish the relationship between injectability and solution viscosity for a model CPC using an injection test through a 12 gauge 10 cm needle.

**METHODS:** The cement powder was a mixture of alpha tricalcium phosphate, barium sulfate, calcium carbonate and monocalcium phosphate monohydrate. Cement solutions with different viscosities were prepared by dissolving water soluble polymers in different concentrations into 0.075 molal sodium phosphate dibasic solution. Water soluble polymers were Hydroxypropyl methyl cellulose (HPMC), carboxymethyl cellulose sodium salt (CMC) and sodium hyaluronate. Two different molecular weights were used for each polymer. For each injection test, cements were mixed and 5 cc of cement was loaded into a 5cc syringe with a 12 gauge 10cm cannula. An Instron was used to displace the syringe plunger and inject cement at a constant rate of approximately 6cc/min while a load cell recorded injection force. The test stopped when a load of 62 lbs was achieved.

**RESULTS:** For the purpose of this abstract, data is presented only for sodium hyaluronate polymer. Figure 1 shows injection profiles for cements mixed with sodium hyaluronate solutions with varying viscosity (molecular weight = 670,000 Da). The injection force and delivered volume increase with increasing solution viscosity. Figure 2 shows 1cc injection force and cement viscosity (determined using the Hagen Poiseuille equation) as a function of sodium hyaluronate molecular weight and solution viscosity. Injection force increases with solution viscosity with very little difference in behavior for the two different molecular weights. Figure 3 shows % injection for the two different molecular weights of sodium hyaluronate. The % injection increases with solution viscosity. CMC and HPMC polymers showed similar behavior as the sodium hyaluronate containing cements.

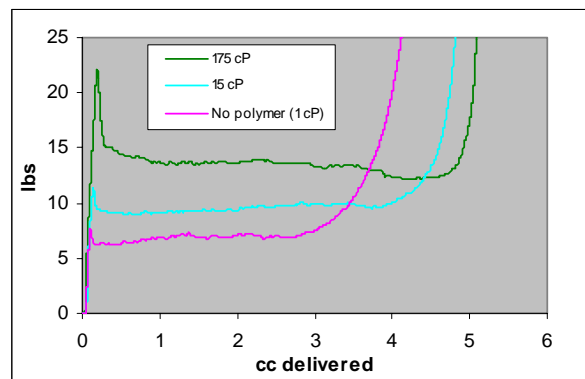


Fig. 1: Injection profiles for cements with sodium hyaluronate (NaHy) 760,000 Da.

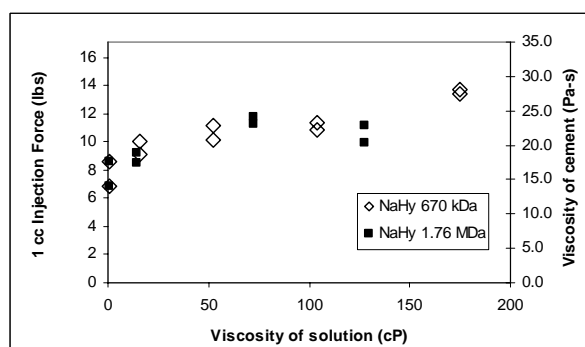


Fig. 2: Injection force and cement viscosity at 1 ml for NaHy.

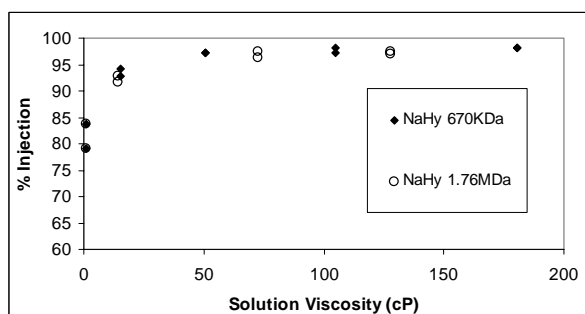


Fig. 3: Percent Injection for cements with (NaHy).

**DISCUSSION & CONCLUSIONS:** Injection force and cement volume delivered (% injection) increased with increasing solution viscosity. Above 50 cP solution viscosity nearly complete injection was achieved with little evidence of phase separation. For a given viscosity of solution, molecular weight of polymer had little or no effect on injectability.

# Injectable Calcium Phosphate Cement with Water Washout Resistance

Y.Wang, J.Weil, H.Hong, H.Guo, C.Liu

*Engineering Research Center for Biomedical Materials under Ministry of Education, Institute of Biomaterials, East China University of Science and Technology, Shanghai CN*

**INTRODUCTION:** Calcium phosphate cements (CPCs) have been paid much attention as bioactive biomaterials for bone defect repair because they can set to form apatite under ambient conditions within short time and bond to natural bone. Although CPCs show excellent bioactivity, the currently available calcium phosphate cements are still insufficient for safe application. One of these problems is the decay of the cement when the paste is in contact with blood and body liquid. The decay of the paste would result in the failure of the operations, which limits the potential application of the CPC. Therefore, there is a requirement of non-decaying type of injectable CPC for application in clinic. In this study, a novel injectable CPC with excellent property of water washout resistance was fabricated by using cellulose acetate as an additive and non-aqueous solvent ethyl lactate as cement liquid.

**METHODS:** Equimolar amounts of DCPA and TTCP powders were mechanically mixed to obtain calcium phosphate cement powders. Different amounts of acetyl cellulose were dissolved in ethyl lactate to obtain polymer solutions. Pastes were prepared by mixing of the CPC powders and the cellulose solution with different P/L (power/liquid ratio). The setting time of the paste samples was measured according to the method set out in international standard ISO1566 for dental zinc phosphate cements. Composition and surface morphology of the CPC hardened body was characterized with XRD, IR and SEM after soaking in water at 36.5° for 3d. The compressive strength of the CPC was determined with a universal material test machine. Cell culture experiment was performed to evaluate the biocompatibility of the CPC and characterized with SEM and optical microscope.

**RESULTS:** The experiments results indicated that the injectable CPC has excellent water washout resistance property, which can set and harden both in air and in physiological saline solution. XRD and IR results showed that only apatite phase was presented after the CPC harden for 3d, the addition of the cellulose acetate did not hamper the CPC change into hydroxyapatite. When the paste was exposed to body fluid, precipitation of cellulose acetate and hydroxyapatite simultaneously occurs

to result in the setting of the paste. The setting time of the CPC decreased with the increase of the P/L ratio and the concentration of the cellulose and the optimized setting time was 15-30min when the P/L was 2:1 and the concentration of the cellulose was 30%. The compressive strength of the CPC increased with the increase of the P/L ratio, the concentration of the cellulose and the time in water. The optimized compressive strength was 23-34MPa when the P/L was 2:1, the concentration of the cellulose was 30% and the time in water was 7 days. SEM and optical microscope analysis results indicated that the cultural cells were attached, dispersed and preferentially proliferated on the surface of the CPC, the results showed that the injectable CPC has excellent biocompatibility.

**DISCUSSION & CONCLUSIONS:** The novel injectable CPC prepared in this study has a reasonable setting time, high mechanical strength, excellent water washout resistance properties and can be easily handled as paste and injectable. The result suggests that the novel injectable cement may be an ideal bone repair or substitute material.

**REFERENCES:** <sup>1</sup> Law FC, James KH, Matthew CA, Rushton N. *Biomaterials* 13(1992)811. <sup>2</sup> Gil-Al barova J, Lacleriga A, Barrios C, Canadell J. *Brit J Bone Jt Surg* 74(1992)825. <sup>3</sup> D. Walsh, J. Tanaks. *J.Mater Sci Mater Med* 12(2001)33. <sup>4</sup> Huipin Yuan, Yubao Li. *Biomaterials* 21(2000)1283.

# **POSTERS**

**In alphabetical order**

# Activation and Biomechanical Assessment of an Injectable Hybrid Osteoconductive – Osteogenic Bone Substitute

S. Becker<sup>1</sup>, I. Boecken<sup>2</sup>, M. Böhner<sup>3</sup>, G. Bigolin<sup>3</sup>, M. Alini<sup>4</sup>

<sup>1</sup>Spine Center Orthopaedic Hospital Speising Vienna AUT, <sup>2</sup>Synthes Biomaterials CH, <sup>3</sup>Robert Mathys Foundation, Bettlach CH, <sup>4</sup>AO-Research Institute Davos-Platz CH

**INTRODUCTION:** Current research is focusing on injectable osteoconductive materials. Injectable CaP cements offer a minimal-invasive use, but lack osteogenic properties. In order to create a combined osteoconductive / osteogenic bone substitute we used in this study a synthetic, injectable and resorbable Brushite /  $\beta$ -tricalcium-phosphate ( $\beta$ -TCP) scaffold (chronOS Inject) and impregnated it with a transglutaminase (plasmatransglutaminase – F XIII). We evaluated the activity of the osteogenic protein and the biomechanics of the mixture

**METHODS:** Activation study: In order to evaluate the reaction of the osteogenic protein F XIII to the fluid phase of chronOS Inject (sodium hyaluronate), different PH solutions (ph 4 – 7), sodium hyaluronate and chronOS Inject were mixed with F XIII, the protein activity and F XIII release detected with ELISA.

Biomechanical study: The injectability of the chronOS Inject / F XIII mixture was assessed measuring the force required to inject the mixture through a 1 ml standard syringe without a cannula. 3 repeats were performed with and without F XIII.

**RESULTS:** Activation study: F XIII is not influenced by low pH and the sodium hyaluronate. The release of F XIII from chronOS Inject could not be measured due to clouding of the liquid.

Biomechanical study: We saw an increase of the injection force which increased with the time after mixture and in the presence of F XIII.

**DISCUSSION & CONCLUSIONS:** F XIII is not affected by the liquid phase of chronOS Inject, which therefore may be a good carrier for the

osteogenic protein. In a further test we could remove the clouding by filtration, however to what extend the amount of protein was also reduced needs to be further investigated. Furthermore the osteogenic protein affects the injectability of the cement which may be due to the fact, that the sodium hyaluronate and the protein increase cement viscosity or a change of the liquid / powder ratio. The injectability needs to be optimized testing various liquid / powder ratios in the future in order to produce a hybrid injectable bone substitute.

**REFERENCES:** Benfer J, Struck H. Factor XIII and fracture healing. An experimental study. *Eur Surg Res.* 1977;9(3):217-23

Claes L, Burri C, Gerngross H, Mutschler W. Bone healing stimulated by plasma factor XIII. Osteotomy experiments in sheep. *Acta Orthop Scand* 1985;56(1):57-62

Schlenzka R, v. Garrel T, Pistro C. Does fibrogammin significantly accelerate bone healing? *JBJS [Br]* 1993;75B:Suppl II:100

Kienapfel H, Swain R, Hettel A, Wilke A, Koller M, Griss P. Recombinant and nonrecombinant factor XIII and its effect on bone ingrowth and strength of fixation. *Arch Orthop Trauma Surg.* 1997;116(4):239-43

Ponomarev I, Becker S, Stoll T, Wrabetz E, Alini M, Wilke I. Preliminary results of enhanced osteogenesis by Fibrogammin and mesenchymal stem cells. *Eur Cell Mater* 2003;5,2:80

# The Effect of Pulsed Jet Lavage in Vertebroplasty on Injection Forces of PMMA Bone Cement, Material Distribution and Potential Fat Embolism; a Cadaver Study

L. M. Benneker<sup>1</sup> & A. Gisep<sup>2</sup>

<sup>1</sup> *Inselhospital, Department of Orthopaedic Surgery, University of Berne, CH* <sup>2</sup> *AO Development Institute, Davos, CH*

**INTRODUCTION:** Percutaneous vertebroplasty is an established procedure for the treatment of osteoporotic vertebral fractures. The technique is highly effective in pain reduction and prophylaxis of further fractures but contains the risks of cement leakage or fat embolism, which limits the volume of injected cement to 30 cc or 6 levels at one session.<sup>1,2</sup> In this study, a lavage technique was developed to investigate its effect in vertebroplasty on injection forces, cement distribution and fat wash out.

**METHODS:** 24 vertebral bodies (Th8 – L04) from 5 osteoporotic cadaver spines were grouped in triplets of similar bone mineral density. Previous to PMMA vertebroplasty (Vertecem, Synthes Inc., CH), a pulsatile jet lavage was performed in two groups with 8 specimens each, using a special adaptor for radial irrigation in one group. 100 cc of Ringer solution were injected through one pedicle and regained by low vacuum via the contralateral side. Eight untreated vertebral bodies were used as controls. All vertebrae underwent transpedicular PMMA cement augmentation under standardized conditions injecting 20% of the vertebral volume at constant speed. Injection forces were measured on an Instron universal testing machine, cement distribution was assessed with digital x-rays and CT (Xtreme CT, Scanco Medial, CH). Fat content of the retrieved lavage solution was analysed biochemically.

**RESULTS:** The lavage technique showed to be feasible and reproducible – in all samples the full lavage solution injected could be regained through the contralateral transpedicular access. To date the analysis of the fat content is not complete yet. Injection forces were significantly reduced in both lavage groups compared to controls (*Figure 1*). System failure due to dilatation of the syringe occurred at forces above 300 N in 6 of 8 untreated vertebrae compared to 2 of 16 lavaged specimens. Extravasation of PMMA through a segmental vein was found in digital x-rays in 2 of 8 controls and 2 of 16 lavaged specimens. Distribution analysis by

CT is still ongoing, preliminary data show a more homogenous cement distribution with less extravasation (*Figure 2*).

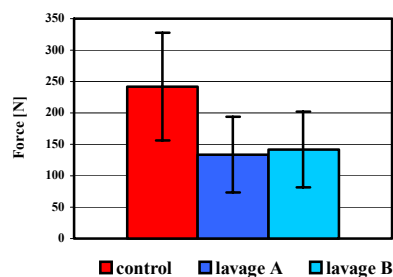


*Fig. 1: Maximal Injection forces [ $\pm 1$  SD, n=8 for each group] at vertebroplasty in untreated (red) and lavaged (blue) vertebrae.*

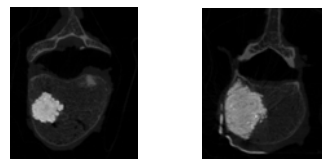


*Fig. 2: CT Sections of a lavaged (left) and an untreated (right) vertebral body.*

**DISCUSSION & CONCLUSIONS:** The data available to date clearly demonstrate a reduced injection force at vertebroplasty after lavage compared to the untreated group. Although we have no complete data yet, the tendency for a more homogenous cement distribution with less extravasation after lavage becomes apparent. The technique of the lavage has shown to be reproducible in intact vertebrae and an easy-to-apply technique. Theoretically the wash out of bone marrow should reduce potential fat embolism at prophylactic cement augmentation of intact osteoporotic vertebrae – clinical trials will be needed.

**REFERENCES:** <sup>1</sup> N. Aebli et al (2002) *Spine* 27:460-6. <sup>2</sup> P. Heini et al (2004) *Orthopaede* 33:22-30.

**ACKNOWLEDGEMENTS:** Synthes Inc. for providing the PMMA cement.

# Biodegradable Polymers in Spinal Surgery - Posterior Lumbar Interbody Fusion with Resorbable Polymer Interbody Cage. Case Report.

D.Bludovsky & M.Choc

Department of Neurosurgery, *Charles University Hospital in Plzen, Czech Republic*

**INTRODUCTION:** We describe a case report of a patient who underwent instrumentation-assisted posterior lumbar interbody fusion with resorbable polymer cages and autograft bone for segmental instability and stenosis of the lumbar spine, and who was the first in Czech Republic treated with resorbable spinal interbody implant.

Bioresorbable polymers have been advocated recently as replacement for metal, carbon fibre and non-resorbable polymeric materials in spinal surgery. These implants can reduce stress shielding having a better match of strength and elasticity to bone [1]. In addition, resorbable polymers are radiolucent, it can facilitate radiographic and neuroimaging analysis of the interbody fusion status.

**METHODS:** Our patient was fifty-four years old man, with a history of fifteen years lasting low back pain with irradiation to inguinal region bilaterally. Objectively he suffered polyradicular sensitive lesion of L3-S1, and light motoric lesion of L2 and L3 bilaterally. X-rays, computed tomography (CT) and magnetic resonance (MRI) of the lumbar spine showed monosegmental L2/3 degenerative changes with disc protrusion and ligamentous hypertrophy in this segment, with pathological motion on dynamic X-rays.

**Operation:** we performed decompressive laminectomy of L2, monosegmental transpedicular fixation of L2-3 segment, discectomy L2/3 and posterior lumbar interbody fusion with two resorbable cages Telamon™ Hydrosorb™ (Medtronic Sofamor Danek) (Fig.1) filled with autograft bone chips from the resected lamina.

The follow up period is twenty four months to date. Subjectively our patient has no pain; he is able to do jogging for long trails from 5 to 15 kilometers as before his problems started. Neurological findings are normal.

**DISCUSSION:** Non-surgical therapies of low back pain are usually unsuccessful for certain injuries and pathologies including degenerative disc disease, stenosis, spondylolysis, and spondylolisthesis. When conservative treatment fails, spinal fusion may be performed.

In our case we used a cage, which consist of 70/30 D,L-poly lactid acid. Polyhydroxy acids are the best known and most studied resorbable polymeric materials for implantation [2].



*Fig.1 Resorbable polymer spinal interbody cage*

The implant slowly degrades by bulk hydrolysis over an 18 to 36 month period, which allows anterior column structural support to gradually shift from the implant do the maturing interbody fusion mass.

In contrary some authors [3] declare, that the disintegration of a polylactid into particles with a very slow hydrolytic degradation rate can induce and maintain a clinically detectable swelling. This fact could imply these polylactid particles can no longer be considered to be fully biocompatible.

We had not found any signs of swelling near the implants, but it was evaluated by CT scans only.

**CONCLUSION:** Early results mentioned in the literature are encouraging, but clinical evaluation is underway. We suppose next studies will show resorbable polymers fully biocompatible and promising spinal interbody devices.

**REFERENCES:** <sup>1</sup> A.R.Vaccaro and L.Madigan (2002) Spinal applications of bioabsorbable implants. *J Neurosurg (Spine 4)* 97:407-412. <sup>2</sup> S.Gogolewski, M.Jovanovic, S.M.Perren et al. (1993) Tissue response and in vivo degradation of selected polyhydroxyacids. *J Biomed Mater Res* 27:1135-1148. <sup>3</sup> J.E.Bergsma, W.C.de Bruijn, F.R. Rozema, et al (1996) Late degradation tissue response to poly(L-lactide) bone plates and screws. *Biomaterials* 16:25-31.

# Fluorcanasite/Frankamenite Based Glass-Ceramics for Bone Tissue Repair

S. Bandyopadhyay-Ghosh<sup>1,2</sup>, A. Johnson<sup>2</sup>, I. M. Reaney<sup>1</sup>, K. Hurrell-Gillingham<sup>2</sup>, I. M. Brook<sup>2</sup>  
and P. V. Hatton<sup>2</sup>

<sup>1</sup>Department of Engineering Materials, Sir Robert Hadfield Building, Mappin Street, University of Sheffield, Sheffield, S1 3JD, UK. <sup>2</sup>Centre for Biomaterials and Tissue Engineering, School of Clinical Dentistry, Claremont Crescent, University of Sheffield, S10 2TA, UK

**INTRODUCTION:** Fluorcanasites/Frankamenites are quadruple chain silicate, have a highly crystalline microstructure of interpenetrating laths that give rise to high flexural strength (>300 MPa) and fracture toughness (>5 MPa m<sup>1/2</sup>)[1]. Miller et al. [2] demonstrated that the addition of excess CaO and P<sub>2</sub>O<sub>5</sub> to the stoichiometric (Ca<sub>5</sub>Na<sub>4</sub>K<sub>2</sub>Si<sub>12</sub>O<sub>30</sub>F<sub>4</sub>) composition induced the early formation of an apatite layer in simulated body fluid. However, no quantitative data regarding their biocompatibility has been published to date, and knowledge of structure-property relationships in these materials remains limited. The aim of this research was therefore to further characterise these modified fluorcanasite glass-ceramics, to evaluate their castability, to compare their *in vitro* biocompatibility with parent glasses. Properties of the fluorcanasite glass and glass-ceramics including ion release, pH were also studied and the data related to biocompatibility.

**METHODS:** Three glass compositions were considered. Glass 1 had the stoichiometric fluorcanasite composition, Glass 2 had an increased calcium concentration and Glass 3 contained P<sub>2</sub>O<sub>5</sub>. These glasses were heat-treated using a two stage heat-treatment process at 520°C/2h and 780°C/2h. The parent glasses and the glass-ceramics were characterised using X-Ray Fluorescence Spectrometry (XRF), Differential Thermal Analysis (DTA), X-Ray Diffraction (XRD) and Scanning Electron Microscopy (SEM). The castability was evaluated with a spiral test piece using lost wax casting route. *In vitro* biocompatibility was investigated using rat osteosarcoma cells (ROS 17/2.8, Merck Inc., USA). The materials were evaluated in both their glassy and crystalline states. Samples and cells were incubated at 37°C in a 5% CO<sub>2</sub> atmosphere for 72 h. SEM was used to observe cell morphology. Quantitative MTT assay was also carried out. Ion release from discs (12 mm diameter × 2 mm thickness) was determined using inductively couple plasma-mass spectrometry (ICP-MS) and the change of pH in de-ionised distilled water was measured using a calibrated pH meter.

**RESULTS:** XRF data showed a close similarity between the pre-melt and post-melt molar compositions. The DTA curves of glasses showed exothermic peaks that were assigned to the crystallisation of various phases, identified by XRD. Essentially Glass 1, 2 and 3 crystallised to form frankamenite (Glass 1), frankamenite, fluorcanasite, xonotlite (Glass 2) and frankamenite, fluorcanasite, xonotlite, and fluorapatite (Glass 3). The microstructures obtained from fractured surfaces of the glass-ceramics consist of interlocking crystals of the strengthening chain silicate phase. These modified fluorcanasite glasses had excellent relative castability. SEM images from samples which had been tested for biocompatibility showed that cells had colonized the surfaces of fluorcanasite glass-ceramics to form a confluent sheet to a greater degree than their parent glasses. Quantitative MTT assay results were in good agreement with the qualitative SEM observations. The ion release and pH data suggested a close relationship between solubility (in particular sodium release) and biocompatibility.

**DISCUSSION & CONCLUSIONS:** Fluorcanasite and Frankamenite are the major crystalline phases in these glass-ceramics. Excellent relative castability of these modified fluorcanasite glasses confirming that they may be useful for the fabrication of custom prostheses via the lost wax casting. Incorporation of excess CaO (Glass 2) and P<sub>2</sub>O<sub>5</sub> (Glass 3) in stoichiometric glass composition (Glass 1) improved *in vitro* biocompatibility. Controlled heat-treatment improved *in vitro* biocompatibility of modified fluorcanasite glass-ceramics compared to their parent glasses. Reduced solubility and related pH effects appeared to be the principal mechanisms responsible for improvement in *in vitro* biocompatibility.

**REFERENCE:** <sup>1</sup>G. H. Beall (1991) *J Non-Cryst Solids*, **129**:163-173. <sup>2</sup>C. A. Miller, T. Kokubo, I. M. Reaney, P. V. Hatton and P. F. James (2002) *J Biomed Mater Res*, **59**: 473-480.

# Synthesis and *In Vitro* Cell Culture of Zn-doped Calcium Phosphates

C. L. Burchfield, A. E. Tate, S. Jalota, S. B. Bhaduri & A. C. Tas

School of Materials Science & Engineering, Clemson University, Clemson, SC 29634, USA

**INTRODUCTION:** The human nutritional need for zinc is small, but its role in growth and well-being is enormous, starting even before birth. Zinc is an essential trace element in a variety of cellular processes including DNA synthesis, behavioral responses, reproduction and virility, bone formation, bone growth and wound healing [1]. The necessity of Zn for bone growth was demonstrated by the observation that normal bone growth was retarded in animals that are Zn-deficient [2], and the addition of zinc to these deficient diets resulted in a stimulation of both bone growth and mineralization [3]. Zinc has been implicated in bone formation, mineralization, and the stimulation of ALP activity in calvarial organ cultures [4, 5], osteoblast-like cell cultures, as well as the stimulation of the bone DNA synthesis via the activation of bone DNA polymerase [6]. We have recently developed inexpensive wet methods for synthesizing Zn-doped (600 to 9000 ppm)  $\beta$ -tricalcium phosphate ( $\beta$ -TCP) or Zn-doped hydroxyapatite (HA) bioceramics. Synthesis procedures and the results of rat calvarial osteoblast culture studies will be presented.

**METHODS:** For the synthesis of Zn-doped  $\beta$ -TCP bioceramics, novel Zn-doped brushite (DCPD:  $\text{CaHPO}_4 \cdot 2\text{H}_2\text{O}$ ) powders were prepared and then used as precursors. Zn-doped DCPD powders were synthesized at RT by using aqueous solutions of  $\text{CaCl}_2 \cdot 2\text{H}_2\text{O}$ ,  $\text{KH}_2\text{PO}_4$ ,  $\text{Na}_2\text{HPO}_4$ , and  $\text{Zn}(\text{NO}_3)_2 \cdot 6\text{H}_2\text{O}$ . Zn-doped DCPD powders were then mixed with small amounts of  $\text{Ca}(\text{OH})_2$  and hydrothermally-converted at  $90^\circ\text{C}$  into Zn-doped Ca-deficient hydroxyapatite ( $\text{Ca/P molar}=1.50$ ). These Zn-doped CDHA powders were finally calcined at  $850\text{--}1000^\circ\text{C}$  to form single-phase Zn- $\beta$ -TCP bioceramics. On the other hand, for the synthesis of Zn-doped HA powders, transparent solutions ( $\text{Ca/P}=1.50$ ) containing  $\text{Ca}(\text{NO}_3)_2 \cdot 4\text{H}_2\text{O}$ ,  $\text{Zn}(\text{NO}_3)_2 \cdot 6\text{H}_2\text{O}$ ,  $\text{NH}_4\text{H}_2\text{PO}_4$  and  $\text{H}_2\text{NCONH}_2$  were first prepared at RT [7]. These solutions were first aged in glass bottles at  $80^\circ\text{C}$ , and then the obtained precipitates were calcined at  $850^\circ\text{C}$  in air. Powder characterization was performed by XRD, FT-IR, TG/DTA, SEM, ICP-AES analyses, and by surface area measurements. Rat osteoblasts (7F2, ATCC) were cultured on these samples from 3 to 7 days. Cell viability histograms (as a function of Zn content) and ALP activities were determined.

**RESULTS:** SEM micrographs of Fig. 1 depicted the morphology of 3000 ppm Zn-doped  $\beta$ -TCP and 3000 ppm Zn-doped HA bioceramics. Prior to calcinations, the obtained Zn-doped CDHA powders had surface areas  $>45\text{ m}^2/\text{g}$ .

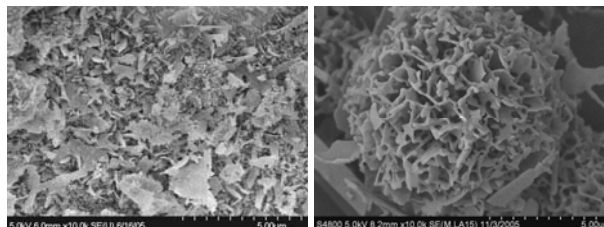


Fig. 1: Morphology of Zn-doped  $\beta$ -TCP (left) vs. Zn-doped HA (right); both heated at  $850^\circ\text{C}$ , 6h.

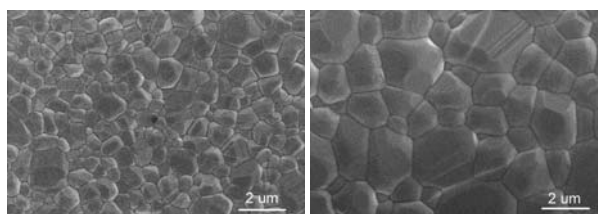


Fig. 2: 3000 ppm Zn-doped  $\beta$ -TCP (left) vs. 4000 ppm Zn-TCP (right); both heated at  $1000^\circ\text{C}$  for 6 h.

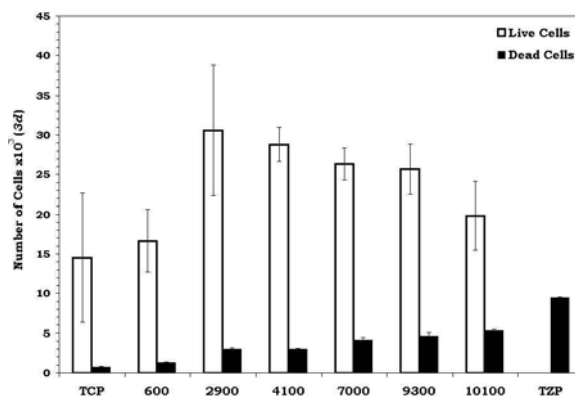


Fig. 3: Cytotoxicity of Zn-doped  $\beta$ -TCP vs.  $\text{Zn}_3(\text{PO}_4)_2$

**CONCLUSION:** Zn-doping improved both the densification behavior and osteoblast viability on the  $\beta$ -TCP and HA bioceramics of this study.

**REFERENCES:** <sup>1</sup> D.G. Barceloux (1999) *J Toxicol Clin Toxic* **37**:279. <sup>2</sup> G. Oner, et al. (1984) *Endocrinology* **114**:1860. <sup>3</sup> M. Yamaguchi, et al. (1987) *Pharmacol* **36**:4007. <sup>4</sup> D.L. Bougle, et al. (2004) *J Trace Elem Med Bio* **18**:17. <sup>5</sup> M. Yamaguchi, et al. (2004) *J Health Sci* **50**:75. <sup>6</sup> Z.J. Ma, et al. (2001) *Calcif Tissue Int* **69**:108. <sup>7</sup> A.C. Tas, et al. (2001) *J Mater Sci Lett* **20**:401.

# Laser Preconditioning on Irradiated Bone: A Preliminary Intravital Study

S.Desmons<sup>1,2</sup>, C.Delfosse<sup>1</sup>, P.Rochon<sup>2</sup>, G.Leroy<sup>1</sup>, S.Mordon<sup>2</sup>, G.Penel<sup>1</sup>

<sup>1</sup>LBM Raman, Faculté de Chirurgie Dentaire, Lille, France <sup>2</sup>UPRES EA 2689 INSERM IFR 114, Pavillon Vancostenobel, CHU Lille, France

**INTRODUCTION:** Radiotherapy used in head and neck cancer, induces a chronic antiangiogenic effect on bone. This leads to a bone remodelling and a healing process reduction (Marx, 1983). The application of a control thermal stress before a second injury induces a cytoprotective effect on tissues and promotes tissue recovering (Perdrizet et al., 1999). So, the present study aims to investigate the effects of a laser preconditioning as a thermal stress on irradiated bone. The use of an intravital model allows a long term follow up of a single bone site.

**METHODS:** An optical transcutaneous chamber is implanted on rabbit calvaria (Penel et al., 2005). Twelve rabbits are divided in four groups:

- group 1) single 18.75Gy X-rays irradiation (n=3),
- group 2) laser irradiation (48J/cm<sup>2</sup>) (n=3),
- group 3) laser irradiation (48J/cm<sup>2</sup>) 24 hours before X-rays irradiation (18.75Gy) (n=3) and,
- group 4) control (n=3).

Intravital microscopic pictures are acquired weekly during 130 days with a digital camera. Image processing is performed to estimate the vascular density (VD). It is defined as the ratio of blood vessel pixels over all pixels in a region of interest. Statistical analysis is performed to compare the evolution of VD between the different groups.

**RESULTS:** After a healing postoperative phase, VD remains stable as it's shown in the group control. The experimentations are achieved during this period. Results are presented on table1. For the group1), vascularisation decreases immediately after X-rays irradiation and remains below the initial value during all the study. We describe a temporary VD's instability in the group 2). For the group 3), which received laser before radiotherapy, VD decreases in a first time, but statistically less than in the group 1) (p<0.001). Then, we observe an increase of VD on the long term tending to reach the initial value.

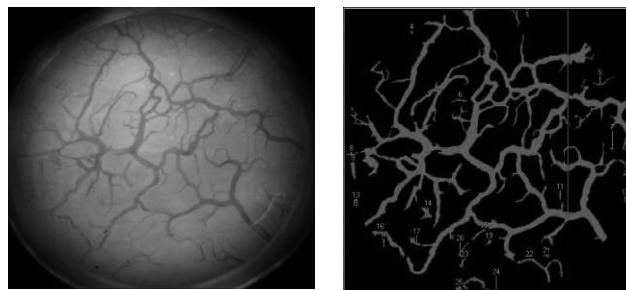
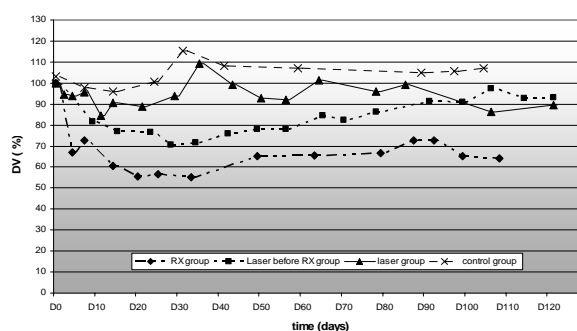


Fig. 1.a: Original picture of the bony site through the optical chamber. Fig. 1.b: Data processing to calculate the vascular density.

Table 1. Evolution of the vascular density.



**DISCUSSION & CONCLUSIONS:** With this new model and imaging technique, microscopic intravital observations allow to evaluate VD in a reproducible manner. Radiotherapy leads to a high decrease of the superficial bone vascularisation which persists at least 120 days. A laser preconditioning seems to induce protective effects opposite to the antiangiogenic effects of X-rays irradiation.

## REFERENCES:

- MARX R. E. (1983) *J Oral Maxillofac Surg* **41**(5), 283-8.  
 PENEL G., et.al (2005) *Bone* **36**(5), 893-901.  
 PERDRIZET G. A., et.al (1999) *Ann N Y Acad Sci* **874**, 320-5.

# Pure and Doped Bioactive Glasses Synthesised by Melt Derived and Sol-gel Methods

E.Dietrich<sup>1</sup>, H.Oudadesse<sup>1</sup>, A.Lucas-Girot<sup>1</sup>, Y.Legal<sup>1</sup>, M.Mami<sup>1,2</sup>, R.Sridi-Dorbez<sup>2</sup>

<sup>1</sup> *Biomatériaux, LCSIM – UMR 6511, Université de Rennes 1, 263 av. du g<sup>al</sup> Leclerc, Rennes, FRANCE*

<sup>2</sup> *Faculté des Sciences de Monastir, Laboratoire de physico-chimie, Monastir, TUNISIE*

**INTRODUCTION:** The bioactivity of glasses was attributed to the apatite layer formed on the surface of glass in the body. Dissolution of ions from the glass was considered to play an important role in forming this layer. This indicated that various kinds of bioactive materials with different characteristics could be developed from CaO-SiO<sub>2</sub>-based glasses. The aim of this work was to study the effect of both composition and synthesis method on the *in vitro* bioactivity of our glasses. Moreover, their reactivity was studied after introduction of magnesium as doping element.

**METHODS:** The glasses compositions are shown in Table 1.

	SiO <sub>2</sub>	CaO	P <sub>2</sub> O <sub>5</sub>	Na <sub>2</sub> O
46S6 (fusion)	46	24	6	24
60S4 (sol-gel)	60	36	4	

Table 1. Glass compositions studied (wt%)

High purity silica and reagent grade calcium carbonate, phosphorus pentoxide and sodium carbonate were weighed and mixed. The glasses were melted in a platinum crucible at 1300°C for 1h and poured into brass moulds to form (13 mm × 10 mm) cylinders. After annealing for 2h at 540°C, the cylinders were cut, coated with resin and polished into discs of 8 mm height. Sol-gel glasses were prepared by hydrolysis and polycondensation of tetraethyl orthosilicate (TEOS), triethyl phosphate (TEP) and Ca(NO<sub>3</sub>)<sub>2</sub>·4H<sub>2</sub>O. Nitric acid 2M was used to catalyse the TEOS and TEP hydrolysis, using a molar ratio of (HNO<sub>3</sub>)/(TEOS + TEP) = 8. The discs of 13 mm diameter and 2 mm height were formed using 0.5g dried gels compacted uniaxially at room temperature at 740 MPa and stabilised by heating in air at 700°C for 3h.

The glass discs were analysed before and after immersion in the SBF-K9 solution, prepared according to the method proposed by Kokubo et al. [1].

**RESULTS:** The variations of ionic concentrations of the SBF solution were studied versus time after immersion using induced coupled plasma spectroscopy (ICP). Changes in the morphology, composition and crystalline phases formed on the

surface of the discs, after soaking in the SBF were also analysed using SEM, XRD and IR methods.

*46S6 (fusion):* The quantitative analysis of the Ca and P ions indicates that hydroxycarbonate apatite (HCA) formation starts after 8h in SBF-K9 solution. This observation was confirmed by XRD pattern, which showed peaks that could be assigned to (211) and (002) apatite reflections. IR spectra reveal the absorption bands of phosphate groups (602 and 565 cm<sup>-1</sup>), which are a characteristic feature of phosphate in crystalline phases.

*46S6 with 1,2% Mg (fusion):* We observed on XRD pattern peaks at 26° and 32° 2θ, but after a longer time of immersion than for pure glass. On IR spectra, others bands appear, characteristic of a new phase formed on the surface of glasses.

*60S4 (sol-gel):* On the XRD pattern and IR spectra, the same apatite reflections ((211) and (002)) and phosphate absorption bands (604 and 572 cm<sup>-1</sup>) are observed. However, the ICP analysis shows that the rate of HCA formation is better: growth of the layer starts only 4h in SBF solution.

**DISCUSSION & CONCLUSIONS:** The non-porous surfaces of melt-derived 46S6 glasses exhibited lower rate of surface HCA layer formation than 60S4 sol-gel glasses. The highly porous texture of our sol-gel glass causes formation of a dense gel layer resulting from the large number of nucleation sites [2].

The presence of magnesium as doping element affects the rate of growing of the HCA layer and the possible formation of secondary phases which compete in stability with the apatite-like phase.

This work will be completed by the study of effects of zinc, strontium and both as doping elements, in order to determine the most interesting composition with introduction of these three elements. *In vitro* tests in a cell culture media are in progress.

**REFERENCES:** [1] T.Kokubo, H.Kushitani, S.Sakka, (1990) *J. Biomed. Mater. Res.*, 721.

[2] P.Sepulveda, J.R.Jones, L.L.Hench (2002) *Biomaterials*, 301-311.

# Injectable Bone Substitutes of Silica-contained Calcium Phosphates and a Hydrophilic Polymer

S.V. Dorozhkin

*Independent, Kudrinskaja sq. 1-155, 123242 Moscow, Russia*

**INTRODUCTION:** In recent years, self-setting calcium phosphate cements have been of considerable interest in orthopedic and dental applications [1]. Calcium phosphates have also been used as components or fillers in polymeric composites in association with polymers such as polysaccharides [2]. However, these products have not proved efficiency for bone osteoconduction and ingrowth. It has already been demonstrated that porosity is required for bone ingrowth [3]. The aim of this study is to present the results obtained from elaboration of an injectable bone substitute paste based on silica-contained calcium phosphates and a hydrophilic polymer.

**METHODS:** The polymer used for this study was hydroxypropylmethylcellulose (HPMC; Walocel<sup>®</sup> HM 100000 PA, Wolff Cellulosics, Germany). This polymer was dissolved in deionized water (polymer concentration: 2% w/w), and the solution was stirred for 2 days. The calcium phosphate fillers were composed of a homogeneous mixture of silicon-substituted  $\alpha$ -tricalcium phosphate (50-60% w/w), hydroxyapatite (30-40% w/w) and  $\beta$ -tricalcium phosphate (balance) synthesized as described elsewhere [4]. Fluidal composites were prepared by mixing calcium phosphate powder with polymer solution under ambient conditions. Afterwards the mixtures were placed in 12-mL glass bottles which were sealed and steam sterilized in an autoclave for 20 min at 121°C according to pharmacopeial procedure. To study the influence of polymer on the suspension properties, viscosity measurements (Brookfield RDV11, 1 rpm) were performed with different ratios of polymer solution/solid calcium phosphates.

**RESULTS:** Injectable bone substitutes need to pass through narrow channels (e.g., syringe tube) without phase alteration or demixing. Previous apparent viscosity measurements and extrusion tests have indicated that macromolecules are most suitable for this purpose [5]. The mixture remains liquid up to a concentration of 57-58% of calcium phosphates and then suddenly becomes plastic, increasing slightly in viscosity. Exceeding 60-61% of the mineral phase, the aqueous suspension becomes solid because the different composite

strata cannot slide. Measurements become impossible since the viscometer only records friction between the heavy mixture and the analysis spindle. Addition of a polymer allows the viscosity of the suspension to increase rapidly and substantially. The plasticity zone in which the material remains injectable is considerably enlarged. In extrusion experiments, a study of molecular weight and polymer concentration showed that the best carrier had a heavy molecular weight. However, the viscosity degree was limited because friction with the needle wall became too strong.

**DISCUSSION:** This material is a viscous suspension. The stability of any suspension depends on many parameters, including the sedimentation laws. The polymer concentration increasing decreases the sedimentation kinetics but does not influence the sedimentation ratio. Rapid phase segregation occurs without HPMC and granule compaction is maximal. With polymer all small pieces of calcium phosphates are separated from each other by the macromolecular gel. Therefore, this suspension can be compared with interconnected macroporous block ceramics.

**CONCLUSIONS:** The experiments reported here facilitate the choice of molecular weight and the degree of substitution suitable for specific medical indications. Unfortunately, the flow behavior of a mixture cannot be predicted with mathematical precision because of the many parameters that influence the rheology. The greatest challenge is to understand the implications of each parameter in order to produce effective injectable bone substitutes.

**REFERENCES:** <sup>1</sup> M. Bohner and G. Baroud (2005) *Biomaterials* **26**:1553-63. <sup>2</sup> O. Gauthier, R. Muller, D. von Stechow, et al. (2005) *Biomaterials* **26**:5444-53. <sup>3</sup> A. C. Tas (2005) *Ceramic Transactions* **147**:15-24. <sup>4</sup> M. Sayer, A. D. Stratilatov, J. Reid, et al. (2003) *Biomaterials* **24**:369-82. <sup>5</sup> G. Grimandi, P. Weiss, F. Millot and G. Daculsi (1998) *J Biomed Mater Res* **39**:660-66.

# Using XRD, FTIR and TGA to Monitor Conversion of a Novel, Injectable Calcium Phosphate Cement

M. Geiger<sup>1</sup>, A. Hina<sup>2</sup>, S. Sofia<sup>1</sup>, N. Warne<sup>1</sup>

<sup>1</sup> Wyeth BioPharma, One Burt Rd, Andover MA 01810, U.S.A. <sup>2</sup> ETEX Corporation, 38 Sidney St., Cambridge MA 02139, U.S.A.

**INTRODUCTION:** For application of rhBMP-2 in bone fracture repair, a calcium phosphate powder based on amorphous calcium phosphate (ACP) and dicalcium phosphate dihydrate (DCPD) is mixed with protein solution to form an injectable paste (Fig. 1). Upon contact with (warm) fluid, the material starts to convert to poorly crystalline hydroxyapatite (pcHA), which is structurally similar to the mineral phase of bone.



Fig. 1: Injection into warm saline – after 5 min

There was some evidence that conversion may also occur upon contact of the powder with moisture from the environment, which is undesirable for stability reasons. The **objective** of this work was to evaluate X-ray diffraction (XRD), Fourier-transform infrared spectroscopy (FTIR), and thermogravimetric analysis (TGA), for characterization and their potential to quantify conversion.

**MATERIALS AND METHODS:** The calcium phosphate matrix (CPM) (supplied by ETEX Corporation) consists of a mixture of ACP, DCPD and sodium bicarbonate powders. Fully converted CPM was obtained by curing in aqueous buffer (37°C for 24 hours) and subsequent drying. Binary mixtures of unconverted and fully converted powders were used to generate standard curves. Powder samples of unknown degree of conversion were generated: 1) in a Dynamic Vapor Sorption instrument (SMS, USA), 2) by long-term storage in monitored incubators, and 3) by interrupting the conversion process of CPM paste in aqueous buffer (37°C) by snap-freezing in liquid nitrogen and freeze-drying. **XRD:** 5-40° (2 Theta; Cu ka) at 0.02°/step. **FTIR:** KBr pellets (transmission), 4000-400cm<sup>-1</sup>. **TGA:** 25 to 250°C at 5°C/min. The data were analyzed using the respective analytical software or with Microcal™ Origin™ 7.0.

**RESULTS:** With XRD and FTIR, there are two approaches to determine conversion: either assessing the decrease in peaks characteristic for

DCPD (which had previously been found to be the slowest in converting to pcHA [2]), or the increase in peaks characteristic for pcHA. Accordingly, the regions selected were 11.6 and 32° in XRD scans, and 527 and 600 cm<sup>-1</sup> in FTIR spectra. TGA profiles show a very reproducible sharp mass loss between 175 and 200°C (loss of crystal water from DCPD). With all three methods, it was possible to generate linear calibration curves with R<sup>2</sup>≥0.96. The paste was shown to fully convert within approx. 4 h (Fig. 2). The powder samples generated in the DVS showed various degrees of conversion after 2 days exposure to elevated temperatures at 75%RH. For all samples analyzed, the three analytical methods yielded comparable results and accordingly similar trends.

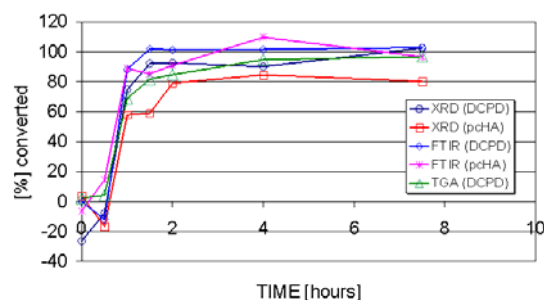


Fig. 2: Conversion kinetics in PBS at 37°C

**CONCLUSIONS:** CaP cement powders may be subject to conversion to pcHA when exposed to humid air and/or elevated temperatures. XRD, FTIR and TGA deliver specific signals for the conversion process. TGA is currently considered to be the most reproducible yet simple method for our material, but the three methods deliver valuable complementary information (e.g. XRD shows that HA of slightly higher crystallinity was forming in powder samples over extended time periods). The techniques are useful for evaluating conversion kinetics of the CaP cement pastes, as well as for stability assessments.

## REFERENCES:

[1] Wikesjo U.M. et al., Clin. Implant Dent. Rel. Res. 4(4) (2002) 174-82. [2] Tofighi A. et al., Sixth World Biomaterial Congress Transactions, Kamuela, Hawaii (2000), #1302.

# Effect of Mg<sup>2+</sup> Content on Lattice Parameter and Phase Transformation Temperature of $\beta$ - $\alpha$ TCP

F. Goetz-Neunhoeffler<sup>1</sup>, J. Neubauer<sup>1</sup>, M. Göbbels<sup>1</sup> & R. Enderle<sup>2</sup>

<sup>1</sup> Department of Mineralogy, University of Erlangen-Nuremberg, D. <sup>2</sup> Department of Materials Science and Engineering, University of Erlangen-Nuremberg, D.

**INTRODUCTION:** Tricalcium phosphate Ca<sub>3</sub>(PO<sub>4</sub>)<sub>2</sub> (TCP), an osteoconductive as well as bioresorbable phase, has found application as bone cement and bone implant material. TCP can crystallize in three polymorphic modifications:  $\beta$ -TCP below 1180 °C,  $\alpha$ -TCP between 1180 °C and 1430 °C, and  $\alpha'$ -TCP above 1430 °C [1]. Mainly  $\beta$ -TCP and  $\alpha$ -TCP have reached acceptance in biomedical applications. At the moment  $\beta$ -TCP ceramics are used for non load-bearing applications in oral surgery. In this investigation the determination of the influence of partial Mg<sup>2+</sup> substitution of Ca<sup>2+</sup> in the solid solution series of  $\beta$ -TCP (Ca<sub>1-x</sub>Mg<sub>x</sub>)<sub>3</sub>(PO<sub>4</sub>)<sub>2</sub> was determined at 1025 °C ± 10 °C in air. The temperatures for  $\beta$ - $\alpha$ -phase transformation were determined in dependence of the Mg<sup>2+</sup> content.

**EXPERIMENTAL METHODS:** Syntheses of  $\beta$ -TCP powders were carried out by solid-state reaction in a chamber furnace at 1025 °C ± 10 °C in air. The starting materials - high purity (NH<sub>4</sub>)<sub>2</sub>HPO<sub>4</sub> (>99 %, Fluka), MgO (>98 %, Fluka) and CaCO<sub>3</sub> (99.99%, Fluka) - were mixed in proper molar ratios, homogenized in an agate disc mill, and dried at 195 °C. After further homogenization in a disc mill, the samples were sintered for 2.5 hours at 1025 °C. Phase composition was examined by quantitative X-ray powder diffraction (XRPD) in combination with Rietveld refinements. All powders were proven to be single-phase  $\beta$ -TCP. Rietveld refinement was performed using the structural models (ICSD Database) of all possible occurring secondary phases listed in Table 1.

Table 1: ICSD data for Rietveld refinements

Phase	Mineral/name	ICSD-Code
$\beta$ -Ca <sub>2</sub> P <sub>2</sub> O <sub>7</sub>	$\beta$ -C <sub>2</sub> P	73712
Ca <sub>10</sub> (PO <sub>4</sub> ) <sub>6</sub> (OH) <sub>2</sub>	HAP (Hydroxyapatite)	87668
$\beta$ -Ca <sub>3</sub> P <sub>2</sub> O <sub>8</sub>	$\beta$ -TCP (Whitlockite)	6191
$\alpha$ -Ca <sub>3</sub> P <sub>2</sub> O <sub>8</sub>	$\alpha$ -TCP	923
(CaMg) <sub>3</sub> P <sub>2</sub> O <sub>8</sub>	Stanfieldit	23642

Refined parameters were scale factor, zero displacement, background as Chebyshev polynomial of 5th grade, crystallite size, micro

strain and lattice parameters. Occupancy factors were included in case of refinement of the Mg-doped solid solutions of  $\beta$ -TCP, whereby the scattering factor of P<sup>5+</sup> was assumed for phosphorous in tetrahedral coordination.

**RESULTS:** Substitution of Ca<sup>2+</sup> by Mg<sup>2+</sup> in the  $\beta$ -TCP structure at 1025 °C ± 10 °C is correlated with a decrease of the lattice parameters. Refinement from lattice parameters led to the composition of the end member of the solid solution. At a temperature of 1025 °C ± 10 °C up to 14 mole% of Ca<sup>2+</sup> can be replaced by Mg<sup>2+</sup> in the  $\beta$ -Ca<sub>1-x</sub>Mg<sub>x</sub>)<sub>3</sub>(PO<sub>4</sub>)<sub>2</sub>. For the described synthesis conditions the Mg-rich end member of the solid solution has the formula (Ca<sub>0.86</sub>Mg<sub>0.14</sub>)<sub>3</sub>(PO<sub>4</sub>)<sub>2</sub>[2]. Additionally the occupation factor of the Ca(4) and Ca(5) sites of the  $\beta$ -TCP structure by Mg<sup>2+</sup> ions could be calculated by Rietveld refinement of the XRD data. The course of lattice parameters can be attributed to the stepwise occupation by Mg<sup>2+</sup> on the two different Ca<sup>2+</sup> sites. Rietveld refinement has proven to be a very powerful tool in terms of characterization of the synthesized TCP samples and optimization of the synthesis conditions.

Transformation temperature of  $\beta$ - $\alpha$  TCP can be increased from 1150 °C (Mg<sup>2+</sup>-free) to 1540 °C with a Mg<sup>2+</sup>-substitution on Ca<sup>2+</sup> sites of 8 mole %. Samples with higher substitution than 10 mole % Mg<sup>2+</sup> are not affected by the  $\alpha$ - $\beta$  transformation since the melting points were reached before transformation could take place. The formed melt fills up existing pores and thus lead to completely dense ceramic. Higher temperatures during sintering process lead to denser TCP ceramics and thus better mechanical properties. Sintering of Mg-containing TCP ceramics can be performed at much higher temperatures.

**REFERENCES:** <sup>1</sup> Elliott, J.C. 1994 *Structure and Chemistry of the Apatites and Other Calcium Orthophosphates* <sup>2</sup> Enderle, R., Götz-Neunhoeffler, F., Göbbels, M., Müller, F., Greil, P. 2005 Influence of Magnesium-doping on the phase transition temperature of  $\beta$ -TCP ceramics; *Biomaterials*; **26**(17): 3377-3769

# A Novel Experimental Approach to Imaging and Quantifying Newly Bone Formation Around Bone Substitutes

A. Gorustovich<sup>1,2</sup>, M. Sivak<sup>1</sup> & M.B. Guglielmotti<sup>1,2</sup>

<sup>1</sup> Department of Oral Pathology, School of Dentistry, University of Buenos Aires. <sup>2</sup> National Research Council (CONICET), Argentina

**INTRODUCTION:** Confocal laser scanning microscopy (CLSM) is a relatively new optical imaging technique that has been exploited extensively in the biological community over the past decade [1]. Despite the widespread use of CLSM, application of CLSM in the field of biomaterials is still limited. The aim of the present study was to use CLSM to image and characterize ground sections of undecalcified rat bone tissue with *in situ* bioceramic implants.

**METHODS:** Male Wistar rats (n: 10) weighing  $100 \pm 20$  g were used throughout. All the animals were anesthetized by i.p. administration of a 4:1 solution of ketamine/xylazine at a dose of 0.15 mL per 100 g body weight. Boron-modified melt-derived 45S5 bioactive glass (BG) particles (300-350  $\mu$ m) [2] were placed inside the medullary compartment of the tibiae following a previously described surgical technique [3]. The animals were killed 30 days after implantation. The guidelines of the NIH for the care and use of laboratory animals (NIH Publication N° 85-23, Rev. 1985) were observed. The tibiae were resected, fixed in 20% formalin solution, and radiographed.

**Histologic Processing-** The tibiae were stained in 1% basic fuchsin in absolute ethanol following the Frost's bulk-staining technique [4], and embedded undecalcified in methyl-methacrylate resin. The samples were then sectioned using a diamond saw (Exakt Apparatebau, Germany) and three slices were cut at approximately 500  $\mu$ m, perpendicular to the longest axis of the tibiae; that is, through the middle of the implant bed and through two points equidistant from the middle. The cross sections were ground using a grinding machine and finished manually with sandpaper to obtain sections about 100  $\mu$ m thick, and mounted on glass slides and coverslipped for histologic analysis. A confocal laser scanning Zeiss Pascal LSM 5 equipped with a HeNe laser and a Zeiss Axioplan 2 Imaging microscope (Carl Zeiss, Germany) was used to image specimens in the confocal fluorescence mode. Ground sections were examined using 543 nm wavelength excitation and a long-pass 560 nm emission filter. Sequential

optical sections at an interval of 10 $\mu$ m/section were collected using a 10X(AN0.30) objective to

build a 50  $\mu$ m thick stack of images. In addition, sequential images taken at 1 $\mu$ m/section were acquired using a 40X (NA1.3) objective so that each final image had an effective thickness of 10  $\mu$ m.

**RESULTS:** Confocal images revealed that a large proportion of BG particles was surrounded by reactive medullary bone. Bone tissue bridges were observed between BG particles (Fig. 1A). A close bone-to-implant contact was detected at the interface (Fig. 1B).

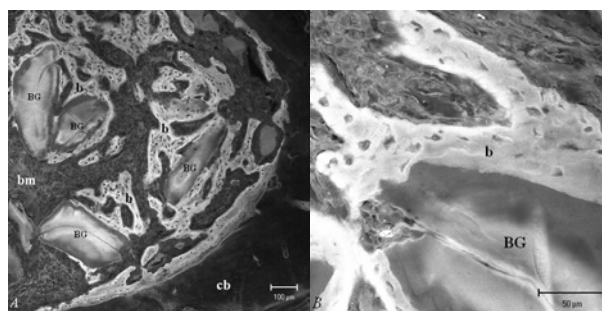


Fig. 1: (A) Stack of images, 50  $\mu$ m thickness. (B) Stack of images, 10  $\mu$ m thickness BG: bioactive glass; b: newly formed bone; bm: bone marrow; cb: cortical bone.

**DISCUSSION & CONCLUSIONS:** In this study we show that CLSM allowed rapid non-destructive optical serial sectioning of thick ground sections of undecalcified bone tissue with *in situ* bioceramic implants. The methodology described herein could prove useful to perform histomorphometric analysis of the bone tissue surrounding implant materials providing optimally thin optical sections in order to obtain reliable results.

**REFERENCES:** <sup>1</sup> J.K. Sugden (2004) *Biotech & Histochem* **79**: 71-90. <sup>2</sup> A. Gorustovich, et al (2005) *Key Eng Mater* **284-286**: 913-16. <sup>3</sup> A. Gorustovich, et al (2002) *Int J Oral Maxillofac Implants* **17**: 644-50. <sup>4</sup> D.B. Burr and T. Stafford (1990) *Clin Orthop Rel Res* **260**: 305-8.

**ACKNOWLEDGEMENTS:** Grants: ANPCyT PICT 0511870, UNSa 1309, UBA 0020 and CONICET PIP 6042.

# Evaluation of *In Vitro* Bioactivity of Different Types of Biomaterials

L. Hermansson<sup>1,2</sup>, A. Faris<sup>2</sup>, and H. Engqvist<sup>1,2</sup>

<sup>1</sup> *Doxa AB, Axel Johanssonsgata 4-6, 754 51 Uppsala, Sweden.* <sup>2</sup> *Materials Science Department, The Angstrom Laboratory, Uppsala University, Box 534, 751 21 Uppsala, Sweden.*

**INTRODUCTION:** Biomaterials are often classified as inert, biodegradable or bioactive materials. For all known bioactive materials an interfacial layer of apatite towards the tissue is formed [1-2]. This finding is used in *in vitro* tests in screening potentially bioactive materials. In this study different types of potentially bioactive materials including a metal, an oxide and some chemically bonded ceramics were evaluated

**METHODS:** The *in vitro* tests were conducted according to the outline in the ISO-standard ISO/WD 23317. This standard describes a procedure for producing simulated body fluid (SBF), sample preparation, immersion and analysis techniques. For analyses of possible apatite formation scanning electron microscope (SEM), energy dispersive X-ray spectroscopy (EDX) and X-ray diffraction (XRD) were used. The samples were also embedded and cross sectioned in attempt to measure the thickness of the layer formed on the sample surface.

**MATERIALS:** The materials tested were cp Ti, Al<sub>2</sub>O<sub>3</sub> and three chemically bonded ceramics, namely a Ca-phosphate, a Ca-aluminate and a Ca-silicate. Ti and Al<sub>2</sub>O<sub>3</sub> were also tested after surface activation. The activation of titanium and alumina was done by immersion in 5.0 M NaOH aqueous solution at 60°C for 24 h followed by a gentle washing in distilled water. After the NaOH treatment the samples were annealed at a rate of 5°C/min and kept at 600°C for an hour. The cooling rate was kept at approximately 5°C/min.

**RESULTS:** The elemental and phase analyses both indicated Ca-phosphate formation on most of the materials tested. The growth rate of the different materials varied. In Fig. 1 the elemental analysis of the layer formed on the Ca-aluminate is presented together with layer of the surface activated titanium. The four largest peaks are O, P, Ca and Al for the Ca-aluminate case and O, P, Ca and Ti for the titanium case. Phase analysis of the layer formed on Ca-silicate showed an amorphous structure.

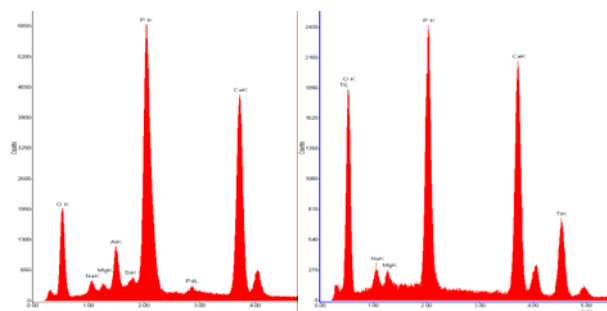


Fig. 1: Elemental composition of layer formed on Ca-aluminate (left) and surface activated Ti (right) in simulated body fluid.

**DISCUSSION & CONCLUSIONS:** From what can be seen from the experiments and analyses in this study all three bone cements show *in vitro* bioactivity. This indicates these materials as promising candidates for implants intended to bond to bone. However in order to determine true bioactivity *in vivo* tests are necessary. Just as the cements, the activated titanium also shows *in vitro* bioactivity. As was seen the alumina could not be activated to form a hydroxyapatite layer *in vitro* by this method. Li et al, however, claim to have activated alumina by a similar process [3]. The interpretation was done based on a cell culture testing by measuring the difference in adhered cells between treated and non-treated alumina. The results will be discussed in relation to established bioactive materials such as hydroxyapatite and Bioglass®.

**REFERENCES:** <sup>1</sup>L. Hench, Biomaterials: a forecast for the future, *Biomaterials* **19** (1998) p 1419-1423, <sup>2</sup>L. Hermansson, L. Kraft, H. Engqvist, Chemically bonded ceramics as biomaterials, *Key Eng. Mat.* **24** (2003) p 437-442, <sup>3</sup>Li, P., Ohtsuki, C., Kokubo, T., Nakanishi, K., Soga, N. & de Groot, K. (1994) Role of hydrated silica, titania, and alumina in inducing apatite on implants. *Journal of Biomedical Materials Research*, **28**, 7-15.

**ACKNOWLEDGEMENT:** Part of this work was financed by Göran Gustafsson Foundation for academic research.

# Vertebroplasty and Kyphoplasty: a Systematic Review of 69 Clinical Studies.

P.A.Hulme<sup>1</sup>, J. Krebs<sup>1</sup>, S.J. Ferguson<sup>1</sup>, U. Berlemann<sup>2</sup>

<sup>1</sup> MEM Research Center, University of Bern, Bern, Switzerland

<sup>2</sup> Das Rückenzentrum, Thun, Switzerland

**INTRODUCTION:** Vertebroplasty and kyphoplasty have been gaining popularity for treating vertebral fractures. Current reviews provide an overview of the procedures but are not comprehensive and tend to rely heavily on personal experience. This paper aimed to compile all available data and evaluate the clinical outcome of the two procedures.

The objective was to evaluate the safety and efficacy of vertebroplasty and kyphoplasty using the data presented in published clinical studies, with respect to patient pain relief, restoration of mobility and vertebral body height, complication rate, and incidence of new adjacent vertebral fractures.

**METHODS:** This is a systematic review of all the available data presented in peer reviewed published clinical trials (69 papers). The methodological quality of included studies was evaluated and data was collected targeting specific standard measurements. Where possible a quantitative aggregation of the data was performed.

Data was collected for each study under the headings: general information, participants, intervention, outcomes, complications, and follow-up. Outcome data was collected detailing: pain relief, general health, functional improvements, satisfaction with treatment, and reduction in kyphosis. Complications included: cement leakage (asymptomatic and symptomatic), neurological deficits, cardiovascular, pulmonary and any other clinically relevant complication. Long term follow-up information included all the items recorded under the heading "outcome" with the addition of new fracture details.

**RESULTS:** A large proportion of subjects experienced some pain relief (87% vertebroplasty, 92% kyphoplasty). Vertebral height restoration

was possible using kyphoplasty (average 6.6°) and for a subset of patients using vertebroplasty (average 6.6°). Cement leaks occurred for 41% and 9% of treated vertebrae for vertebroplasty and kyphoplasty respectively. New fractures of adjacent vertebrae occurred for both procedures at rates that are greater than the general osteoporotic

population but approximately equivalent to the general osteoporotic population that had a previous vertebral fracture.

**DISCUSSION & CONCLUSIONS:** The problem with stating definitely that vertebroplasty and kyphoplasty are safe and effective procedures is the lack of comparative, blinded, randomized clinical trials. Standardized evaluative methods should be adopted.

The pain relief experienced by patients appears to be promising for both kyphoplasty and vertebroplasty in the short term (<1 year).

Leakage of the PMMA is the most common complication and may pose significant physical danger, even in small quantities. Higher leakage rates have been reported for single-group cohort vertebroplasty studies compared to kyphoplasty studies. However, the only study that compared kyphoplasty and vertebroplasty using matched groups found little difference in leakage rates (28% and 23% of vertebra had cement leaks for vertebroplasty and kyphoplasty, respectively).

Both kyphoplasty and vertebroplasty have the ability to reduce the kyphotic angle and restore vertebral height associated with vertebral fractures. The critical factor for the restoration of vertebral height would appear to be fracture age rather than the technique used.

**ACKNOWLEDGMENTS:** AO Spine, Switzerland, Grant #SRN 02/105

# Mechanical Evaluation of a Bioactive Calcium Aluminate Cement for Vertebral Body Augmentation

P.A.Hulme<sup>1</sup>, P.F. Heini<sup>2</sup>, T. Persson<sup>3</sup>, H. Spengler<sup>3</sup>, K. Björklund<sup>3</sup>, L. Hermansson<sup>3</sup>, S.J. Ferguson<sup>1</sup>

<sup>1</sup> MEM Research Center, University of Bern, Bern, Switzerland, <sup>2</sup> Inselspital, University of Bern, Bern, Switzerland, <sup>3</sup> DOXA AB, Sweden

**INTRODUCTION:** Bioactive cements for vertebral augmentation may offer the advantage of providing better integration between the material and the bone, lower curing temperatures and no toxicological effects. The injection characteristics and the ability to restore vertebral strength and stiffness of PMMA and a bioactive calcium aluminate cement (CAC) were compared.

**METHODS:** Injection Characteristics: Cement was injected through standard 11G cannulae at a constant rate. Injection force and displacement data were recorded continuously.

**Mechanical Testing:** Twenty human thoracolumbar vertebral bodies (VB) were prepared and assigned as matched-pairs to two groups based on volumetric bone density measurements. Vertebrae were maintained at 37°C at all times, except when performing compression tests or cement injection. Mechanical testing, to determine the strength and stiffness of the VBs, was performed in three stages: 1) intact, 2) fractured and 3) after unipedicular augmentation with cement (24 hours curing). Differences in outcome parameters were evaluated using a matched-pairs Student's t-test (significance level  $p \leq 0.05$ ).

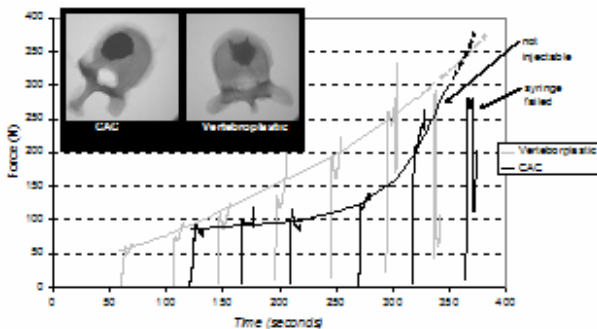


Fig. 1: Injection force versus time from initial mixing. Also shown is a representative CAC and Vertebroplastic AP fluoroscopic image. Qualitatively, the cement border appeared more distinct for CAC injected VBs.

**RESULTS:** Injection characteristics for the two cements were distinctly different (Figure 1). CAC

demonstrated a prolonged plateau in injection force, followed by a rapid increase as cement setting progressed, while PMMA viscosity constantly increased with time. Strength was restored to fractured vertebrae,  $139\% \pm 67$  and  $176\% \pm 88$  of initial values for CAC and PMMA augmented vertebrae respectively ( $p=0.06$ ). Stiffness values were  $37\% \pm 18$  and  $60\% \pm 47$  of the intact values for CAC and PMMA specimens respectively ( $p=0.25$ ).

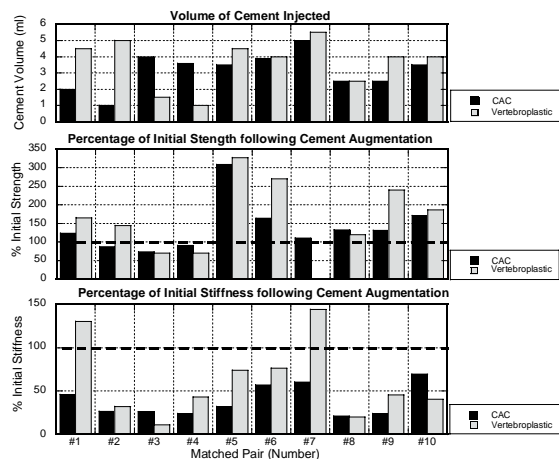


Fig. 2: Strength and stiffness of CAC and Vertebroplastic cement augmented VBs.

**DISCUSSION & CONCLUSIONS:** CAC demonstrated a more constant injection force, possibly allowing a surgeon to better determine filling response (leak or obstruction) through tactile force feedback. The strength and stiffness of vertebrae augmented with PMMA and CAC cements were similar. The advantages of the tested bioactive cement, combined with its consistent injection characteristics, enhanced radio-opacity and similar mechanical properties to PMMA, may make it an attractive option for VB cement augmentation.

# Comparison of Milling Techniques in the Production of $\alpha$ -TCP

V.Jack<sup>1</sup>, F.Buchanan<sup>1</sup>, N.Dunne<sup>1</sup>, M.Bohner<sup>2</sup>

<sup>1</sup> *School of Mechanical and Aerospace Engineering, Queen's University of Belfast, Northern Ireland*

<sup>2</sup> *Robert Mathys Foundation, Bischmattstrasse 12, CH-2544 Bettlach, Switzerland*

**INTRODUCTION:** Calcium phosphate bone cements (CPC) are becoming increasingly popular as a bone substitute material. The osteoconductiveness of calcium phosphates and their ability to be resorbed and gradually replaced by the surrounding bone have proved attractive. CPC consist of a powder and a liquid, which when mixed form a paste that sets as porous cement. Initial research was conducted on CPC for which the main component was tetracalcium phosphate (TTCP). As knowledge in the subject increased studies have spread into other forms of calcium phosphate, i.e. tricalcium phosphate (TCP). Alpha-tricalcium phosphate ( $\alpha$ -TCP) has shown great potential with regards mechanical properties (e.g. compression strength) and setting properties.  $\alpha$ -TCP reacts with water to form calcium deficient hydroxyapatite (HA).

The objective of this study was to compare the conventional ball milling technique with cryogenic grinding and planetary milling methods for the reduction of particle size of  $\alpha$ -TCP.

**METHODS:** A calcium phosphate and calcium carbonate mix was turboblended and furnace treated for 6 hours at 1400°C. The samples were initially reduced to powder form using a pestle and mortar. Further particle reduction experiments were carried out under the conditions in Table 1.

Table 1: Details of the milling experiments.

Technique	Sample size	Grind time
Ball milling	10g-100g	Up to 10hrs
Cryogenic	10g-30g	2min-30min
Planetary milling	Up to 100g	5min-30min

Laser particle size analysis was carried out using the Sympatec HELOS Particle Sizer (Sympatec Limited, UK). Shape and surface characteristics of particles were examined using SEM, Jeol 6500 FEG Scanning Electron Microscope (Advanced MicroBeam, Inc). Compressive strength of cement samples was determined through tests using EZ50 Universal Material Test System (Lloyd Instruments Ltd, UK) and setting times were monitored using the Gillmore needle apparatus.

## RESULTS & DISCUSSION:

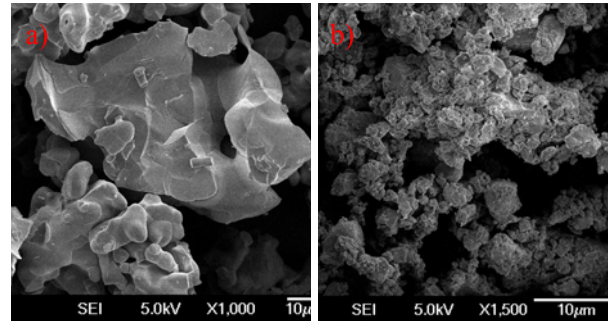


Fig 1: SEM images showing cryogenically ground TCP particles (a) after 2min and (b) after 40min grinding.

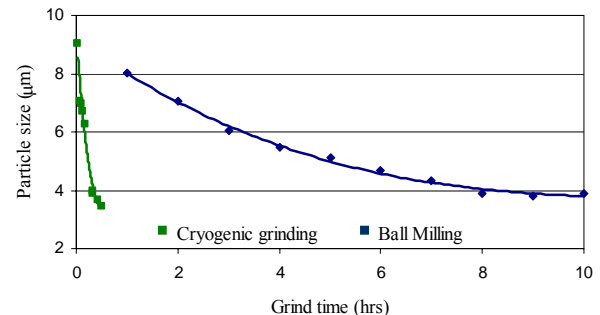


Figure 2: Particle size measurements.

Wide ranges of particle sizes were found in all the samples (Figure 1), although the general trend was that particle size decreased with increasing grind time (Figure 2). Ball milling takes a significantly longer time to achieve small particles than the other milling methods (1, 2).

**CONCLUSIONS:** An increase in grind time generally led to stronger cements. It is postulated that smaller particles will result in more homogenous cements. Crack propagation within the cement is thought to be limited due to this factor.

It is characteristic of smaller particles to have a larger surface area, this led to faster curing reactions.

**REFERENCES:** 1. Jack V. Presented at ESB 2005. 2. Camiré *et al.*, Biomaterials 2005 (26) 2787-94.

# Powder Metallurgy(pm) Processed Titanium Based Biocomposite for Bone Substitute Material

M. Karanjai<sup>1</sup>, R. Sundaresan<sup>1</sup> & T. R. Ramamohan<sup>2</sup>, B. P. Kashyap<sup>2</sup>

<sup>1</sup> International Advanced research center for powder metallurgy and new Materials, Balapur P.O, Hyderabad- 500 005, India. <sup>2</sup> Indian Institute of Technology Bombay, Powai, Mumbai-400 076, India

**INTRODUCTION:** Titanium is very important for use as implant material in body for its excellent mechanical properties, corrosion resistance and biocompatible nature[1,2]. For load bearing implants, the prevalent practice is to coat a titanium substrate with calcium hydroxylapatite to render the titanium metal which is bio inert by nature to actively interact with the surrounding host environment when implanted within the body[3]. In this experimental work, a different technique of forming hydroxylapatite or calcium phosphatic compounds which are biocompatible in nature are formed in-situ in titanium based matrix. The process adopted can be used for load bearing implants because of its high strength, combined with its bioactive nature.

**METHODS:** Calculated quantities of precursors of calcium and phosphorus are mixed in titanium base matrix, all in powder form and are milled together for uniform and intimate contacts of the constituents. The milled mixture is then compacted and subjected to vacuum calcination at different temperatures to find the optimum calcination temperature. The calcined compacts are crushed, and calcined powders compacted for vacuum sintering at 1150°C. The phases obtained during calcination and their stability during sintering have been studied by X ray diffraction studies. The mechanical properties like biaxial flexural strength and Transverse rupture strength were measured. In vitro studies were undertaken to test the biocompatibility of the composites obtained by the above PM processing route by immersing into simulated body fluid (SBF). The growth of deposits were monitored at intervals of 7, 14, 21 and 28 days. The morphology of the composites before and after immersing in SBF was studied using SEM. Also Fourier transform infra red (FTIR) studies were undertaken to characterize the growth of deposits on the composite surface. The composites were then subjected to in vitro cytotoxicity tests.

**RESULTS:** In-situ calcium-phosphatic phases were obtained in the titanium based matrix. The phases obtained during calcination and sintering

were titanium oxide[Ti<sub>2</sub>O], nitride[TiN<sub>0.3</sub>], different forms of hydroxylapatites[Ca<sub>5</sub>(PO<sub>4</sub>)<sub>3</sub>OH, Ca<sub>10</sub>(PO<sub>4</sub>)<sub>6</sub>(OH)<sub>2</sub> Ca<sub>8</sub>H<sub>2</sub>(PO<sub>4</sub>)<sub>6</sub>.5H<sub>2</sub>O], tri calcium phosphate [Ca<sub>3</sub>(PO<sub>4</sub>)<sub>2</sub>] and calcium based titanates [CaTiO<sub>3</sub>]. The quantitative analysis of the phases were different during calcination and sintering. The biocomposites were found to be non toxic during in vitro cytotoxicity tests.

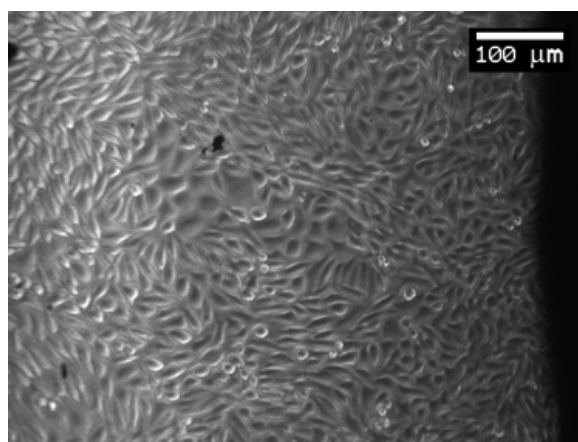


Fig. 1: Fibro blast cells around sample having 10wt % Ca-P precursor content in the ratio of 1.7:1

**DISCUSSION & CONCLUSIONS:** PM processing can be adopted for making titanium based biocomposites with required calcium phosphatic phases, ensuring the composite to be bioactive in nature and having adequate mechanical strength for use as bone substitute implant application.

**REFERENCES:** <sup>1</sup>Mitsuo Niinomi *Recent metallic materials for Biomedical applications* Met. and Mat. Trans. A(2002) 33A 477-486. <sup>2</sup> J.B.Park (1987) *Biomaterials Science and Engineering* Plenum Press, NewYork). <sup>3</sup>L.L.Hench, E.C.Ethridge(1987) *Biomaterials: An interfacial Approach* Academic Press, New York.

**ACKNOWLEDGEMENTS:** Authors gratefully acknowledge the funding of this research work by Department of Biotechnology, New Delhi, Govt. of India for financially supporting this work.

# Preparation of Hydroxyapatite-gelatin Composite Scaffold for Bone Tissue Engineering

M. Kazemzadeh Narbat<sup>1</sup> & M. Solati<sup>1</sup> & M. Pazouki<sup>1</sup>

<sup>1</sup> *Materials and Energy Research Center (MERC)*

**INTRODUCTION:** Calcified tissue, such as long bone and jaw bone is considered a biologically and chemically bonded composite between HA (HA:  $Ca_{10}(PO_4)_6(OH)_2$ ) and type-I collagen. Gelatins are compositionally virtually identical to the collagen from which they are derived. Therefore In this study, to mimic the mineral and organic component of natural bone, hydroxapatite[HA] and gelatin[GEL] composite scaffolds were prepared using solvent-casting method combined with freeze drying process. Glutaraldehyde [GA] was used as cross linking agent in the making of gelatin-tricalcium phosphate composites rendering them no longer water soluble but since GA is cytotoxic the bisulfite sodium was used as excess GA discharger. Prepared composite scaffold of HA and gelatin is expected to show increased biodegradation together with sufficient mechanical strength.

**METHODS:** The slurry composites were prepared using solvent casting method. Definite GEL concentration was dissolved in deionized water [DI] at temperature  $45^\circ C$ . Desire volumetric content (30wt%, 40wt% and 50wt%) of fine HA particles relative to gelatin were added. The reinforced slurry composite was then heat treated on magnet stirrer under constant mixing for 1h at  $45^\circ C$ . The slurry was deagglomerated by magnet stirring meanwhile the temperature was monitored continuously. Then to avoid air bubbles the slurry immediately was injected by using a syringe into cylindrical Teflon molds. The molds were frozen at  $-70^\circ C$  and were dried in a commercial freeze-dryer for 6h for solvent (DI) removal. After that, the white composites were removed and placed in room temperature for 24 h, they were immersed in a 8% solution of GA for 3 h then. To remove the residues of GA agent, the cylinders were washed with DI for 24 h, during which time the water was changed every 6 h. Besides, the sodium bisulfite was used to discharge the excess GA.

**DISCUSSION & CONCLUSIONS:** FT-IR spectroscopy was used to estimate the conformational change of the HA/GEL composite structure. FT-IR spectrum for the cross-linked HA-

GEL composite indicates chemical bond formation between carboxyl ions in GEL and HA phases. The compressive strength, Young's modulus and elongation of composites were measured with an Instron materials testing machine. The compressive modulus of HA-GEL scaffolds increased with HA content. It was found that the mechanical properties of GEL/HA with ratio of 50wt% was similar to that of trabecular bone. Water absorption of HA-GEL composites with different HA content were studied to evaluate the effect of HA content on the size and stability of material. The water absorption of composites reduced with HA content. A liquid displacement method was used to measure the porosity and density of HA scaffolds. It was found that the addition of HA results in more dense and thicker pore walls with lower porosity. The morphology and microstructure of the scaffolds were examined using SEM and light microscopy (fig. 1). The scaffold prepared has an open, interconnected porous structure with a pore size of  $80-400 \mu m$ . The biological responses of scaffolds carried out by L929 fibroblast cell culture. Cells exhibited rather good proliferation and partially covered the composite surface after 48h.

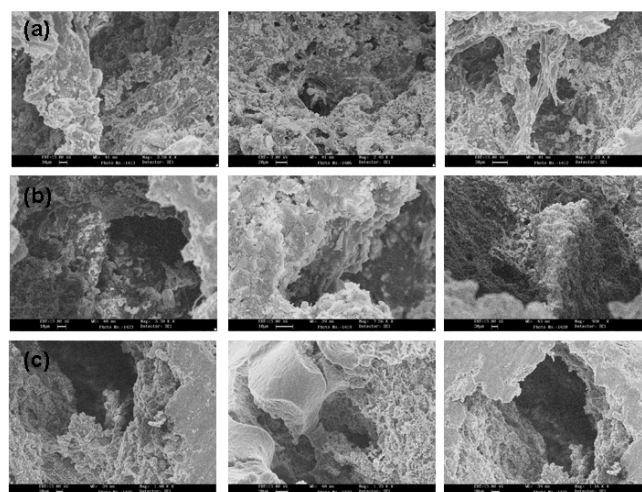


Fig. 1. SEM micrographs of the pores in the cross-section of different HA-GEL scaffolds (a)HA30% (b) HA40% (c)HA50%

**REFERENCES:** Stephan F. Badylak. Methods of Tissue Engineering , 2001. etc.

# Poly(lactide-co-glycolide)/Nano-hydroxyapatite Composite for Bone Regeneration

S.-S.Kim<sup>1,2</sup>, M.S.Park<sup>3</sup>, O.Jeon<sup>3</sup>, C.Y.Choi<sup>2,4</sup>, B.-S.Kim<sup>1</sup>

<sup>1</sup>Department of Bioengineering, Hanyang University, <sup>2</sup>Interdisciplinary Program for Biochemical Engineering and Biotechnology, Seoul National University, <sup>3</sup>Department of Chemical Engineering, Hanyang University, <sup>4</sup>School of Chemical and Biological Engineering, Seoul National University, Seoul, Korea

**INTRODUCTION:** Biodegradable polymer/bioceramic composite scaffolds can overcome the limitations of conventional ceramic bone substitutes such as brittleness and difficulty in shaping. However, conventional methods for fabricating polymer/bioceramic composite scaffolds often use organic solvents (e.g., the solvent-casting and particulate-leaching (SC/PL) method), which might be harmful to cells or tissues. Furthermore, the polymer solutions may coat the ceramics and hinder their exposure on the scaffold surface, which may decrease the likelihood that the seeded osteogenic cells will make contact with the bioactive ceramics. In this study, a novel method for fabricating a polymer/nano-bioceramic composite scaffold with high exposure of the bioceramics on the scaffold surface was developed for enhanced bone regeneration.

**METHODS:** Poly(lactic-co-glycolic acid)/nano-hydroxyapatite (PLGA/HA) composites were fabricated by the gas-forming and particulate-leaching (GF/PL) method without the use of organic solvents<sup>1</sup>.

**RESULTS:** The GF/PL method exposed HA nanoparticles at the scaffold surface significantly more than the conventional SC/PL method does. The GF/PL scaffolds showed interconnected porous structures without a skin layer and exhibited superior mechanical properties to those of scaffolds fabricated by the SC/PL method. Both types of scaffolds were seeded with rat calvarial osteoblasts and cultured *in vitro* or were subcutaneously implanted into athymic mice for eight weeks. The GF/PL scaffolds exhibited significantly higher cell growth, alkaline phosphatase activity, and mineralization compared to the SC/PL scaffolds *in vitro*. Histological analyses and calcium content quantification of the regenerated tissues five and eight weeks after implantation showed that bone formation was more extensive on the GF/PL scaffolds than on the SC/PL scaffolds. Compared to the SC/PL

scaffolds, the enhanced bone formation on the GF/PL scaffolds may have resulted from the higher exposure of HA nanoparticles at the scaffold surface, which allowed for direct contact with the transplanted cells and stimulated the cell proliferation and osteogenic differentiation.



Fig. 1: A macroscopic image of three types of scaffolds (GF/PL-no HA, PLGA scaffold with no HA, fabricated by the GF/PL method; SC/PL, PLGA/HA scaffold fabricated by the SC/PL method; GF/PL, PLGA/HA scaffold fabricated by the GF/PL method) stained to reveal HA exposed on the scaffold surfaces. A hydrophilic dye (trypan blue) selectively stained the ceramics exposed on the scaffold surface.

**DISCUSSION & CONCLUSIONS:** These results show that the biodegradable polymer/bioceramic composite scaffolds fabricated by the novel GF/PL method enhance bone regeneration compared with those fabricated by the conventional SC/PL method.

**REFERENCES:** <sup>1</sup> S.S. Kim, M.S. Park, O. Jeon, C.Y. Choi, B.S. Kim. (2006) *Biomaterials* **27**: 1399-1409.

**ACKNOWLEDGEMENTS:** This work was supported by a grant (SC 3220) from the Stem Cell Research Center of the 21st Century Frontier Program funded by the Ministry of Science and Technology, Republic of Korea.

# Effects of Vertebral Bone Augmentation on Intervertebral Discs

J. Krebs<sup>1</sup>, S.J. Ferguson<sup>1</sup>, B.G. Goss<sup>2</sup>, N. Aebli<sup>3</sup>

<sup>1</sup> *MEM Research Centre, University of Bern, Bern, CH;* <sup>2</sup> *AO Spine Reference Centre, Queensland University of Technology, Brisbane, AUS;* <sup>3</sup> *Swiss Paraplegic Centre, Nottwil, CH*

**INTRODUCTION:** Reported clinical results suggest that vertebroplasty is a safe and effective technique for providing pain relief. However, information about the long-term effect of PMMA on the adjacent intervertebral discs and the augmented bone is lacking. Adjacent intervertebral discs may be at higher risk of degeneration due to nutritional constraints. Bone loss in augmented vertebrae may occur due to mechanical stress-shielding or toxicological effects.

The aim of the present study was therefore to investigate the effect of augmenting vertebrae with PMMA on intervertebral disc and bone tissue after 6 and 12 months, using an animal model.

**METHODS:** In 12 skeletally mature sheep, 2.0ml PMMA (Simplex P) was injected into three lumbar vertebrae (approved by Animal Ethics Committee).

Two injection holes were drilled into the middle of three vertebrae at a distance of 5.0mm from the cranial and caudal endplate and 1.0ml PMMA was injected into each hole. Four weeks before euthanasia, animals received an injection of tetracycline for bone labeling.

Postmortem, T1- and T2-weighted sagittal and axial MR images were taken prior to fixation in 80% ethanol. Spines were cut into specimens containing one intervertebral disc and half of the two adjacent vertebrae. The discs which were two levels above the first augmented vertebra served as controls. Microsections were stained with H&E, Goldner, Alcian blue-PAS and Safranin O.

MRI signal intensity and morphology of discs were evaluated qualitatively. Histomorphological analysis of discs and endplates was conducted using published criteria [1]. Presence of bone remodeling, fibrous tissue and foreign body reaction in the vertebrae was also recorded.

**RESULTS:** There was no distinguishable loss of MRI signal intensity in the discs in between augmented vertebrae.

Cement injection resulted in blocking 50-75% of the endplate lengths. Most discs (~83%) that were in between augmented vertebrae showed signs of degeneration (chondrocyte proliferation, necrosis) both after 6 and 12 months (Fig. 1). Inflammatory

reaction to PMMA was observed in some specimens, mainly after 6 months. Cement had been covered with fibrous tissue in all augmented vertebrae, but tetracycline labeling revealed new bone formation in the vicinity of PMMA.

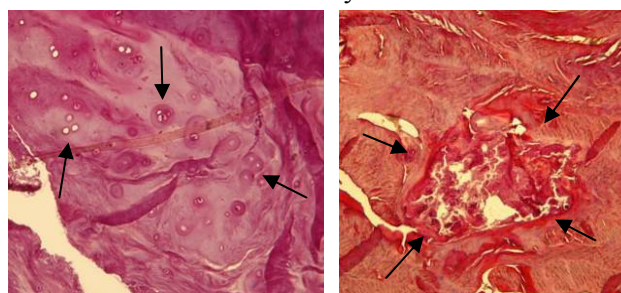


*Figure 1: Histology sections (H&E, original magnification 5x) showing (left): chondrocyte clusters (arrows) in the nucleus and (right): calcified necrotic area (arrows) in annulus 12 months postoperatively.*

**DISCUSSION & CONCLUSIONS:** The augmentation of three adjacent vertebrae with PMMA initiated degenerative changes of intervertebral discs in between two augmented vertebrae. This is in contrast to previous animal studies [2,3] where no degenerative changes after cementing endplates were observed.

Investigations were performed with the specific aim to block the endplates. Clinically, endplates may not get blocked as effectively. On the other hand, discs in older patients are nutritionally constrained due to endplate calcification [4] and even partial blockage may lead to degenerative changes as documented presently.

The risk of degenerative changes of intervertebral discs should be considered in patients undergoing vertebroplasty.

**REFERENCES:** <sup>1</sup> N. Boos, S. Weissbach, H. Rohrbach, et al (2002) *Spine* **23**:2631-44. <sup>2</sup> W.C. Hutton, H. Murakami, J. Li, et al (2004) *J Spinal Disord Tech* **17**:53-63. <sup>3</sup> J.J. Verlaan, F.C. Oner, P.J. Sloopweg, et al (2004) *JBJS* **86-A**:1230-8. <sup>4</sup> L.M. Benneker, P.F. Heini, M. Alini et al (2005) *Spine* **30**:167-73.

**ACKNOWLEDGEMENTS:** Histology: Ladina Ettinger; Grant from AO Foundation, Davos, CH.

# Cardiovascular Consequences of Pulmonary Cement Embolism

J. Krebs<sup>1</sup>, N. Aebli<sup>2</sup>, B.G. Goss<sup>3</sup>, S. Sugiyama<sup>3</sup>, S.J. Ferguson<sup>1</sup>

<sup>1</sup> MEM Research Centre, University of Bern, Bern, CH; <sup>2</sup> Swiss Paraplegic Centre, Nottwil, CH; <sup>3</sup> AO Spine Reference Centre, Queensland University of Technology, Brisbane, AUS

**INTRODUCTION:** Cement leakage into adjacent structures is the main complication during vertebroplasty. The majority of these leaks is asymptomatic, but pulmonary cement embolism has been reported to cause cardiovascular disturbances and even death [1,2]. Furthermore, the use of calcium phosphate (CaP) cements for vertebroplasty may aggravate cardiovascular deterioration in the event of cement embolism by stimulating coagulation [3].

The cardiovascular effects of pulmonary cement embolism were investigated using an animal model.

**METHODS:** In 18 skeletally mature sheep, 2.0ml cement was injected into the pulmonary artery during general anesthesia (approved by Animal Ethics Committee). Three different cements were used: 1) PMMA (Simplex P, Stryker); 2) PMMA with 10% hydroxyapatite (PMMA & HA) (Vertecem, Synthes); 3) Experimental injectable CaP cement (Synthes). The following cardiovascular parameters were recorded continuously (endpoint: 60min post-injection): arterial, central venous, pulmonary arterial and left ventricular pressures, cardiac output. Blood gases were measured pre-injection, 5, 30 and 60min post-injection.

**RESULTS:** There were no fatalities. After 1min, mean pulmonary arterial pressure had increased by approximately 10% (PMMA) or 20% (PMMA & HA; CaP) respectively (Fig. 1). Values stayed elevated for the duration of the experiment. After 50min, mean pulmonary arterial pressure had increased further in the CaP group (increase of 35% or 8mmHg compared to the pre-injection value). At the same time, mean arterial pressure had decreased by 8% in the CaP group. Furthermore, a trend of respiratory acidosis was observed in this group. However, there were no statistically significant changes in any of the cardiovascular or blood gas parameters from pre- to post-injection values and no statistically significant differences between material groups.

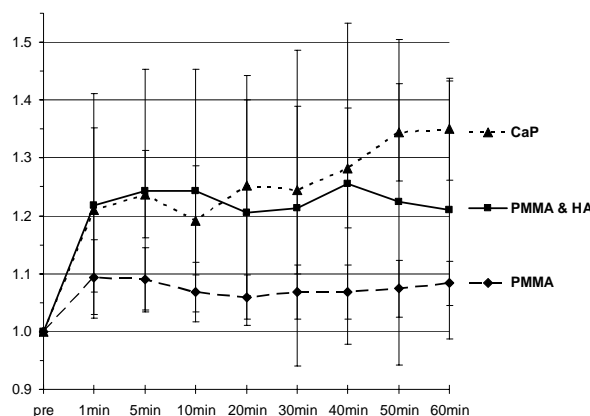


Figure 1: Normalized values of mean pulmonary arterial pressure prior (pre) and after (1, 5, 10, 20, 30, 40, 50, 60min) intravenous injection of cement.

**DISCUSSION & CONCLUSIONS:** Pulmonary cement embolism did not lead to significant cardiovascular changes regardless of the injected material. Present results are in contrast to earlier reports (pig model) of fulminant cardiovascular deterioration after CaP cement embolism [3]. This may be due to differences in the cement formulation or the animal model. Further investigations are needed to elucidate the clinical significance of the mild pulmonary hypertension (statistically not significant) observed in the PMMA & HA and CaP groups

Cement embolism during vertebroplasty should be prevented but cardiovascular consequences of considerable leaks (2ml) may not be severe in individuals with a healthy cardio-pulmonary system.

**REFERENCES:** <sup>1</sup>H.L. Chen, C.S. Wong, S.T. Ho et al. (2002) *Anesth Analg* **95**:1060-2. <sup>2</sup>K. Stricker, R. Orler, K. Yen et al (2004) *Anesth Analg* **98**:1184-6. <sup>3</sup>C.M. Bernardis, J. Chapman and S. Mirza (2004) *ORS* #0254.

**ACKNOWLEDGEMENTS:** Synthes GmbH, Switzerland

# Fabrication of Porous $\text{Al}_2\text{O}_3$ and $\text{t-ZrO}_2$ Ceramics and Evaluate their Biocompatibility

B. T. Lee<sup>1</sup>, A. K. Gain<sup>1</sup> and H. Y. Song<sup>2</sup>

<sup>1</sup>School of Advanced Materials Engineering, Kongju National University, 182, Shinkwan-dong, Kongju City, Chungnam, 314-701, Korea <sup>2</sup>Department of Microbiology, School of Medicine, Soonchunhyang University, 366-1 Ssang-dong Cheonan, Chungnam 330-090, Korea

**INTRODUCTION:** Recently, yttria stabilized zirconia ( $\text{t-ZrO}_2$ ) and  $\text{Al}_2\text{O}_3$  have been considered as a typical bioceramics for implants such as prostheses, dental materials and femoral heads due to their excellent biocompatibility, as well as desirable material properties such as strength, chemical stability and wear resistance [1]. However, the pore size, shape and porosity are also important factors to consider improving the compatibility of ceramics for implants because they are closely related to cell attachment, growth behavior and bond strength between the tissue and the artificial implant in the human body [2]. Suitable pore sizes for implants were reported to be approximately 100-150, 140-160 and 200-1000 $\mu\text{m}$  in diameter [3].

**METHODS:** To fabricate the continuously porous  $\text{Al}_2\text{O}_3$  and  $\text{t-ZrO}_2$  bodies, the starting ceramic powders /EVA/ stearic acid with a 50/40/10 volume fraction, were homogeneously mixed using a shear mixer. This mixture was used to produce tubes by warm press. On the other hand, to make the rod, a pore-forming agent (carbon, Aldrich Chemical Company, USA), polymer and stearic acid (volume fraction 50/40/10) were also mixed using a shear mixer at 120°C for 1hr. The tubes and rods were assembled together to prepare a feed roll and extruded at 120°C to make the 1<sup>st</sup> passed filaments with a diameter of 3.4 mm. The 1<sup>st</sup> passed filaments were cut 80mm in length and reloaded into the extrusion die and re-extruded to make the 2<sup>nd</sup> passed filaments. To remove the polymer binder (EVA) and pore forming agent carbon, the 1<sup>st</sup> and 2<sup>nd</sup> burnout was performed at 700°C and 1000°C, respectively. Finally, the pressureless sintering process was carried out at 1450°C-1600°C for 1 hr in flowing air.

**RESULTS:** Fig.1 (a) and (b) are SEM and TEM images of porous  $\text{Al}_2\text{O}_3$  bodies and (e) (f) are SEM images of  $\text{t-ZrO}_2$  bodies. The pore sizes of the 2<sup>nd</sup> passed samples were 260 $\mu\text{m}$ , in diameter. The average grain sizes of  $\text{Al}_2\text{O}_3$  and  $\text{t-ZrO}_2$  bodies were about 0.8 $\mu\text{m}$  and 0.7 $\mu\text{m}$  in diameter, respectively. In case of  $\text{Al}_2\text{O}_3$  porous body, in pore frame region also many fine pores less than 100nm in diameter were clearly observed. Figure 1(c) and

(h) are the light microscopic images of osteoblast cells grown behaviour of porous  $\text{t-ZrO}_2$  and  $\text{Al}_2\text{O}_3$  bodies, respectively. The spindle shape osteoblast cells grew well in both samples and most of the cells went down through the pores. On other hand, the pebble stone appearance osteoclast cells fully covered the pore frame region with in 12 days as shown in Fig. 1(d) and (h).

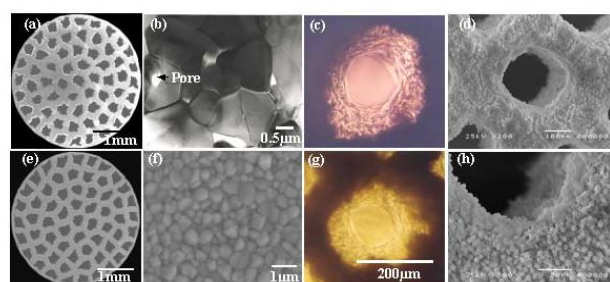


Fig. 1: SEM (a), (e), (f) and TEM (b) images of porous  $\text{Al}_2\text{O}_3$  and  $\text{t-ZrO}_2$  and their grown behaviour of osteoblast (c), (g) and osteoclast (d), (h) cells.

**DISCUSSION & CONCLUSIONS:** Continuously porous  $\text{Al}_2\text{O}_3$  and  $\text{t-ZrO}_2$  ceramics were fabricated by multi-pass extrusion process using commercial  $\text{Al}_2\text{O}_3$  and  $\text{t-ZrO}_2$  powders. The pore forming agent and binder were successfully removed during the burn out process and fabricate the continuously porous  $\text{Al}_2\text{O}_3$  and  $\text{t-ZrO}_2$  bodies. Their biocompatibility was evaluated through in-vitro investigation. All kinds of cells were grown well on top and bottom surface as well as inside the surface of the porous bodies. The growth of osteoblast cells showed spindle shape, three-dimensional and network type structures. In contrast, osteoclast revealed the growth behavior like pebble stone in appearance.

**REFERENCES:** <sup>1</sup>M. C. Heisel, M. M. Silva, M. T. P. Schmalzried, J. Bone & Joint Surgery **85** 1366-1379. <sup>2</sup>B. T. Lee, I. C. Kang, S. H. Cho, H. Y. Song, J. Am. Ceram. Soc. **88** 2262-2266 <sup>3</sup>L. L. Hench, J. Am. Ceram. Soc. **81** 1705-1728

**ACKNOWLEDGEMENTS:** This work was supported by NRL research program of the Korean Ministry of Science and Technology.

# Phases Evolution of Bioactive Glasses during Crystallization for Orthopaedic and Tissue Engineering Applications

L. Lefebvre<sup>1</sup>, J. Chevalier<sup>1</sup>, D. Bernache<sup>2</sup>, L. Gremillard<sup>1</sup> & R. Zenati<sup>3</sup>

<sup>1</sup>GEMPPM, INSA, Lyon, FR, <sup>2</sup>CIS, EMSE, St Etienne, FR, <sup>3</sup>Noraker, Lyon, FR

**INTRODUCTION:** Bioactive glass 45S5 is currently used for dental and ear implants. We aim at extending its application to the orthopaedic and tissue engineering fields, via the processing of porous scaffolds. Our goal is the optimisation of the porous bioactive glasses mechanical and biological properties, via a careful understanding of the process–microstructure–biomechanical properties relations. In this study we report on the thermal transformation of the glass.

**METHODS:** High purity SiO<sub>2</sub>, Na<sub>2</sub>CO<sub>3</sub>, CaCO<sub>3</sub> and P<sub>2</sub>O<sub>5</sub> powders were mixed and melted in a Pt crucible to obtain the 45S5 bioaglass<sup>®</sup> (45%SiO<sub>2</sub>; 24,5% Na<sub>2</sub>O; 24,5% CaO and 6% P<sub>2</sub>O<sub>5</sub> in weight). The melt were quenched in water and ground to a fine powder.

The thermal transformations of the material were first characterized via dilatometric measurements and differential thermal analysis (DTA). The crystallization process and the transformation kinetics were investigated by Differential Scanning Calorimetric analysis coupled with TGA (DSC/TGA). Several thermal treatments in the range of 600 to 1000°C were carried out on the glass powder. The different crystallized phases were studied with XRD and Infrared analysis. A rietveld analysis was performed on the XRD results to measure the cells parameters. Furthermore, SEM and TEM techniques were used on all the samples to observe the microstructure.

**RESULTS:** TGA analysis gives two main weight losses at 100 and 400°C which are due to the departure of free water and -OH groups principally. DTA, DSC and dilatometric analysis show that the glassy transition takes place at 550°C and that the crystallization process begins at 600°C. DSC results allow us to find out the necessary enthalpy need for crystallization and its kinetics. XRD diffractograms shows that the system crystallized principally under the Na<sub>6</sub>Ca<sub>3</sub>(Si<sub>6</sub>O<sub>18</sub>) phase. This structure shows a separation of its two principals peaks at 800°C. At this temperature a minor phase appears identified as Na<sub>2</sub>Ca<sub>4</sub>(PO<sub>4</sub>)<sub>2</sub>SiO<sub>4</sub>. This steps corresponds to a shrinkage on the dilatometric curves. Fourier

Transform Infrared analyses confirm the presence of a cristallized phosphate phase and shows that amorphous phosphate is still present. DTA analysis gives a melting point of 1100 °C.

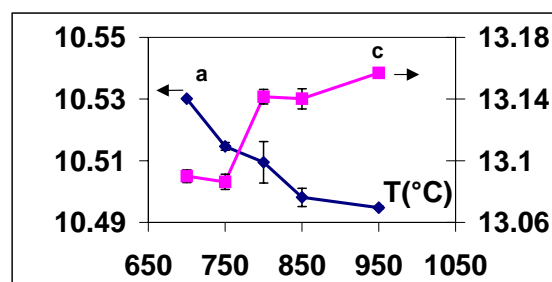


Fig 1: Evolution of the cell parameters with thermal treatment.

**DISCUSSION & CONCLUSIONS:** Several studies<sup>[1],[2]</sup> show that the bioglass crystallizes principally in the Na<sub>4</sub>Ca<sub>4</sub>Si<sub>6</sub>O<sub>18</sub> with Na<sub>2</sub>CaSi<sub>3</sub>O<sub>8</sub> as a minor phase. We found no evidence of the second phase and the major phase appears more likely to be Na<sub>6</sub>Ca<sub>3</sub>Si<sub>6</sub>O<sub>18</sub> which has the same structure as Na<sub>4</sub>Ca<sub>4</sub>Si<sub>6</sub>O<sub>18</sub>. On the other hand we found a crystallized phosphate phase which can lead to a decrease in bioactivity of the crystallized 45S5 bioglass after 800°C. After the glassy transition and before the crystallization process, a separation of the glassy phase into two immiscible phases occurs<sup>[3]</sup> (one phase rich in silicon and the other rich in phosphorus). We suppose that the first one leads to the major crystalline phase and the second one to the crystalline phosphate phase. The evolution of the crystalline phase (Figure 1) differs from this reported by Oshato and Takéuchi<sup>[4]</sup> for pure Na<sub>4</sub>Ca<sub>4</sub>Si<sub>6</sub>O<sub>18</sub>. The difference between the two evolutions can be attributed to the presence of phosphate glassy phase. The behavior of phosphorous ions is not yet very clear and is under investigation.

**REFERENCES:**<sup>1</sup>O. Peitl, E. D. Zanotto, L.L. Hench (2001). Elsevier Biomat. 292: 115-126. <sup>2</sup>H.A. El Batal, M.A. Azooz, E.M.A. Khalil, A. Soltan Monem, Y.M. Hamdy (2003). Materials Chem. and Phys. 80: 599-609. <sup>3</sup>A. El-Ghannam, E. Hamazawy, A. Yehia. J Biomed Mater res 2001; 55: 387-398. <sup>4</sup>H. Oshato and Y. Takéuchi (1990), Acta Cryst, B46, 125-131.

# The Study of PLGA/TCP Scaffold with Bovine BMP were Implanted in Bone Defects Peri-implant

P.Lei<sup>1</sup> & X.E.Xing<sup>1</sup>

<sup>1</sup> *Department of Orthopaedics, The Second Affiliated Hospital Wenzhou Medical College, China.*

**INTRODUCTION:** Compound PLGA/TCP triaxiality and porous frames and BMP extracted from cortical bone to make the composite material that have nature bone matrix ingredient and osteoinductive. The study is based on the model of porous titanium in distal bone defects peri-implant in femur of rabbit, observe the effect of prosthesis and rabbit adapted virusgical fixation, and apply for femur prosthesis of canine to check the effect of the composite material in enduring gravity in arthroplasty, to establish foundation for further clinical experiment.

**METHODS:** The PLGA/TCP scaffold was loaded with bovine BMP and then the composites were implanted into distal bone defects peri-implant in femur of adult rabbits and around femur prosthesis of canine. Using X-ray, SEM EDX and Bone mineral density means to inspect the effect of BMP loaded PLGA/TCP on peri-prosthesis.

**RESULTS:** New bone quantity on the porous area of Titanium with BMP loaded PLGA/TCP were higher than those of PLGA/TCP at 6 weeks. At 12 weeks on the bone defects area peri-titanium, new bone in BMP loaded PLGA/TCP group were more mature than that of control group(p<0.05). At 6 and 12 weeks there was higher shearing force in experimental group than control group. At 20 weeks point There was new bone formation mainly made of woven bone on the pores of Titanium and bone graft area. trabecula of which had matured. The biomaterial had been degraded completely.

Shear stress Equations: 
$$\sigma = \frac{F}{\pi dt} \quad (1)$$

$\sigma$  is shear stress;  $F$  is maximum fracture load;  $d$  is diameter of implanted sample;  $t$  is height of implanted sample.



Fig. 1: X-ray scan after operation for 4months.

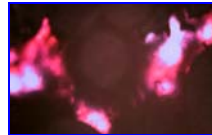


Fig. 2: New bone ingrowths on Ti/HA pores HE staining at 20 weeks.

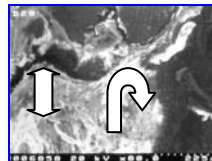


Fig.3:Break area mainly on bone-graft-Ti border at 6 and 12 weeks.

Table 1. Push-out test results

	6W	12W	24W
CP	10.2411	21.3481	43.2689
BCP	15.1248	27.2562	48.1587

**DISCUSSION & CONCLUSIONS:** Histological observation indicated that the presence of BMP not only had promoted osteogenesis but also had accelerated degradation of the biomaterials. Which are beneficial of new bone growth in the pores of prosthesis. The composite of HA coating/porous titanium is promising to increase fixation between prosthesis and bone. At the same time BMP loaded PLGA/TCP as a new kind of bone grafts will be applied widely in clinical orthopedics because of its excellent biological properties.

**REFERENCES:** <sup>1</sup>Tagil M,Jeppsson C,Aspenberg P.Bone grafte incorporation effects of osteogenic protein-1 and impaction. Clin Orthop 2000;371:240-5.<sup>2</sup>Hamadouche M,Blanchat C,Clingerlla BS et al.Histological findings in a proximal femoral structural allograft ten years following revision total hip arthroplasty Clin Orthop 2001 378.258-64.

**ACKNOWLEDGEMENTS:** This template was modified with kind permission from European cells and Materials Journal.

# Autologous Marrow Stromal Cells Enhance Further Osseointegration Earlier in Porous Coated-apatite Titanium Implants in Rabbit

P.Lei<sup>1,2</sup> & W.Mingxi<sup>1</sup> & X.E.Xing<sup>2</sup>

<sup>1</sup>*School of Life Science and Technol., Xi'an Jiaotong University, China.* <sup>2</sup>*Department of Orthopaedics, The Second Affiliated Hospital Wenzhou Medical College, China*

**INTRODUCTION:** Titanium inoculated with cells *in vitro* is an method to increase bone integration directly. Although the osteoinductive effect of osteoblasts and bone marrow cells as combined with pure titanium or other biomaterials has already been demonstrated, it has not been addressed in the literature whether apatite-coated porous titanium implants inoculated with osteoblastic cells can further increase bone osseointegration *in vivo* at early stage.

**METHODS:** Porous titanium ( $\phi 4\text{mm} \times 10\text{mm}$ ) with maximal pore size about  $240\mu\text{m}$  were coated with apatite by alkali- and heat-treatment and were inoculated with autologous marrow stromal cells obtained from the rabbit proximal femur. The cell-inoculated implants (group I) were inserted into the rabbit distal femora and uninoculated implants were inserted in the contralateral femora as controls (group II). The animals were sacrificed after 10, 20 and 42 days. Intravital fluorochrome labeling was used for the histological assessment of bone ingrowths.

**RESULTS:** There is not significant different bone-implant contact at the surrounding of implants for both groups at 20 days after operation. But the bone tissue formation in the porous channels for group I is significantly more than that for group II. At 42 days after operation, the average bone-implant contact section and bone tissue formation in porous channels are similar for both groups. Inoculation with autologous osteoblasts accelerates the osseointegration of apatite-coated porous titanium implants, especially in early stage after operation.



Fig. 1: Apatite-coated porous titanium implants ( $\phi 4 \times 10\text{mm}$ ) with maximal pore size about  $240\mu\text{m}$ . The implants are inserted into the rabbit distal femur.

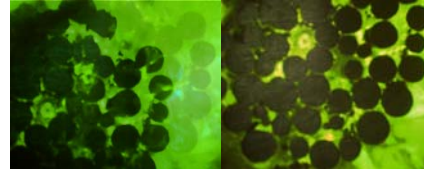


Fig. 2: Fluorescence micrographs at 42 days after operation. (left): For group I and (right): For group II, the bone labeling was observed in the most porous channels.

Table 1. The proportion of mineralized tissue in the channel and the bone-implant contact are given respectively for both groups at 20 days after operation.

	Porous section	Bone-implant contact
Group I	15.4±5.72%	35.8±16.87%
Group II	3.5±5.24%	30.5±17.50%

**DISCUSSION & CONCLUSIONS:** It is known well that autologous transplanted osteoblastic cells as well as bone marrow cells have an osteoinductive effect on the osseointegration of biomaterials. Cell-inoculation significantly accelerate the formation of bone tissue and improve osseointegration at early stage after operation, especially in porous channels.

**REFERENCES:** <sup>1</sup> Davies JE. In vitro modeling of the bone/implant interface. *Anat Rec* 1996;245:426-445. <sup>2</sup> Goshima J, Goldberg VM, Caplan AI. The origin of bone formed in composite grafts of porous calcium phosphate ceramic loaded with marrow cells. *Clin Orthop* 1991;269:274-283. <sup>3</sup> Bunker BC, Rieke PC, Tarasevich BJ, Campbell AA, Fryxell GE, Graff GL, Song L, Liu S, Virden JW, Mcvay GL. Ceramic thin film formation on functionalized interface through biomimetic processing. *Science* 1994;264:4855.

**ACKNOWLEDGEMENTS:** This template was modified with kind permission from European cells and Materials Journal.

# Study of Degradability of the $\text{CaO-MgO-B}_2\text{O}_3\text{-P}_2\text{O}_5\text{-SiO}_2$ Glasses

X.Li<sup>1,2</sup>, L.We<sup>2</sup>, W.Wu<sup>3</sup>, H.Guo & C.Liu<sup>1</sup>

<sup>1</sup> Engineering Research Center of Biomedical materials under Ministry of Education, ECUST, Shanghai, 200237.

<sup>2</sup> Qiqihaer University, Qiqihaer, Heilongjiang province, China, 161006.

<sup>3</sup> Shanghai Rebone Biomaterials CO.,LTD,200237

**INTRODUCTION:** Due to its favorable bioactivity and biocompatibility, bioactive glasses have been widely used in biomaterials field. However, the long-term biocompatibility and the degradability of bioactive glasses are not very ideal. So many attentions have paid to sol-gel glasses, melting glasses with new compositions, organic-inorganic composite materials. Some materials had shown promising, but the above-mentioned degradable glasses presently have not been in accordance with human's natural bone growth. We prepared a new bioglass composite by combining sol-gel and melting methods and studied its degradability *in vitro*.

**METHODS:** *Materials preparation:* Using chemical reagents  $\text{SiO}_2$ ,  $\text{Ca}_3(\text{PO}_4)_2$ ,  $\text{CaCO}_3$ ,  $\text{Mg}(\text{OH})_2$  and  $\text{H}_3\text{BO}_3$  to prepare  $\text{CaO-MgO-B}_2\text{O}_3\text{-P}_2\text{O}_5\text{-SiO}_2$  systematic glasses. The mixed raw materials were melt at  $1300\text{-}1550^\circ\text{C}$  in crucibles of corundum with electric cookers for 2-3 hours and cooled it quickly. The  $\text{CaO-P}_2\text{O}_5\text{-SiO}_2$  sol-gel glasses were synthesized using TEOS, TEP, deionic water, ethanol and compounds containing Ca elements. Then, smashed two kinds of glasses to super-fine powders, and mixed them together by suitable press and sintered at  $800\text{-}1000^\circ\text{C}$ , crashed the product to  $450\text{-}900\mu\text{m}$  particles. *In vitro degradability experiment:* Placed the Prefabricated glass particles in SBF solution, then put them in training box and kept temperature at constant  $37^\circ\text{C}$  and took them out in turn after 0.5, 1, 3, 7, 14, 28, 42, 56, 70, 84, 98, 112 days, filtrated the samples using middling-rate filters and washed, removed the waters in the materials with vacuum drying-box, then weighted the samples in electronic balance and calculated the weights lost in percentage ratio eventually.

**RESULTS:** The results of the *in vitro* tests indicated that the degradation of the composite glass is 94.44% after immersing in SBF solution 112 days; silica, phosphorus and calcium ions were tested in SBF solution; holes appeared in glass particles' and apatites micro-particles could be found.

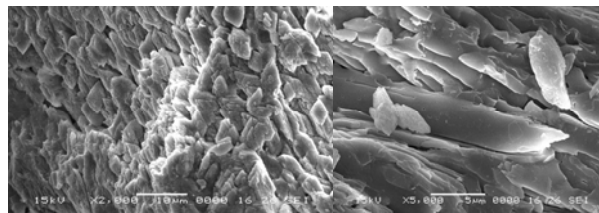


Fig. 1: The SEM photographs of sample 12-1 before *in vitro* experiment.

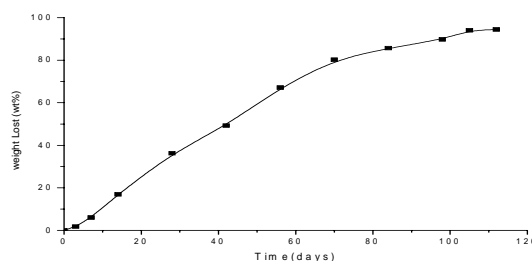


Fig. 2: The curve of Weight lost with time after sample 12-1 emerging in SBF solution for four months.

## DISCUSSION & CONCLUSIONS:

Two factors contribute to the composite degradability: the soluble capability and amount of sol-gel glass produces preliminary holes in the composite product leads to large surface areas in the melting glass; phosphate phase with defects in the melting glass promotes more degradation and bring composite dissolution entirely; the prepared sample combines strength and degradability characters together.

**REFERENCES:** <sup>1</sup>A.G.Dias, M.A.Lopes, I.R.Gibson, et al (2003) *Journal of Non-Crystalline Solids* **330**:81-89.

<sup>2</sup>J.M.Oliveira,R.N.Correia,M.H.Fernandes (2002) *Biomaterials* **23**:371-379.

**ACKNOWLEDGEMENTS:** The Author would like to acknowledge Professor Lihui Zhou, Zhiyun Xue, Lizhong Zhang, JiazhenHuang from The Testing Center of ECUST for their help in samples testing.

# Development of an Advanced Injection Device for Highly Viscous Materials

M. Loeffel<sup>1</sup>, J. Kowal<sup>1</sup>, P. F. Heini<sup>2</sup>, J. Burger<sup>3</sup>, L.-P. Nolte<sup>1</sup>

<sup>1</sup> MEM Research Center, Institute for Surgical Technology and Biomechanics, Bern, Switzerland

<sup>2</sup> Department of Orthopaedic Surgery, Inselspital, University of Bern, Switzerland

<sup>3</sup> School of Engineering and Information Technology, HTI Biel, Switzerland

**INTRODUCTION:** In several interventions on the spine, such as Vertebroplasty and disc nucleus replacement, highly viscous fluids are injected into bony or cartilaginous structures through a cannula. Currently, the material is delivered with traditional syringes, which suffer from low pressure, or screw plunger systems<sup>1</sup>, which eliminate tactile information.

We are presenting an advanced injection device that overcomes the limitations of current injectors and provides real time parameter assessment.

**METHODS:** An injection device generating 5 MPa peak pressure in a 6 ml polycarbonate syringe has been built. It is driven by a DC motor, which creates 640 N compressive force on the syringe plunger. An integrated encoder provides precise position and speed information used to calculate the injected volume and flow rate. Furthermore, strain gauges measure the force applied to the plunger, which is proportional to the pressure created in the syringe barrel. The system is controlled from a syringe-like actuator with force feedback for precise operation.



Fig. 1: The motorized injection device loaded with a 6 ml polycarbonate syringe

In most procedures dealing with the injection of substitution materials, the viscosity of the substitute is a central parameter relating to complications. When viscosity is to be assessed in a standard viscometer during the injection procedure, material curing is affected by the measuring process itself. Therefore, measurements do not correspond to the viscosity of the material contained in the syringe barrel. Our system however provides all necessary parameters for

viscosity estimation during injection based on the capillary rheometer principle<sup>2</sup>:

$$\eta = \tau/\dot{\gamma} = (PD/4L)/(32Q/\pi D^3) \quad (1)$$

( $\eta$ : viscosity,  $\tau$ : shear stress,  $\dot{\gamma}$ : shear rate, P: applied pressure, D,L: diameter, length of the cannula, Q: volumetric flow rate)

**RESULTS:** The device has been used in animal and cadaver studies investigating various aspects of Vertebroplasty. Furthermore, verification of viscosity estimation has been performed against Newtonian standard fluids rated at 41, 72, 200 and 380 Pa·s, as shown in Fig. 2.

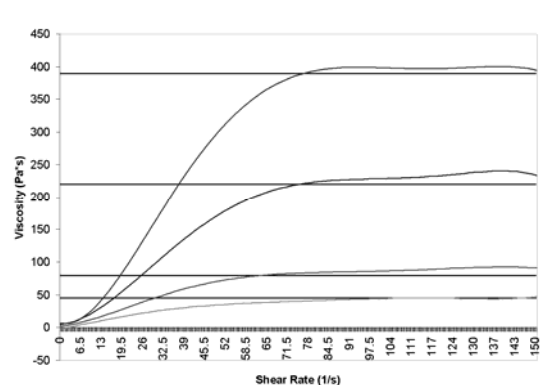


Fig. 2: Viscosity estimation against four different Newtonian fluids (horizontal lines) at increasing shear rate.

**DISCUSSION & CONCLUSIONS:** The presented injection device provides the means for consistent, repeatable and well-documented research and interventions. The integrated parameter assessment capabilities pave the way for identification and prevention of injection related complications, such as leakage due to low viscosity or excessive volume.

**REFERENCES:** <sup>1</sup>S.T. Lee and J.F. Chen, *A syringe compressor for vertebroplasty: technical note*, Surg.Neurol., 61-6: 580-584 (2004). <sup>2</sup>A. Allahham, D. Mainwaring, P. Stewart, et al, *Development and application of a micro-capillary rheometer for in-vitro evaluation of parenteral injectability*, J.Pharm.Pharmacol., 56-6: 709-716 (2004)

# Bone Substitutes Produced by Wet Shaping Techniques

J. Luyten, S. Mullens, I. Thijs, J. Coymans & S. Impens

*Materials Technology, Vito, Boeretang 200, B-2400 Mol, Belgium*

**INTRODUCTION:** Large bone defects, caused by trauma or bone cancers, are still a big challenge for surgeons. A porous bone substitute mimicking the properties of the trabecular bone to be replaced is a way to go.

To have a solution for both young people and old people, metals (stainless steel, Ti) and calcium phosphate (CaP, e.g. Hydroxyapatite (HA),  $\beta$ -TCP) are the materials for this application. The metals are load bearing and will allow the patient to re-use rapidly his defected body part. This is very important for older patients. The disadvantage is that the metal scaffold stays in the body which requires inertness with respect to reaction with the human body.

The CaP on the other hand, is a rather brittle material which cannot be used as a load bearing component but it has the advantage that it is replaced by new bone after some time.

**METHODS:** Two shaping procedures, based on aqueous powder suspensions, were developed to produce these porous scaffolds designed to promote bone ingrowth.

The two foam manufacturing routes are the PU-replica technique and gel casting.

In both cases the starting product was a stable suspension containing 25 vol% of powder in water with a dispersing agent and other additives, depending of the specific powder and shaping technique. For the replica technique a PU sponge with the desired macrostructure is dipped in a stable suspension. The excess slurry is removed by rolling. After 24 hours of drying in air, the PU sponge is burned out and the structure is sintered to gain its final strength. For the gel casting technique, a comparable suspension is used with an addition of foaming and gelling agents. This suspension is foamed by mechanically stirring and the foamy structure is gelled by cooling down. After drying in air, the organic components are burned out and the green structure is sintered. The pore diameter can be adjusted to the desired pore size distribution by the composition of the slurry and the stirring time.

In the case of metal powder, the thermal treatments have to be performed in vacuum or in a protected atmosphere.

**RESULTS AND DISCUSSION:** With both techniques, porous scaffolds can be produced with a mean pore size varying from 100  $\mu\text{m}$  to a few mm.

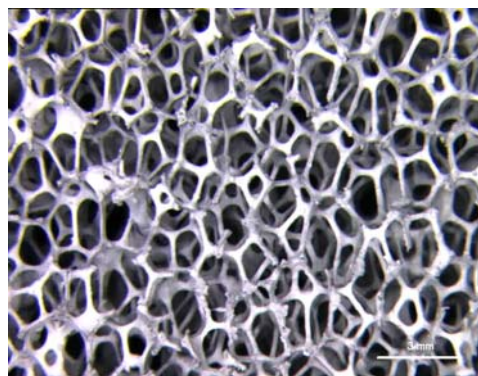


*Figure 1: Ti foam structure produced by the PU replica technique.*

To validate the performance of the scaffolds, they were characterized by different techniques. Important parameters are the pore size distribution, strut thickness (Image analysis,  $\mu\text{C}$ -Tomography), specific surface area (BET-measurement), mechanical strength and stiffness (compression, bending tests), and chemical composition (XRD and EDX).

After cyto-toxicity tests, preliminary in vivo tests were performed. Porous HA and Ti-materials were implanted in mice and rabbits. Here, bone ingrowth in the scaffolds could clearly be demonstrated.

To improve the osteoconductivity of the Ti-scaffolds, Ti-foams were coated with CaP. The first results show the feasibility of this process.

Future activity aims at incorporation of a drug delivery system in such scaffold in order to have local interaction with possible infections.

## Distal Radius Fracture and Injectable Cement : Usefull or Not ? Prospective Continue Study of 48 Cases with Minimal Follow Up of 3 years

*L.Obert, G. Leclerc, D. Lepage, Y. Tropet, P. Garbuio*

*Orthopedic and Plastic Surgery Unit - University Hospital Jean Minjoz. bd Fleming  
Besancon, France*

**INTRODUCTION:** The purpose of the study was to evaluate the feasibility of Norian SRS bone cement injected into a distal radius following reduction and stable fixation in preventing shortening and loss of pronation-supination.

**METHODS:** Between 1998 and 2000 48 patients with a mean age of 65 (54-82) sustained distal radius fracture (AO classification stage A in 26 cases, B in 15 cases, C in 7 cases) with metaphyseal comminution. Functionnal and radiological outcomes of the wrist (O'Brien scoring, Gartland and Werley scoring, DASH) were evaluated with a mean follow up of 46 months (36-56) by a surgeon not involved in treatment. Fixation was performed in 34 cases by pins, in 14 cases by dorsal plate, in 2 cases by external fixator.



*Fig 1 : Reduce the fracture and the volar cortical wall, locate the comminution, and pack the comminution*

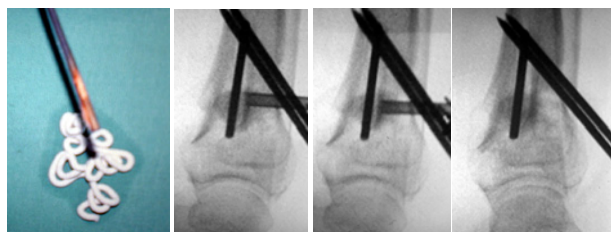


*Fig 2 :The injection of the cement is performed under X Ray control to fill the void without intraarticular or volar injection.*

**RESULTS:** 4 patient lost of follow up and 5 mal union were excluded of final evaluation. 3

RSD were pointed on the 39 evaluated patients. O' Brien scoring reached 84/100 (54-100), Gartland and Werley scoring reached 4,6 (0-11) with 89% excellent and good results, DASH reached 23,6 (5,8-62,7). Ulnar variance changed less than 2mm between postoperative time and maximal follow up in 88%. There were no clinically adverse effects but one case of volar extrusion of injected Norian was pointed with resolutive evolution. Bone substitute was always in place at the longest follow up.



*Fig 3 : Male, 42 yo...*



*Fig 4 : ... Follow up 4 years*

**CONCLUSIONS :** Adams, Pogue, Mc Queen pointed the biomechanical and clinical advantage to fill the void secondary to the comminution to avoid the shortening of the radius. First cases reported by Kopylov and Jupiter, and prospective series of Kopylov, Sanchez Sotello and Cassidy proved the interest of an adaptative injectable cement in case of comminution. Injectable bone substitute allows to maintain the ulnar variance in competition with bone graft or bio ceramic.

# Post Traumatic Arthritis Secondary to Intra Articular Malunion of the Distal Radius Treated by Chondro-costal Graft

L. Obert, D. Lepage, J. Pauchot, Y. Tropet, P. Garbuio

Orthopedic and Plastic Surgery Unit - University Hospital Jean Minjoz, bd Fleming  
Besancon, France

**INTRODUCTION:** 4 cases of postraumatic arthritis of the distal radius treated by chondro costal graft are reported with a minimum follow up of 2 years

**MATERIAL and IMETHODS:** One 22 years old patient with a dislocated radiocarpal joint 6 months after an injury, 2 patients (48 and 53 years old) respectively 1,5 and 2 years after a intraarticular fracture of distal radius and a patient (74 years old) with radio lunate arthritis reported two mains complaints : pain and stiffness. Location of the loss of cartilage was central in two cases and palmar in the others. A dorsal approach in one cases, a palmar approach in the three others allowed reduction and reconstruction of the destroyed radial part of joint. A chondro costal graft harvested on the eight's rib was inserted and fixed by plate in place of the articular impaction. Plaster cast of 3 months in the first case and 1 month in the three others cases followed the articular reconstruction

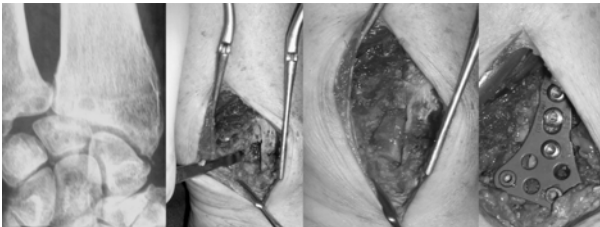


Fig. 1: Pre and per operative aspect of distal Radius with the graft

**RESULTS:** No complication have been pointed. Union was achieved in all 4 cases. Integration and viability of the graft were evaluated with RMI. At the highest follow up fonctionnal result are excellent in the first case. Motion and grasp are similar than the controlateral side. For the three others patients motion in flexion - extension reached respectively 74%, 69%, 54% of controlateral side, and grasp reached respectively 62%, 73% and 68% of controlateral side.



Fig 2 : post operative Xray

**CONCLUSIONS** Reconstruction of a partially destroyed articular surface by a costal graft is reliable and allows filling and resurfacing an articular cartilage void. If chondro costal graft is currently used in maxillo facial surgery it is the first report in post traumatic arthritis secondary to intra articular mal union.

# Extra Articular Malunion of the Distal Radius Treated by Corrective Osteotomie and Injectable Cement

L. Obert, D. Lepage, S. Rochet, Y. Tropet, P. Garbuio

Orthopedic and Plastic Surgery Unit - University Hospital Jean Minjoz, bd Fleming  
Besancon, France

**INTRODUCTION:** The purpose of the present study was to report on the author's experience using injectable cement as a bony substitute in distal radius corrective osteotomies. The interest of such a bone substitute is the real capacity to adapt itself to the bone defect. Harvesting a trapezoidal cortico spongious graft which can fill very precisely the void and not more remains a challenging objective in treating extra articular mal union.

**METHODS:** Three patients with an average age of 41yo (24-48) had a corrective osteotomy for a malunited distal radius fracture using Injectable bone substitute (Eurobone, Jectos, Kasios Inc) as an alternative to an autogenous bone graft. Internal fixation of the osteotomy was achieved by using one plate without post operative immobilisation. Two patients were stiff at preoperative time.



*Fig 1 : pre and per operative view with injection of the cement secondary to the corrective osteotomy*

**RESULTS:** At an average follow-up evaluation of 26 months (14-37 mo) all the osteotomies united. Wrist flexion-extension motion improved from 56° to 110°, forearm rotation increased from 112° to 142°, and grip strength had an average increase of 120% at the time of the final follow-up evaluation. All patients were satisfied but there one report of persistent pain. Radiographic evaluation showed an average volar tilt improvement from a preoperative dorsal angulation shifting into a neutral position in the sagittal plane; Radiographically the injectable cement showed evidence of progressive re-absorption over time but with no complete disappearance.

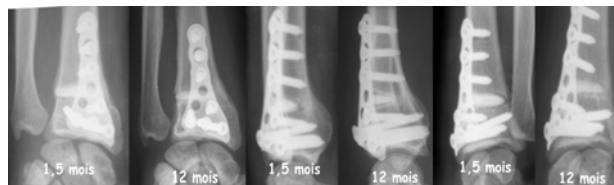


*Fig 2 : X ray aspect at short and at one year of follow up on three different view*

**CONCLUSIONS :** On the basis of this preliminary experience it is reasonable to consider injectable cement as a viable alternative to bone grafting in conjunction with surgical correction and internal fixation of extra articular distal radius malunion.

# Impact Simulation for Cranioplasty using Non-Linear Finite Element Model

H.K.Park, J.H.Park, H.D.Han & J.H.Chung

Biomedical Education Center, Department of Biomedical Engineering, School of Medicine

Kyung Hee University, Seoul, Korea

**INTRODUCTION:** Understanding the mechanical reasoning of injuries can help to determine injury tolerance and develop how to protect from injury and quantify its relationship with the degree of injury. The brain movement inside the skull has a complex three-dimensional dynamic boundary condition, which means a dynamic head injury induces transient stress distribution in three dimensions. The internal biomechanical response due to brain injury is difficult to analyze by the present outcomes from experimental animal models because mechanical transducers cannot measure the transient stress changes internally due to the current limitations of the technique. The changes after cranioplasty indicated in selected cases that cranioplasty can improve cerebral circulation and protect from neuronal deterioration [1, 2] with a good cosmetic result.

In previous studies in our laboratory, we evaluated a cranioplasty that used four different implant materials to reconstruct the normal contours of the skull. The result presented the particular reference to the safety and suitability of cranioplasty and the behavior of the implanted material over secondary impact injury. In order to improve the limitation of a previous model, we designed a redefined model close to the human skull and analyzed dynamic behavior with new implant materials. In this study, large cranioplasty that used triple layer implant materials was simulated during the injury by weight drop impact.

**METHODS:** The CT image (1 mm slice thickness) of the male patient skull was transferred to the line data in order to create an accurate surface patch. The data transferred from the CT scan was filtered by imaging data protocol to verify the integrity of the data set for slice and volumetric viewing.

In order for any computer model to provide useful information, an accurate material with constitutive laws and material properties of the patch are essential. For the finite element analysis of the computational model of the patch, four-node quadrilateral isotropic shell element is mainly used.

**RESULTS:** The overall model consists of 4,740 nodes, 2,168 solid elements, and 4,736 shell elements. The average size of the element was 2 mm<sup>2</sup>, and the thickness of the patch was 7 mm. Four peripheral areas were fixed by using titanium mini-plates and screws to secure the patch to the skull.

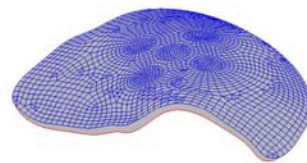


Fig.1: oblique view of inner, outer and middle layer

Table1. Comparison of the simulation results by composite implant

	Force (kN)	Displacement (mm)		Equivalent Stress (MPa)
		Peripheral	Center	
Spongy/cortical bone	2.8	2.96	29.2	47.1
HDPE/HA	5.7	1.44	64.7	172
HDPE/PMMA	1.8	4.48	25.2	100.

**DISCUSSION & CONCLUSIONS:** As a result of dynamic analysis, the composite structure of the implantable material was responding differently by the injury. However, when severe circumstances are considered, such as hitting by baseball or bat, the impact can be occurred at remarkably short time duration. When the impact energy is extremely high, the exact result is still unknown. It may be assumed that severe response can be reduced by change of location of the fixed point or of material properties without consideration of change of the geometric shape.

**REFERENCES:** <sup>1</sup> Segal, D.H., et.al(1994) Neurological recovery after craniectomy, Neurosurgery, Vol. 34, No.4, pp. 729-731. <sup>2</sup>Dujovny, M., et.al(1997) Post-cranioplasty cerebrospinal fluid hydrodynamic changes: Magnetic resonance imaging quantitative analysis, Neurological Research, Vol. 19, pp. 311-316

**ACKNOWLEDGEMENTS:** supported by MOCIE of Korea

# Preparation and Characterization of Nanofiber Matrices for Tissue Engineering

H.H.Park<sup>1</sup>, K.E.Park<sup>2</sup>, K.Y.Lee<sup>1</sup> & W.H.Park<sup>2</sup>

<sup>1</sup> Department of Bioengineering, Hanyang University, Seoul 133-791, South Korea. <sup>2</sup> Department of Textile Engineering, Chungnam National University, Daejeon 305-764, South Korea

**INTRODUCTION:** Tissue engineering is an exciting and revolutionary strategy to treat patients who need a new organ or tissue. In this approach tissues or organs can be potentially engineered with a number of different strategies, but a particularly appealing approach utilizes a combination of a patient's own cells and polymer scaffolds. Polymer scaffolds act as analogues to the natural extracellular matrices, which can provide a space for new tissue formation and potentially control the structure and function of the engineered tissue.<sup>1,2</sup>

Various polymers have been utilized to date in tissue engineering. A copolymer of poly(lactic acid) and poly(glycolic acid) (PLGA) is one of the most widely used synthetic polymers.<sup>3</sup> Fibroin is a main component of silkworm silk, and has been frequently used in the areas of biomedical science and engineering.<sup>4</sup> In this study, nanofiber matrices were prepared as synthetic extracellular matrices by electrospinning a solution of either PLGA or silk fibroin (SF), and their characteristics were investigated. The effects of structural changes of the nanofiber matrices on cellular responses were also studied.

**METHODS:** Nanofibers were prepared by electrospinning a solution of either silk fibroin or PLGA (50:50) dissolved in hexafluoro-2-isopropyl alcohol (HFIP), and were collected on a target drum. A voltage of 16 kV was applied to the collecting target, and the flow rate of the solution was 2 mL/min. A scanning electron microscope was used to investigate morphology of nanofibers. Characteristics of the nanofibers were also investigated using FT-IR, <sup>13</sup>C solid-state CP/MAS NMR, XPS, and contact angle measurements. Normal human epidermal fibroblasts were cultured in Dulbecco's modified Eagle's medium supplemented with 10% fetal bovine serum. Adhered cells on nanofiber matrices were photographed with an optical microscope, and the number of cells on the matrices was quantified using an MTS solution.

**RESULTS:** Nanofibrous nonwoven matrices were prepared by electrospinning a regenerated silk fibroin solution, and their mean diameter was 380 nm. Changes in the characteristic absorption peak

of the amide I and II bands of SF nanofibers during water vapor treatment were investigated using time-resolved measurements of IR absorption bands. The water vapor-treated SF nanofiber matrices showed good cellular compatibility, compared with traditional methanol-treated ones. PLGA nanofiber matrices with the mean diameter of 340 nm were also prepared, and treated with plasma in the presence of either O<sub>2</sub> or NH<sub>3</sub> gas. The hydrophilic characteristics of the plasma-treated PLGA nanofiber matrices dramatically increased, and the growth rates of cells on the matrices were also increased, compared with non-treated PLGA nanofiber matrices.

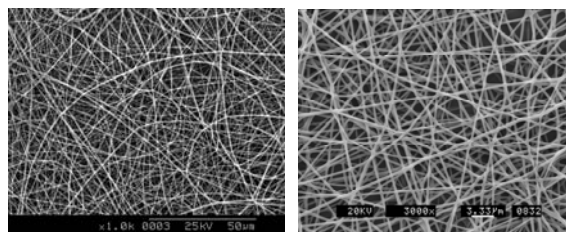


Fig. 1: SEM images of SF (left) and PLGA (right) nanofiber matrices.

**DISCUSSION & CONCLUSIONS:** Structural changes of PLGA and SF nanofiber matrices treated with plasma and water vapor, respectively, influenced cellular behaviour on these synthetic extracellular matrices. This approach to controlling the adhesion and proliferation of cells by varying chemical and/or physical structures of nanofibers may be useful in the design and tailoring of novel biomaterials for tissue engineering applications.

**REFERENCES:** <sup>1</sup> K. Y. Lee, D. J. Mooney (2001) *Chem Rev* **101**:1869. <sup>2</sup> J. J. Marler, J. Upton, R. Langer, J.P. Vacanti (1998) *Adv Drug Deliv Rev* **33**:165. <sup>3</sup> R. C. Thomson, et al (1999) *Biomaterials* **20**:2007. <sup>4</sup> A. Motta, et al (2004) *J Biomat Sci Polym Edn* **15**:851.

**ACKNOWLEDGEMENTS:** This work was supported by the Biotechnology Development Program (Grant No. 2005-00009 and 2005-00115) from Ministry of Science and Technology (MOST), Korea.

# **In Vitro Biocompatibility Test of Nano Alumina and Characterization by Rietveld Analysis**

D. Sahal<sup>1</sup> & S. Dhabal<sup>2</sup>

<sup>1</sup> *Mechanical Engineering , Jadavpur University, Kolkata, 700032, India.*

<sup>2</sup> *Department of Physics, Indian Institute of Technology, Kharagpur, 721302, India.*

Biocompatibility test of nano alumina, has been done by cytotoxicity test method. The crystalline size of nano alumina determined by Rietveld analysis of X ray diffraction studies and Transmission electron microscopy. Cytotoxicity results indicate that cells proliferations has been taken place. So we can conclude that nano alumina

is highly biocompatible material. Rietveld analysis of X-ray diffraction and transmission electron microscopy showed that the sample is composed of crystalline and a small fraction of amorphous phases. In view of these, nano alumina may be considered to be future potential for bone substitute material.

# The Effect of Sintering Temperature on Mechanical Properties of Aluminium-Oxide Reinforced Hydroxyapatite (BHA) Composites

S.Salman,<sup>1a</sup> O.Gunduz,<sup>1b</sup> & F.N.Oktar,<sup>2a,b</sup>

<sup>1a,b</sup>Marmara Uni., School of Technical Education, Metal Education Dep., Istanbul, Turkey

<sup>2a,b</sup>Marmara Uni., School of Engineering, Industrial Engineering Dep., School of Health Related Professions, Radiology Dep., Istanbul, Turkey

**INTRODUCTION:** Because of its superb biocompatibility to the human body, hydroxyapatite [HA,  $\text{Ca}_{10}(\text{PO}_4)_6(\text{OH})_2$ ] ceramics have been used as implants in bone and teeth restorations. Nevertheless, its poor mechanical properties have restricted wider applications in load-bearing devices. Hence, composite materials of HA, with ceramic oxides or metallic dispersants as reinforcing agents, have been proposed. With regards to ceramics, which can be potentially used as reinforcements, alumina ( $\text{Al}_2\text{O}_3$ ) ceramics are probably the most typical structural ceramics. Therefore, they have been used for implants and prostheses, largely in orthopaedic applications, since several decades [1, 2]. Alumina ceramics feature excellent biocompatibility (in terms of bio-acceptability), and high mechanical strength, hardness and fracture resistance. The high wear resistance is of particular interest for implant components with articulating surfaces, such as artificial joints. This is the major reason for the predominant use of alumina ceramics to produce femoral joint heads. It has been suggested that HA- $\text{Al}_2\text{O}_3$  composites can exhibit better mechanical properties than pure HA. Some studies have been addressed in the reinforcement of HA with  $\text{ZrO}_2$  and  $\text{CaF}_2$ . However, all these studies have been performed by merely using synthetic HA supplied by the open market or produced with conventional methods in the laboratory. To the knowledge of the authors, there is no study systematically tackling the production of HA- $\text{Al}_2\text{O}_3$  composites. In this general framework, this study aims to present the effect of sintering on the mechanical properties HA- $\text{Al}_2\text{O}_3$  composites, where the source of HA is natural from bovine bones (BHA).

**METHODS:** The BHA material was obtained from bovine bones. The experimental procedure has been described in details in our earlier paper [3]. The derived BHA mater was first ball milled to a fine powder and then mixed (separately) well with 5 wt% and 10 wt%  $\text{Al}_2\text{O}_3$ . The homogeneous powder mixture was uniaxially pressed into pellets using hardened steel dies, according to the British Standard 7253. The pellets were sintered at several different temperatures, between 1000-1300°C. The characterization of the mechanical properties

comprised measurements of compression strength and microhardness. The results are discussed in the light of microstructure (by SEM) and the crystallography (by X-ray diffraction) of the samples.

**RESULTS:** Microstructural SEM analysis indicated typical densification behaviour, similar to that observed in earlier studies on the sintering behaviour of HA. The experimental results of compressive strength ( $\sigma$ , in MPa) and microhardness are summarized in Table 1.

Table 1: Mechanical properties of the present study.

T (°C)	$\sigma$ 5 % $\text{Al}_2\text{O}_3$	$\sigma$ 10 % $\text{Al}_2\text{O}_3$
1000	42.566	28.94
1100	55.07	32.55
1200	76.32	54.36

**DISCUSSION & CONCLUSIONS:** Table 2 allows the comparison of the results of this study with results of earlier ones [4]. Other investigators have used much higher amounts of reinforcing phases, such as 20%  $\text{Al}_2\text{O}_3$  [5], or 70 vol %  $\text{ZrO}_2$ - $\text{Al}_2\text{O}_3$ . Nevertheless, such big amounts may jeopardize the overall bioactivity of the resultant composites.

Table 2: Mechanical properties of the other studies [4].

T (°C)	$\sigma$ 5 % $\text{La}_2\text{O}_3$	$\sigma$ 10 % $\text{La}_2\text{O}_3$
1000	26.17	61.29
1100	42.98	48.36
1200	86.21	104.13

This study showed that the addition of 5 %  $\text{Al}_2\text{O}_3$  results in increase of mechanical strength of BHA. It is very surprising to get lower mechanical values for increasing content of  $\text{Al}_2\text{O}_3$ . Further studies must be achieved with 15 and 20 %  $\text{Al}_2\text{O}_3$  why the adding  $\text{Al}_2\text{O}_3$  cause decrease at the mechanical values. But it will be also interesting to conduct some cell culture studies.

**REFERENCES:** <sup>1</sup>H-W. Kim et al., (2003) *Mat Sci and Eng C* **23** : 515. <sup>2</sup>H. Fischer et al. (2005) **26**: 6151. <sup>3</sup>L.S. Ozyegin, F.N. Oktar, et al. (2004) *Mater Lett* **58**: 2605. <sup>4</sup>Oktar et al., (2006) *Key Eng Mater* **309-311**: 101. <sup>5</sup>Knepper et al., (1997) *Biomater* **18**: 1523.

# Fabrication of Silver Nanoparticles and Their Antimicrobial Mechanisms

H.Y Song<sup>1,a</sup>, K.K Ko<sup>1</sup>, I.H Oh<sup>2</sup>, B.T Lee<sup>3,a</sup>

<sup>1</sup>Department of Microbiology, College of Medicine, Soonchunhyang University, Cheonan, Chungnam, Korea, <sup>2</sup>Gwangju Research Center, Korea Institute of Industrial Technology(KITECH), Gwangju, Korea, <sup>3</sup>School of Advanced Materials Engineering, Engineering College, Kongju National University, Kongju, Chungnam, Korea, <sup>a</sup>Human NanoTech, Kongju National University, Kongju, Chungnam, Korea

**INTRODUCTION:** Silver is one of the most universal antimicrobial substances. Nano-technology enables us to expand the surface area of silver particles markedly. However, the exact mechanism of the antimicrobial effects of silver is still unknown. Therefore the antimicrobial activities and mechanisms of silver nanoparticles for several pathogenic bacteria were investigated.

**METHODS:** To synthesize nano-sized Ag colloid, silver nitrate as a source of silver was dissolved in ammonia water. Formaldehyde as a reducing agent and polyvinyl pyrrolidone (PVP) as the stabilizing agent were used. The temperature of the reaction vessel was maintained at 40 °C, and the pH of reaction solution was maintained at  $10 \pm 0.5$ . PVP coated silver colloids were washed with acetone. Finally, the silver gel was centrifugally separated and washed with deionized water and then dried at 150°C for 3 hours. To examine the bactericidal effect of silver nanoparticles on *Escherichia coli*, *Staphylococcus aureus*, *Salmonella typhi* and *Mycobacterium tuberculosis*, bacteria were incubated with a bead (0.1g) of silver and silver nanoparticles at a dilution of 0.5, 1, 5, 10 and 30 ppm for 1 hour. Then, bacteria were cultured on BHI agar plates and CFU was determined. Antituberculosis activity of nanosilver was examined using the BACTEC MGIT 960. <sup>1</sup>To explore the antimicrobial mechanisms, several pathogenic bacteria cultured with nanosilver suspension for 1 hour were observed by TEM and SEM.

**RESULTS:** Silver nanoparticle was successfully produced less than 10nm in size (Fig. 1). It showed excellent antibacterial activities against *S. typhi*, *E. coli*, *P. aeruginosa* around 1 ppm and *S. aureus* and *M. tuberculosis* around 10 ppm. Three types of antimicrobial mechanisms were observed. 1) Plasmolysis, cytoplasm of bacteria separated from bacterial cell wall, was observed in Gram negative bacteria (Fig. 2). 2) The synthesis of bacterial cell wall was inhibited in *S. aureus*.

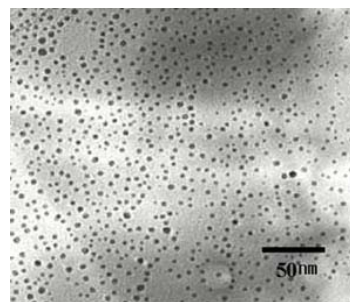


Fig. 1. TEM images of silver nanoparticles.

3) Nanosilver particles found in the cytoplasm of *M. tuberculosis* may induce metabolic disturbance.



Fig. 2. Scanning (top) and transmission (bottom) electron micrographs of *E. coli* after treatment of 0.1 ppm of nanosilver for 1 hour.

**DISCUSSION & CONCLUSIONS:** Silver nanoparticle was successfully synthesized around 5 nm in size. They showed excellent antibacterial activity. Antimicrobial mechanisms of nanosilver were different according to the species of bacteria. From the result, Silver nanoparticles will be available as a good antibiotic alternative.

**REFERENCES:** <sup>1</sup> P.R Murray, K.S Rosenthal, et al (2002), Medical Microbiology, P 11-24, <sup>2</sup> I. Sondi, B.S. Sondi (2004), Journal of Colloid and Science Vol.275, p.177.

**ACKNOWLEDGEMENTS:** This work was supported by the research grant from Soonchunhyang University in the year of 2005.

# Morphological Changes During 42 Months of PMMA Vertebroplasty: A Case Study

C.M.Sprecher<sup>1</sup>, A.Gisep<sup>2</sup>, S.Milz<sup>1</sup>, U.Haupt<sup>3</sup>, K.Yen<sup>4</sup>, P.Heini<sup>3</sup>

<sup>1</sup> *AO Research Institute, Davos, CH* <sup>2</sup> *AO Development Institute, Davos, CH* <sup>3</sup> *Department of Orthopaedic Surgery, Inselspital, Bern CH* <sup>4</sup> *Institute of Legal Medicine, University of Bern, CH*

**INTRODUCTION:** Vertebroplasty has proven to be highly efficient in the treatment of osteoporotic vertebral compression fractures (OVCF) [1-2]. However, questions related to heat necrosis during setting of the PMMA cement and trabecular bone remodelling in and around the augmented volume are still open. Another open question relates to ageing processes of the cement itself.

**METHODS:** This investigation used macerated vertebral bodies of a 80 year old female treated with PMMA vertebroplasty of Th07 – Th10 in August 2001. Vertebral bodies were explanted post-mortem 3.5 years after the initial operation. High resolution CT scans were obtained using a Xtreme CT (Scanco). A field emission scanning electron microscope (Hitachi S-4100) was used to detect changes in the cancellous bone morphology in the topography and density mode. Composition of the cement was assessed by EDX (Oxford Isis300).

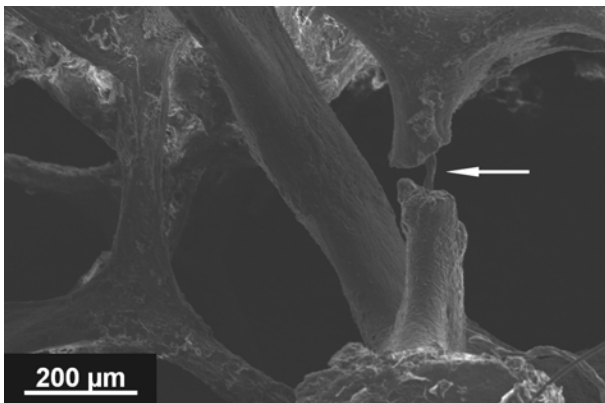


*Fig. 1: SEM image (in the topography mode) of a fractured trabeculi. Part of it is embedded in the cement (bottom right). Note the small bridging piece of macerated bone at the fracture (arrow).*

**RESULTS:** Trabecular bone generally appeared to have normal structure within and outside the cemented region. However, in the vicinity of the cement block some fractured trabeculi could be observed. Some of these trabeculi showed signs of bridging (figure 1). CT scans exhibited different density-levels within the cement block. Slightly higher values were observed in the centre when compared to the periphery. EDX showed that ZrO<sub>2</sub> was used as a contrast medium in the cement. In

most regions, there was a gap (<100 µm) between the individual trabeculi and the surrounding cement. The cement itself was fragmented, showed many microcracks, holes and rests of unpolymerized MMA powder (figure 2).

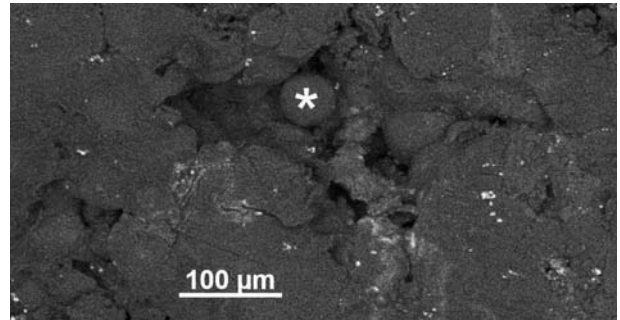


*Fig. 2: SEM image (in the density mode) of a sawcut through the cement. Note the MMA sphere (asterisk) which resembles a prepolymerized part of the cement powder. Also note the surrounding excavation and the network of cracks. The small white dots are contrast material (ZrO<sub>2</sub>).*

**DISCUSSION & CONCLUSIONS:** The results suggest that some bone healing / remodelling is occurring around the cement block in treated osteoporotic vertebrae. The altered mechanical loading of trabecular bone, which connects the cement to the rest of the vertebra may cause fracture of individual trabeculi. In general however, the bony interface between the cement block and the surrounding vertebra (at least in the presented case) does not seem to fail on a broader scale. An inhomogeneous distribution of ZrO<sub>2</sub> within the injected cement can be interpreted as the result of incomplete mixing prior to injection. Alternatively a separation of the different phases of the liquid cement during the injection into the cancellous meshwork could be discussed.

**REFERENCES:** <sup>1</sup> D. Togawa, et al (2003) *Spine* 28:1521-7 <sup>2</sup> G. Lewis, et al (2005) *J Biomed Mater Res B Appl Biomater*. (accepted).

**ACKNOWLEDGEMENTS:** Ricco Soder from AO Development Institute for performing and evaluating CT Scans.

# Determination of Impurities in Calcium Phosphates Ceramics

E.I.Suvorova, P.A.Buffat

Centre Interdépartemental de Microscopie Electronique – EPFL, Lausanne, CH.

**INTRODUCTION:** This investigation was undertaken in the frame to developing efficient synthetic materials that can be osteoconductive for rapid integration with bone and biodegradable at an optimal rate for replacement by newly formed bone tissue.

**METHODS:** Transmission and scanning electron microscopy were used to characterize bioceramics based on hydroxyapatite (HAP) and tricalcium phosphates (TCP) to reveal the possible impurities formed during the preparation.

Three kinds of HAP ceramics were synthesized: (i) spherical HAP aggregates with diameter up to 1-2  $\mu\text{m}$  in boiling suspensions of nanocrystalline HAP [1], and hard HAP ceramics (ii) annealed at 870°C for 2 hours and (iii) at 1000°C (3 hours) + 1200°C (2 hours).

Samples of  $\alpha\text{-Ca}_3(\text{PO}_4)_2$  porous ceramics with a continuous pore structure were synthesized through a conventional sintering procedure that utilizes a slurry composed of  $\beta\text{-Ca}_3(\text{PO}_4)_2$  and potato starch sintered at 1400 °C for 12 h in air [2].

The calculation and interpretation of the TEM data were carried out with the DigitalMicrograph 3.6.1(Gatan, Inc., Pleasanton, CA, USA) and Java Electron Microscopy (JEMS) Software (P. Stadelmann, CIME-EPFL, CH). Also X-ray diffraction patterns were calculated for several mixtures of  $\beta\text{-TCP}$  in  $\alpha\text{-TCP}$ , as well as CaO in  $\alpha\text{-TCP}$  phases and CaO in HAP in different proportions using CaRIne Crystallography 3.1 software (C. Boudias & D. Monceau, Divergent S.A., Compiègne, France).

**RESULTS:** Our results showed that the final TCP product contained mainly  $\alpha\text{-TCP}$ , about 3.4 weight % remaining of the raw material  $\beta\text{-TCP}$  phase and CaO up to 15.4% as an impurity formed by decomposition of TCP at high temperature. X-ray diffraction method failed to detect CaO impurity. The CaO inclusions were found to be embedded into the  $\alpha\text{-TCP}$  matrix (Fig.1) or even as individual aggregates of a few microns in size (Fig.2). HRTEM image and dynamical electron diffraction simulation by JEMS show a good agreement with the experimental images and confirms the presence

of CaO. While TEM showed only the HAP phase in all kinds of HAP ceramics.

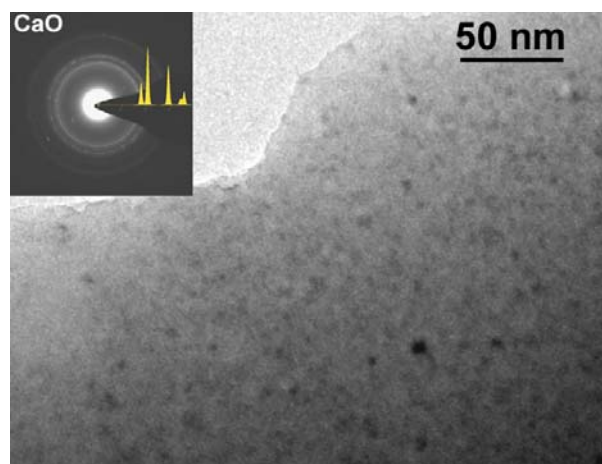


Fig. 1: TEM image and diffraction pattern from an area containing CaO nano-crystals

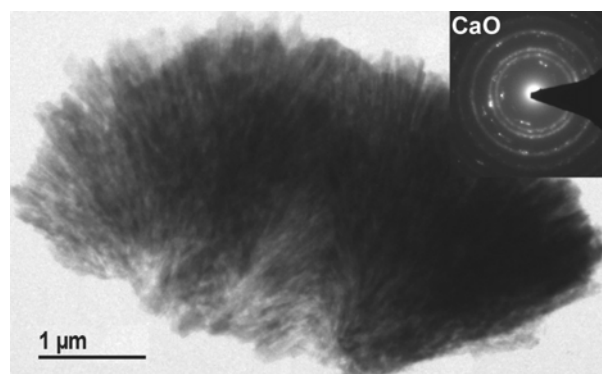


Fig. 2: TEM image and diffraction pattern from a CaO agglomerate.

**DISCUSSION & CONCLUSIONS:** TEM shows that high-temperature sintered  $\alpha\text{-TCP}$  product contained CaO inclusions due to decomposing. The presence of CaO is a potential danger in particular for bio-applications. Its high reactivity with water (exothermic reaction) constitutes an internal heat source in tissues, and in addition its volume nearly doubles during the reaction.

**REFERENCES:** <sup>1</sup> A.V. Severin, V.F. Komarov, et.al (2005) *Russian Journal of Inorganic Chemistry* **50** (1): 72-77. <sup>2</sup> M. Kitamura, C. Ohtsuki, at.al (2004) *Key Engineering Materials* **254-256**: 965-968.

# Acrylic Vertebroplasty Alters Vertebral Load Distribution and Causes Reduction in Strength of Adjacent Vertebrae

W. Tawackoli<sup>1</sup>; K. Sun<sup>1</sup>; M. Fukshansky<sup>3</sup>; A. Burton<sup>3</sup>; L. Rhines<sup>2</sup>; E. Mendel<sup>2</sup>; M. Liebschner<sup>1</sup>  
<sup>1</sup>*Department of Bioengineering, Rice University, Houston, TX*

<sup>2</sup>*Departments of Neurosurgery and* <sup>3</sup>*Anesthesiology, MD Anderson Cancer Center, Houston, TX*

**INTRODUCTION:** Percutaneous vertebro-plasty, specifically polymethylmethacrylate (PMMA), to treat vertebral defects has proven clinical success in alleviating back pain. However, the compact distribution of PMMA within the vertebrae has been shown to cause stress concentrations in the bone tissue directly above and below the PMMA bolus. This in turn is believed to cause secondary fractures of the adjacent vertebrae [1, 2]. The overall goal of this study was to test the hypothesis that vertebral body augmentation through acrylic vertebroplasty reduces the ultimate stress in adjacent untreated vertebrae due to changes in load-transfer along the spinal column.

**METHODS:** Twelve fresh-frozen cadaveric spinal segments (3VB+ 2Discs) from 6 human spines were utilized in this study (mean age  $73 \pm 3$  years). To simulate a worst-case scenario, the L1 and L3 vertebrae (treated group) were injected with PMMA using a transpedicular-bilateral approach with the middle vertebra left untreated. Through each pedicle 5 cc of PMMA (SimplexP, Stryker) was injected into the anterior 2/3 of the vertebral body. The cement was allowed to cure for 24 hours with the specimens kept at 4°C. Specimens were mounted to a 6DOF robotic arm in load control. Pure compressive load was applied while eliminating shear forces and bending moments, thereby following the path of least resistance. The compressive load was increased till the segment has fractured or compressed 20% of its initial height. The load-deformation curve was extracted from the load-cell data and cross-head coordinates. At each 600 N load increment, plane X-rays were taken to identify fractures. The ultimate stress of the control group was used to predict the failure stress of the treated group.

**RESULTS:** The average ultimate stress of the vertebroplasty treated spinal segments was 36% less compared to the ultimate stress of their counterparts in the control group. The bilateral vertebral body augmentation resulted in all but one specimen in a significant loss of strength of the middle vertebra ( $p < 0.01$ ). A comparison in the fracture types by X-rays showed that the superior and inferior endplates of all L2s in the treatment group were fractured whereas in the control group,

the segment failure were mostly due to cancellous bone failure resulting in a wedge fracture pattern (Figure 1).

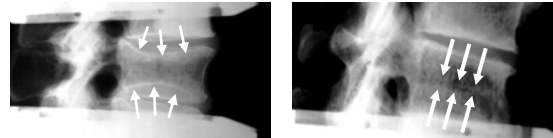


Figure 1: (Left) Spinal segment with top and bottom vertebrae treated with PMMA resulted in fractures at the endplates of the middle untreated vertebra upon compression. (Right) Compression of an untreated spinal segment resulted in a wedge fracture pattern.

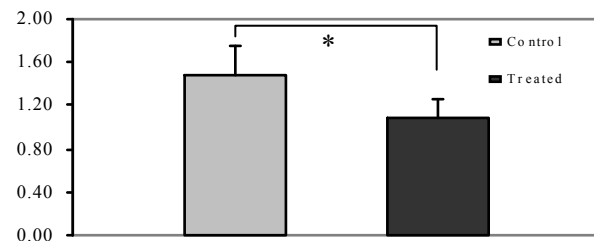


Figure 2: Ultimate Stress [MPa] of the treatment group is on average 36% lower than the ultimate stress of the control ( $p < 0.01$ ;  $n = 6$ ).

**DISCUSSION & CONCLUSION:** The goal of this cadaveric study was to investigate the effect of vertebroplasty on adjacent vertebral strength. The lowered strength and the distinct failure pattern at the endplates of the adjacent vertebrae after vertebroplasty indicate a change in load transfer along the spinal column due to the procedure. The results supported the hypothesis that the presence of the PMMA cement within the vertebra prevented normal deformation of the treated vertebra upon compression, forcing an increased endplate bulge into the adjacent untreated vertebrae and hence initiate premature tissue damage leading to catastrophic failure. Similar conclusions have been drawn in previous numerical studies [2,3]. New types of bone cements with different distribution patterns may be able to reduce adjacent bone failure.

**REFERENCES:** <sup>1</sup>Uppin AA, et al. (2003) *Radiology* **226**:119-24. <sup>2</sup>Polikeit A, et al. (2003) *Spine* **28**: 991-996. <sup>3</sup>Baroud, G, et al. (2003) *Eur Spine J.*, **12**: 421-6.

# Strength Restoration by Sacroplasty of Simulated Sacral Insufficiency Fractures

M.D. Waites<sup>1</sup>, S.C. Mears<sup>1</sup>, J.M. Mathis<sup>2</sup>, & S.M. Belkoff<sup>1</sup>

<sup>1</sup> Johns Hopkins International Center for Orthopaedic Advancement, Baltimore, MD <sup>2</sup> Dept. of Radiology, Virginia College of Osteopathic Medicine, Blackburg, VA

**INTRODUCTION:** Sacral insufficiency fractures are a cause of severe pain and morbidity. Treatment currently involves rest, use of ambulatory aids and pain medicines. By injecting bone cement into the broken pelvis, it may be possible to relieve pain and strengthen the bone<sup>1,2</sup>. This is similar to the technique of vertebroplasty in the osteoporotic spine. The current study tests the hypothesis that sacroplasty restores pelvic strength after sacral insufficiency fracture to intact levels.

**METHODS:** Cadaveric pelvises were stripped of tissue and tested for osteoporosis using DEXA scanning. Pelvises had a mean age of 82 years (SD 9) and mean T-score of -4.7 (SD 1.5). Pelvises were assessed with CT scan to rule out the presence of hardware or previous fractures. 14 pelvises were potted and mounted on a materials testing machine. L5 was displaced inferiorly at a rate of 1 mm per second until fracture occurred. Load at fracture was recorded and fractures were verified using CT. A 10 - gauge needle was then placed into the sacrum at the fracture site of S1 using fluoroscopy. Each specimen was injected bilaterally with 4cc of polymethylmethacrylate cement (Spineplex, Stryker) and the cement was allowed to polymerize. Pelvises were then retested as before to measure the repaired strength.

**RESULTS:** Fractures were seen on CT scan in 12 of 14 pelvises. 10 fractures were unilateral and two bilateral. Fractures were lateral to the foramen in all cases. 3 specimens had a horizontal component to the fracture. Mean load at fracture (strength) of the specimens was 3178 N (SD 1373). After sacroplasty the mean restored strength was 2018 N (SD 1036).

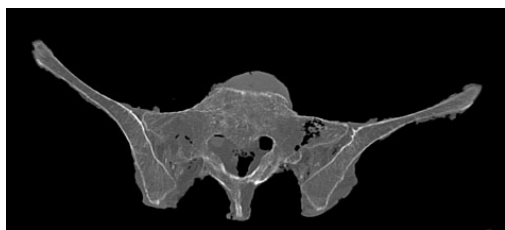


Fig. 1: Unilateral fracture lateral to the S1 foramen

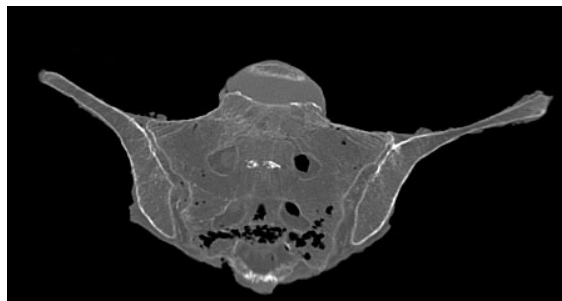


Fig. 2: Horizontal extension of a fracture through the S3 body

**DISCUSSION & CONCLUSIONS:** Sacroplasty was tested in a cadaveric model of a sacral insufficiency fracture. The fracture model created fracture patterns that mimic those seen clinically. The broken pelvis was strengthened with the bilateral injection of 4cc of bone cement to 63% of its intact strength. Future studies are required to determine the strengthening effects of different doses of bone cement. The safe placement of cement into the fractured sacrum will require the use of a CT scanner to avoid extravasation of cement into nearby neurovascular structures. The volume and placement of cement necessary to relieve pain must be determined in the clinical setting.

**REFERENCES:** <sup>1</sup> W. Pommersheim, F. Huang-Hellinger, M. Baker, P. Morris. Sacroplasty: a treatment for sacral insufficiency fractures. (2003) *AJNR Am J Neuroradiol.* **24**:1003-1007. <sup>2</sup> M. Garant. Sacroplasty: a new treatment for sacral insufficiency fracture. (2002) *J Vasc Interv Radiol.* **13**:1265-1267.

**ACKNOWLEDGEMENTS:** SCM is supported by the Jahnigen Career Development Scholarship Program funded by the American Geriatrics Society and the John A. Hartford Foundation

# Injectable Bioactive Nano Biomaterials for Bone Tissue Engineering

Y.Wang, J.Weil, H.Guo, H.Hong, C.Liu

*Institute of Biomaterials, East China University of Science and Technology, Shanghai 200237.  
P.R.China*

**INTRODUCTION:** The search for an osteoconductive and injectable bone tissue engineering material has been the quest of many researchers being interested in reconstructing bone defects. It is well known that the mineral in natural bone exists in the form of nano-hydroxyapatite (n-HA), forming an inorganic and organic nano-composite with collagen. From biomimetic point of view, synthesized apatite nanocrystals can be made to be similar to bone apatite in morphology, composition, crystal structure and crystallinity. Biodegradable polyamide6 (PA66) is an excellent medical polymer, which has a structure similar to collagen and has a good compatibility with human tissue. At present, a biomimetic nano-composite of nano bone-like apatite and PA6 was designed and developed. By using the nano-composite, a new type of injectable biomimetic composite bone cement was developed as tissue repair and tissue engineering materials.

**METHODS:** The as-prepared apatite precipitate in a solid-solution ratio of 1 wt% was treated in water in a glass container at 90-100°C under normal atmospheric pressure for 4 hrs. After treatment, the apatite precipitate became apatite nanocrystals in a slurry state. Composite was prepared by mixing nano apatite slurry and dissolved PA in N, N-dimethyl acetamide (DMAC) solution at 120~ 150°. After fully washed by hot deionized water, the composite was dried at 110° for 48 hrs. The composite was ground and sieved through 400 meshes sieve to get the cement fine powder. The cement solution was composed of ethanol solution and a little metal salt. The composite powder and the cement solution were mixed with different liquid-solid (L/S) ratio to form injectable cement paste.

**RESULTS & DISCUSSION:** The injectable nano-composite cement can be handled as paste, easily injected, and set at 37° within 7~30 minutes in physiological saline solution. It has an excellent washout resistance, and can set and harden not only in physiological saline, but also in blood, which is very suitable for tissue engineering and clinical application. The setting time increases with the increasing of L/S ratio and the metal salt content both in air and in saline. When the L/S ratio is less than 0.40 ml/g and the metal salt is less than 14wt %, the cement is difficult to be injected; when the L/S ratio is more than 0.45, the injectable property of the cement becomes better.

Concerning the injectability, the compressive strength and setting time, the L/S ratio should not be higher than 0.55. A L/S value of 0.5 is found to yield good injectability, reasonable setting time and high mechanical property in saline. The compressive strength of the injectable cement increases with time in saline, a normal value of 38MPa can be obtained at 48 hours for 48wt% n-HA in composite. Increasing the apatite content in composite can also improve the compressive strength and injectability of the cement. The maximum value can reach 44MPa for 64wt% apatite content in the composite. When the content of apatite in the composite is more than 64wt%, the compressive strength of the cement decreased with the apatite content. The result indicates that L/S ratio significantly affects the injectability of the cement and the mechanical strength. The injectability of the cement increases with the increasing of L/S ratio, accompanying the compressive strength decreases and the setting time prolongs. After the cement setting in saline, the cement block shows a porous structure, containing macropores and micropores. There are abundant micropores on the walls of the macropores and the cement surface. When the cement hardened in saline, the ethanol and the soluble metal salt are dissolved in water, allowing the formation of interconnected macropores and micropores. The interconnected micropores and rough surface of the cement will also enhance osteogenic precursor cell adhesion, differentiation, proliferation and bone matrix deposition. The porous apatite/PA cement scaffold will be a high performance biomaterial for repair and bone tissue engineering.

**CONCLUSIONS:** The results suggest that nano-apatite/PA biomimetic composite cement has a reasonable setting time, excellent washout resistance property, high mechanical strength and bioactivity, which can be developed as a bioactive material for bone repair and tissue engineering.

**ACKNOWLEDGEMENTS:** The financial support from the Ministry of Science and Technology of China is gratefully acknowledged.

# Research and Expressions of the Bioglass Cement

L.Weij, X.Li & G.Wu

Department of Material science and Technology, Chemical Institute of Science and Engineering, Qiqihaer University, 161006

**INTRODUCTION:** Biocement injection is one of research hotspot in biomaterial areas. In this paper the authors studied another cement—bio-glass cement which was formed by reaction of the  $\text{CaO-P}_2\text{O}_5\text{-SiO}_2$  systemic glasses with ammonia phosphate liquid. Using  $\text{CaO-MgO-CaF}_2\text{-P}_2\text{O}_5\text{-SiO}_2$  systemic glass and ammonia phosphate composite solution prepared self-hardening biocement. XRD and IR analysis proved P=O bond in glass network were unclosed and replaced by P-O-M bond to form  $(\text{NH}_4)_2\text{Ca}(\text{HPO}_4)_2\cdot 2\text{H}_2\text{O}$  crystal. SEM observations showed phosphate network were founded. The highest strength reached to 34.980 MPa; the haemolytic test showed all samples fit biocompatibility requirement. This Bioactive glass bone cement is a promising injectable planting material with good compatibility and plasticity.

**METHODS:** 1. Preparing bio-glass: Using reagent-grade chemical  $\text{CaCO}_3$ ,  $\text{SiO}_2$ ,  $\text{Ca}_3(\text{PO}_4)_2$ ,  $\text{MgCO}_3$ ,  $\text{CaF}_2$  to confect raw materials. Mixed materials were melted at  $1500^\circ\text{C}$ , cooled, heated at  $1050^\circ\text{C}$ , cracked and sieved through 300 mesh and the powder were stored. 2. Preparing of hardening liquids: The reagent-grade analytical  $(\text{NH}_2)\text{HPO}_4$  and  $\text{NH}_4\text{H}_2\text{PO}_4$  in different ratio were dissolved in 100 ml distilled water, and formed a series of 1M hardening liquid (H) (PH at 6-8). 3. Solidifying process: The bio-glass powders and H liquid were mixed and ground and made into  $\phi 10 \times 10\text{mm}$  column maintained 3 days after solidifying, then tested. Haemolytic test were done in Qiqihaer Medical College. Samples were immersed in Tis-HCl (SBF) solution to do in vitro experiment.

**RESULTS:** All the samples were solidified in 30 minute. Mechanical property and bio-haemolytic properties (see table 1) was ideal. XRD analysis (see fig.1) and IR showed the product of hardening is  $(\text{NH}_4)_2\text{Ca}(\text{HPO}_4)_2\cdot 2\text{H}_2\text{O}$  but not hydroxyapatite. IR analysis illuminated that  $\text{Ca}^{2+}$  released continuously from self-hardening glass into solidifying liquid, and reacted with  $\text{HPO}_4^{2-}$  and  $\text{NH}_4^+$  ions in liquid to form amido calcium phosphate,  $[\text{SiO}_4]$  networks in the glass were

broken and polymerized complex lined structure over again, this was sustained by the band abruption. Fig.2 showed that the structure network of phosphate had been formed.

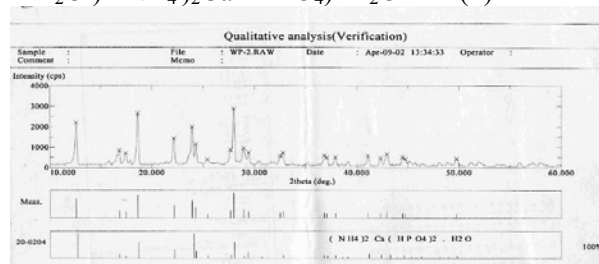
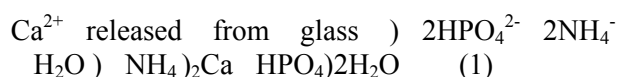


Fig.1: XRD analysis of typical sample immersed in SBF solution about 15 days.

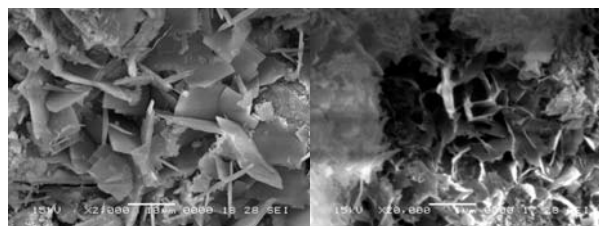


Fig2. SEM photograph of typical sample.

Table1: Results of mechanical and haemolytic test.

Code/Data	1#	4#	6#
$\sigma_{bc}$ (M Pa)	31.20	32.40	34.98
$\sigma_{bc}$ (Mpa)	31.200	32.400	34.980
$\sigma_{sc}$ (Mpa)	16.975	19.364	20.210
hemolysis	non	non	non

**DISCUSSION & CONCLUSIONS:** The main crystal of self-hardening products were  $(\text{NH}_4)_2\text{Ca}(\text{HPO}_4)_2\cdot 2\text{H}_2\text{O}$  and in vitro experiment found no hydroxyapatite the glassy composition and PH value of solidifying liquid could affect the strength and biocompatibility.

**REFERENCES:** <sup>1</sup>Suchanek W, Yoshimura M (1998) *J Mater.Res* 12:94-117. <sup>2</sup>Kasuga T., Sawada M., Nogami M (1999) *AbeY* 20:1415-1420. <sup>3</sup>E.W White (1977) *J.Mat.Res.Lnnovations* 1:57-63.

# Chemical- Physical Characterization and Histological Outcomes after Implantation of KyphOs™ and KyphOs R™ in Vertebral Bodies of Sheep

R. Wenz<sup>1</sup>, J. Meyer<sup>1</sup>, M. Sankaran<sup>2</sup>, J. Schwardt<sup>2</sup>

<sup>1</sup>Sanatis GmbH, Kirchstrasse 9, Rosbach, Germany <sup>2</sup>Kyphon Inc., Sunnyvale, CA, USA

**INTRODUCTION:** KyphOs and KyphOs R are self-setting calcium phosphate bone substitutes, with and without BaSO<sub>4</sub> radiopacifier. These biomaterials contain TCP and magnesium phosphate compounds in the powder, which set into a hardened mass when mixed with an aqueous ammonium phosphate solution. These bone substitute materials provide the combined advantages of biomechanical support and the inherent potential to be replaced by natural bone.

**METHODS:** 10 grams of KyphOs powder was mixed with a 3.5 molar aqueous (NH<sub>4</sub>)<sub>2</sub>HPO<sub>4</sub> solution at a liquid to powder ratio of 0.50 (ml liquid / g powder) to form a paste, which was transferred into cylindrical molds (6x12mm) and incubated in 0.9% NaCl for 1 hour, and 12 weeks. After the respective incubation times the samples were fixed in acetone and crushed, then XRD analysis was performed to determine the crystallographic compositions after these setting times.

Four sheep underwent implantations in L3, L4 and L5 with KyphOs or KyphOs R. Implantation was made by a retroperitoneal lateral approach through the oblique abdominal muscle to the lateral aspect of the vertebral body (VB). All animal surgeries were performed under general anaesthesia. A defect of 7 mm in diameter and 15 mm in depth was created on the lateral aspect of the VB and the defect was completely filled with biomaterial.

Four months after implantation the sheep were sacrificed, the VB's retrieved and processed for undecalcified histology and for back scattered microscopy.

**RESULTS:** Figures 1 and 2 show the XRD pattern of KyphOs 1 hour and 12 weeks after preparation of the test samples. The first setting phase that forms at 1 hour is struvite (MgNH<sub>4</sub>PO<sub>4</sub>) while TCP remains unchanged. At 12 weeks struvite remains the predominant phase, TCP occurs in a lesser amount, and there is a broadening of the peaks in the 30°-35° 2θ angle. Struvite seems to be the primary initial crystallographic phase. Figure 3 shows a CT scan of a retrieved sheep VB demonstrating the status of the implant in the VB.

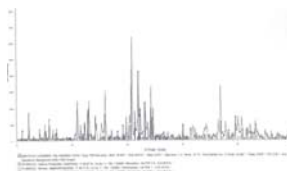


Fig. 1: XRD, 1 hour

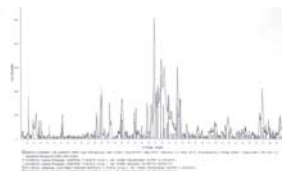


Fig. 2: XRD, 12 weeks

Undecalcified sections (Fig. 4) revealed a tight connection between host bone and both KyphOs and KyphOs R.



Fig. 3 Post-operative CT image.

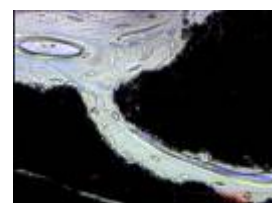


Fig. 4: 4-month implant, undecalc. sect. (black=KyphOs mat'l.)

Resorption lacunae are observed on the surface of the biomaterial, indicating remodelling and new bone formation in direct apposition to the material surface. In some areas BaSO<sub>4</sub> particles are embedded in newly-formed bone.

**DISCUSSION & CONCLUSIONS:** The predominant crystalline phase of KyphOs and KyphOs R is struvite, which forms due to the transformation of magnesium phosphate salts with ammonium phosphate solution<sup>(1)</sup>. This explains the early biomechanical support provided by the setting biomaterial. At later incubation times the peak height of TCP gets smaller with a concomitant broadening of the superpositions of the peaks, indicating the formation of an apatite<sup>(1)</sup>. Apatite forms through the conversion of TCP and strontium carbonate into an apatitic structure. The undecalcified histological sections of implanted KyphOs and KyphOs R reveal the active resorption of the material by osteoclasts with concomitant formation of new bone by osteoblasts, thus resembling the remodelling process of bone. The material demonstrates excellent biocompatibility with direct apposition of new bone and viable osteocytes on the surface.

**References:** Mulliez, M.A. (2002) ESB abstracts

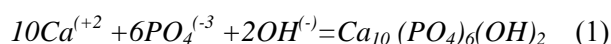
# Hydroxyapatite Coating for Fixation of Biomedical Implants

K.L. Yadav

*Smart Materials Research Laboratory, Department of Physics, Indian Institute of Technology, Roorkee-247 667, India*

**INTRODUCTION:** Hydroxyapatite (HAp) forms the main mineral constituent of human hard tissues and its biocompatibility makes it attractive for use in medical devices [1-4]. It is one of a limited number of materials that forms strong chemical bonds with bone in vivo, while remaining stable under the harsh conditions encountered in the human body. These properties place hydroxyapatite into the class of biomaterials known as surface active or bioactive materials [5, 6]. Most metallic orthopaedic and dental implants are bioinert and do not bond chemically to bone as does hydroxyapatite. Consequently they can become encapsulated by fibrous tissue. Thus, the only means of biofixation is mechanical interlock, whereby the implant must be manufactured in such a way that it possesses surface porosity with interconnections and pores so that hard tissue can grow into the implant and anchor it in place. If the implant does not integrate well with the surrounding bone, or is not held rigidly with a fastening device, the implant will be subjected to micro-movement, and surrounding bone will remodel. This may lead to implant loosening over a period of time. Coating a load bearing substrate, such as titanium metal, with HAp overcomes the physical inadequacies of HAp. The main goal is to accelerate bone ingrowth's to implant surface and thus fixation of the prosthesis. Coatings of hydroxyapatite have been done by a variety of techniques that suffer from various drawbacks which will be discussed during presentation of the paper. Pure HAp coatings are necessary for medical implant because other phases and constituents could accelerate the degradation of HAp coatings in the human body. In the present work a unique chemical method for the deposition of hydroxyapatite coating on Stainless steel substrate is described.

**METHODS:** The idea of chemical bath deposition is based on a controlled performing of the following reaction:



A chemical bath was prepared for Hydroxyapatite coating. The chemical bath deposition was performed in a 50 ml beaker by immersing the steel plate in the prepared solution.

**RESULTS AND DISCUSSIONS:** Phase purity was confirmed by X-ray Diffraction (XRD) and Fourier transforms infrared (FT-IR). SEM micrographs of HAp after the completion of coating at 95 oC are shown in Fig. 1(a-b). The HAp formed is of flake like morphology. The HAp formed appears in flaky to needle-like morphology with smaller crystallite size.

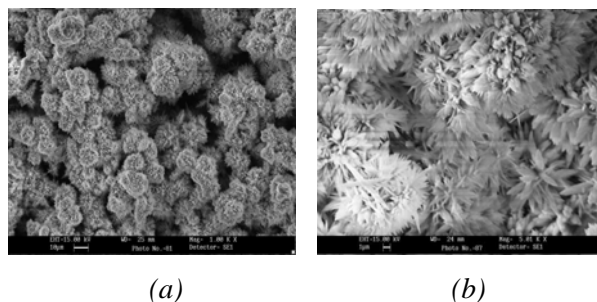


*Fig. 1. SEM micrographs of Hap*

The described method is very simple and produces stoichiometric hydroxyapatite coatings with Ca/P=1.6. It can be applied for deposition onto complex shaped implants. Note that the deposition temperature is below 100 °C with potential for deposition onto polymer substrates. The method can be optimized by designed experiments to control the growth kinetics of stoichiometric Hap coatings. The dense fracture free coating with preferentially oriented grains can improve adhesion with the substrate and also act as a barrier layer between implant surface and body fluids preventing dissolution of the metal. These properties are appropriate for the initial layer in the bi-layer Hap coating designed to satisfy the essential requirements considering its application as a surgical implant material.

**REFERENCES:** <sup>1</sup>B.R. Constantz, et.al. (1995), Science <sup>2</sup>C. Durucan and P.W. Brown, (2000), J. Mat. Sc: Mat. Med. <sup>3</sup>C.P.A.T.Klein, et.al. (1983), J. Biomed. Mater. Res. <sup>4</sup>C.P. A. T. Klein, et.al (1990), "Handbook of Bioactive Ceramics", Vol. II <sup>5</sup>K. de Groot, (1983), Bioceramics of calcium Phosphate <sup>6</sup>K. L. Yadav and P. W. Brown, (2003), J. Biomed. Mater. Res.

# Sponsors

We gratefully acknowledge the financial support of our sponsors.

*DePuy*  
*Kyphon*  
*Stryker*

*Synthes*  
*Heraeus*  
*Promedics*  
*Tecres*

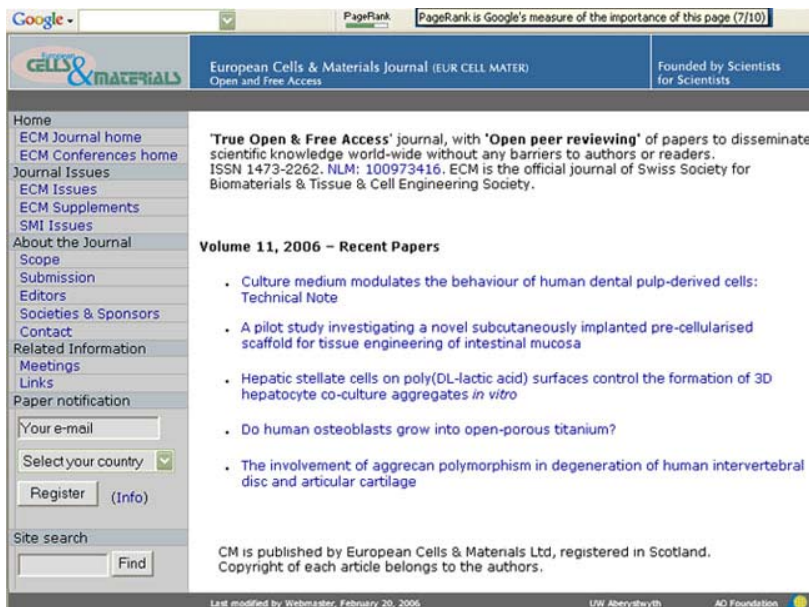
*Kasios*  
*ReGen Lab*  
*Zimmer*

ISSN 1473-2262 NLM: 100973416

European Cells & Materials (ECM) journal is a true Free, world-wide Open Access peer reviewed online journal. ECM was founded by scientists for the benefit of scientists and provides an international and interdisciplinary forum for publication and discussion in the following fields:

- Interaction of tissues, cells or bacteria with biomaterials (in vivo, in vitro, ex vivo).
- Properties of bone, cartilage & connecting tissues, including ligaments & tendons.
- Tissue engineering (scaffolds; stem cells & more differentiated cells; techniques including culture, implantation, bioreactors etc.)
- Surface characterisation of biomaterials.

ECM carries original research papers, reviews and tutorials on the advances made in these fields of activity. All articles are peer-reviewed by 3 specialists and reviewer comments, together with responses by authors, are published along with the paper. The main aim is to provide rapid publication and efficient dissemination of scientific knowledge, without profit.



The screenshot shows the homepage of the European Cells & Materials Journal. The header includes the journal's name and ISSN. A navigation menu on the left lists various sections like Home, Journal Issues, and About the Journal. The main content area features a 'True Open & Free Access' statement and a list of recent papers from Volume 11, 2006. A registration form is visible on the left side of the page.

### Paper notification

If you register for the paper notification, we will send you maximally a monthly e-mail with information about the ECM Journal and the ECM Conferences (Country reader list). We will not give your e-mail addresses to any third party.

[www.ecmjournal.org](http://www.ecmjournal.org)

### Ten good reasons for publishing a paper in ECM

1. World-wide 'True Open & Free access to all'. Over 4600 registered readers (100 countries).
2. ECM is indexed in BIOSIS, CAS, Medline and Index Medicus databases and can be searched directly from Pubmed and DOAJ.
3. No submission or publication charges of any kind (incl. colour illustrations & videos).
4. Authors retain copyright to their articles.
5. Open Peer reviewing minimises both favouritism and prejudice.
6. Discussion with reviewers feature allows sensible arguments included in the paper.
7. High standard of reviewing.
8. Speed of publication (2-3 weeks after acceptance).
9. No payment for reprints: refer colleagues directly to the open access journal site.
10. ECM was founded by scientists for the benefit of Science rather than profit.